| | |
|---|---|
| Title | AN ELECTROPHYSIOLOGICAI STUDY OF NEURONAL ORGANIZATION IN THE RABBIT OLFACTORY BULB |
| Author(s) | 森, 憲作 |
| Citation | 大阪大学, 1978, 博士論文 |
| Version Type | VoR |
| URL | https://hdl.handle.net/11094/2524 |
| rights | |
| Note | |

# AN ELECTROPHYSIOLOGICAL STUDY OF NEURONAL ORGANIZATION IN THE RABBIT OLFACTORY BULB

# ウサギの嗅球におけるニューロン機構の電気生理学的研究

BY

KENSAKU MORI

森 憲作

From Department of Physiology
School of Medicine
Gunma University
Maebashi, Gunma

Contents

This thesis is based on the following articles.

I. K. Mori and S. F. Takagi, Spike generation in the mitral cell dendrite of the rabbit olfactory bulb. Brain Research, 100, 685-689. (1975)

II. K. Mori and S. F. Takagi, Inhibition in the olfactory bulb; dendro-dendritic interactions and their relation to the induced waves. In Food Intake and Chemical Senses ed. by Y. Katsuki, M. Sato, S. F. Takagi & Y. Oomura, Univ. of Tokyo Press, 33-43. (1977)

III. K. Mori, S. Kogure and S. F. Takagi, Alternating responses of olfactory bulb neurons to repetitive lateral olfactory tract stimulation. Brain Research, 133, 150-155. (1977)

IV. K. Mori and S. F. Takagi, An intracellular analysis of dendrodendritic synapses on mitral cells in the rabbit olfactory bulb. J. Physiol. (1978) In press.

V. K. Mori and S. F. Takagi, Activation and inhibition of olfactory bulb neurons by anterior commissure volleys in the rabbit. J. Physiol. (1978) In press.

VI. M. Nakashima, K. Mori and S. F. Takagi, Centrifugal influences on olfactory bulb neurons in the rabbit. Brain Research, (1978) In press.

# 1. GENERAL INTRODUCTION AND PURPOSE OF THE PRESENT STUDY

In order to understand the neural mechanisms for processing the sensory signals in the central nervous system, it is important to analyze the detailed neuronal or synaptic organization of the system as well as the nature of the input signals. The olfactory bulb represents a good substrate for such an analysis in that its neuronal elements are arranged in a well defined laminated structure. Taking advantage of this simple neuronal arrangement, Rall and Shepherd (1968) succeeded in constructing a powerful mathematical model and proposed a new concept of "dendrodendritic synaptic action". In this new concept, it was postulated that the dendrite can be a presynaptic structure as well as a postsynaptic one. This is contrary to the generally accepted view that the dendrite functions mainly as a postsynaptic structure. In parallel with this theoretical advance, there has been a great progress in the electronmicroscopic investigations of the olfactory bulb which were greatly facilitated by the laminated neural structures. One of the important outcome of these studies was a discovery of the "reciprocal synapses" between the dendrites of bulbar neurons which fully corroborated the concept of the dendrodendritic synaptic action (e.g. Hirata, 1964; Andres, 1965; Rall et al. 1966). Furthermore, recent electron-microscopic investigations have demonstrated such dendrodendritic synapses in many other parts of the nervous system. Such a generality of the dendro-dendritic synapses suggests that the dendrodendritic synaptic interactions may not be an unusual phenomenon but occur widely in various parts of the nervous system.

In contrast to the theoretical and anatomical data supporting the new concept, which undoubtedly is of great significance for the understanding of the nervous system in general, electrophysiological data substantiating it have been relatively scanty. Considering the importance of the understanding of the electrophysiological properties of the synaptic transmission in the olfactory bulb, it seemed desirable to undertake a more detailed analysis of the synaptic potentials of bulbar neurons using intracellular recording techniques. This study is divided into five sections (Section A-E). The detailed introduction of each subject and the purpose of each section will be described in the head of the respective section.

## 2. ANATOMY OF THE OLFACTORY BULB

The schematic diagram of the morphology of the olfactory bulb is illustrated in Fig. 1. The nomenclaturs ~~names of~~ each layer in the olfactory bulb are also shown at the left of this figure. They are;

1. Olfactory Nerve Layer (ONL)
2. Glomerular Layer (GL)
3. External Plexiform Layer (EPL)
4. Mitral Cell Layer (MCL)
5. Internal Plexiform Layer (IPL)
6. Granule Cell Layer (GCL)

Olfactory nerves, which are the axons of olfactory receptors in the olfactory epithelium, enter the olfactory bulb from its surface. Thus the most superficial layer of the olfactory bulb contains mainly the olfactory nerves (ONL). The olfactory nerves then enter the glomerular layer (GL) and ramify within the glomeruli. They synapse on terminal dendritic tufts of secondary olfactory neurons, i.e. mitral cells, tufted cells and periglomerular cells. About 500 μ deep to this layer is mitral cell layer, where the somata of large mitral cells lie in a thin sheet. The mitral cell sends its axon to the lateral olfactory tract (LOT) and usually one primary dendrite to a glomerulus. In addition to this, each mitral cell has several secondary dendrites which run obliquely and terminate within the external plexiform layer. Deep to the mitral cell layer, there exist many small axonless cells (granule cells). The granule cell has two types of dendrites. The peripheral processes of the granule cells run to the external plexiform layer and branch repeatedly there. The peripheral process in the EPL has spine-like appendages called gemmules. In contrast to this, the deep dendrites of the granule cells run to the deep portion of the GCL. Beside the mitral and granule cells, the olfactory bulb contains tufted cells in the EPL and periglomerular cells in GL. The bulb also contains small number of short-axon cells scattered in the GL, EPL and GCL.

According to Allison (1953), there are about 50,000,000 olfactory receptor cells in the right or left olfactory epithelium of the rabbit. Each receptor cells seemed to send one axon to only one glomerulus in the olfactory bulb. Since one olfactory bulb contains approximately 1900 glomeruli, a massive convergence of olfactory nerves to one glomerulus

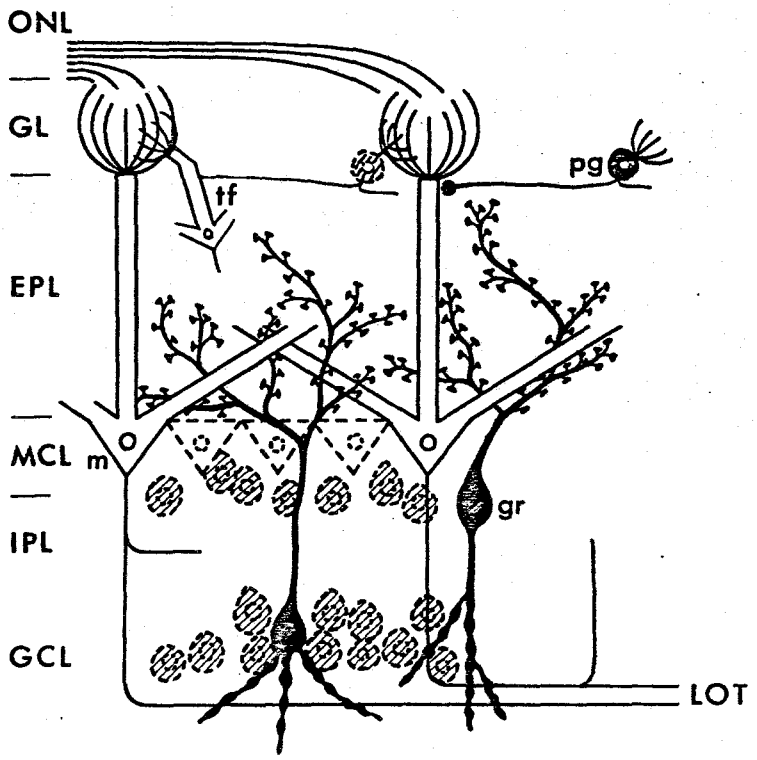


Fig. 1 Schematic diagram of the neuronal organization in rabbit olfactory bulb: ONL, olfactory nerve layer; GL, glomerular layer; EPL, external plexiform layer; MCL, mitral cell layer; IPL, internal plexiform layer; GCL, granule cell layer; pg, periglomerular cell; tf, tufted cell; m, mitral cell; gr, granule cell; LOT, lateral olfactory tract.

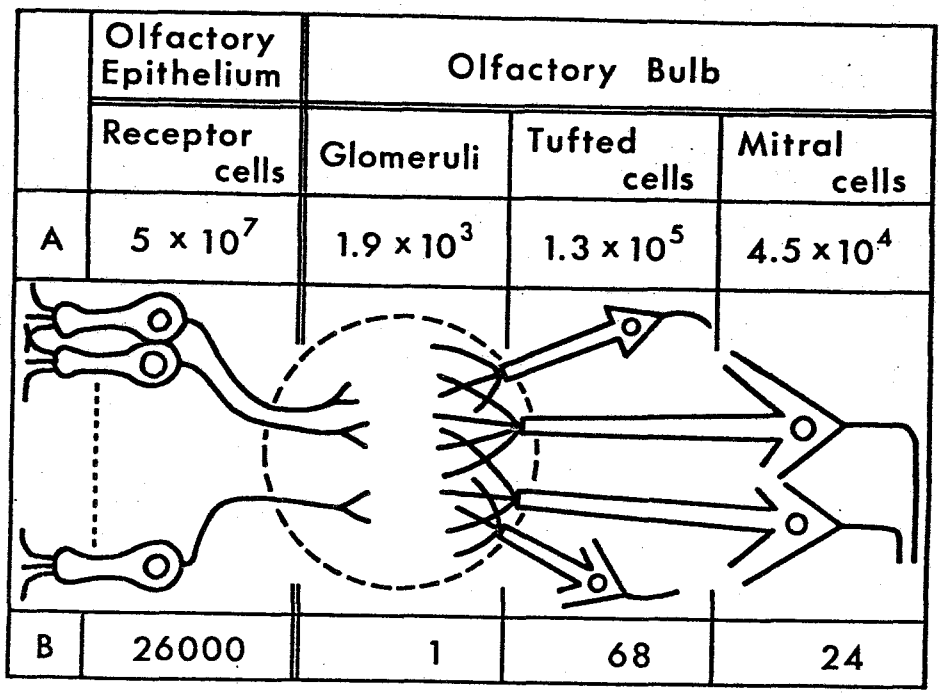


Fig. 2 Number of receptor cells, tufted cells and mitral cells which project their processes into a single glomerulus (B). Total number of them (in one side of the olfactory epithelium and the olfactory bulb) are shown in A. After Allison (1953)

can be estimated (about 26,000 olfactory nerves to one glomerulus). In addition, one can calculate from the total number of the tufted and mitral cells in the olfactory bulb that one glomerulus receive dendritic projections from about 68 tufted cells and 24 mitral cells as indicated in Fig. 2.

In addition to the primary afferent input (olfactory nerves), the olfactory bulb receives various central inputs from the telencephalon (Fig. 3). According to Price and Powell (1970e), there are at least three types of extrinsic inputs from telencephalon to the olfactory bulb. The first is the fibers from anterior commissure (AC) that end upon the deep dendrites and somata of granule cells. The second is the fibers which arise from cells in the ipsilateral anterior olfactory nucleus (AON). The third is the centrifugal fibers (CF) which arise from cells in the ipsilateral nucleus of the horizontal limb of the diagonal band, run foward in the LOT and terminate upon the peripheral processes of the granule cells.

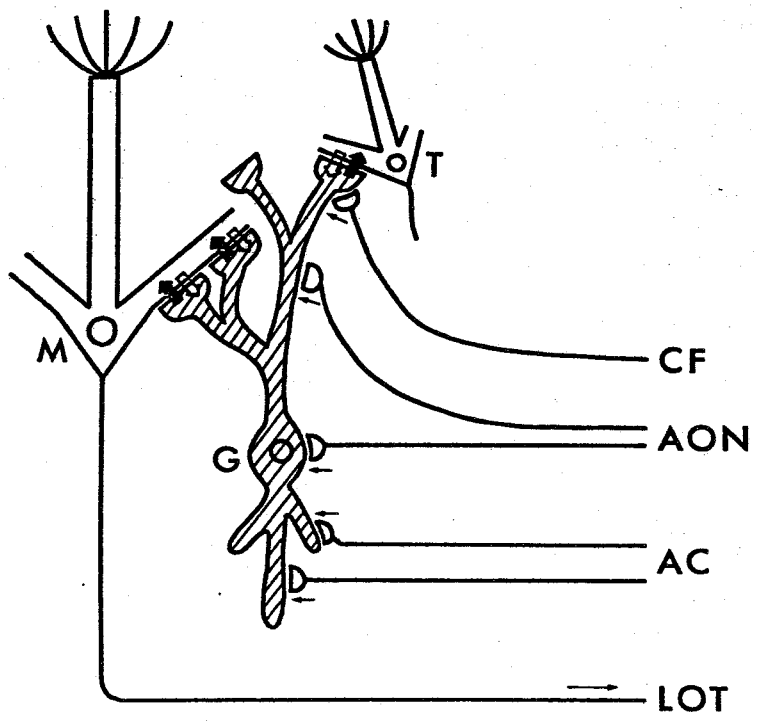


Fig. 3 Centrifugal fiber inputs to granule cells. CF, centrifugal fibers running in the lateral olfactory tract; AON, fibers from ipsilateral anterior olfactory nucleus; AC, anterior commissure fibers; LOT, lateral olfactory tract; M, mitral cell; T, tufted cell; G, granule cell.

# 3 EXPERIMENTAL RESULTS AND DISCUSSIONS

## A, SPIKE GENERATION IN THE MITRAL CELL DENDRITE

The ability of spike generation in dendrites of chromatolyzed motoneurons (Eccles, Libet & young, 1958; Kuno & Llinás, 1970) and some normal mammalian neurons (Maekawa & Purpura, 1967; Purpura, Desiraju, Prelevic & Santini, 1968; Purpura & McMurtry, 1965; Purpura & Shofer, 1964; Purpura, Shofer & Scorff, 1965; Spencer & Kandel, 1961) has been suggested by the findings of brief, depolarizing partial responses or fast pre-potentials (FPPs). Purpura (1966) pointed out that 'in the experimental situations in which impulse initiation has been suspected in the dendrites of mature mammalian neurons, anatomical evidence has indicated the operation of relatively powerful axodendritic excitatory synaptic pathways in the production of dendritic spikes'. From anatomical studies (Allison, 1953; Cajal, 1955), it is well known that the mitral cells of the rabbit olfactory bulb receive olfactory nerve inputs on the primary dendrites exclusively within the glomeruli, about 500 μm from the soma, as shown schematically in Fig. 4. Previous investigators (Shepherd, 1963; Yamamoto, Yamamoto & Iwama, 1963) have shown that a mitral cell discharges one or a few impulses in response to olfactory nerve or olfactory mucosa stimulation. Yamamoto et al. (1963) reported, in their intracellular recordings from the mitral cells, that olfactory mucosa stimulation elicited a small depolarization with superimposed spikes, but that not infrequently spikes were evoked without remarkable depolarization. It seems necessary, however, to acquire more detailed information about the electrical properties of the mitral cell dendrite.

### A-1, METHOD

Experiments were performed on adult albino rabbits anesthetized with urethane (ethyl carbamate) or a mixture of urethane and chloralose, and in half the cases, immobilized with gallamine triethiodide (Flaxedil) and artificially ventilated. The experimental arrangement is shown in Fig. 4. A bipolar electrode was used for lateral olfactory tract stimulation and a concentric electrode was placed at the most rostral part of the dorsal surface of the olfactory bulb for olfactory nerve stimulation. Intracellular recordings from mitral cells were obtained with micropipettes filled with 2 M KCl or 2 M potassium citrate. Although most neurons were damaged by

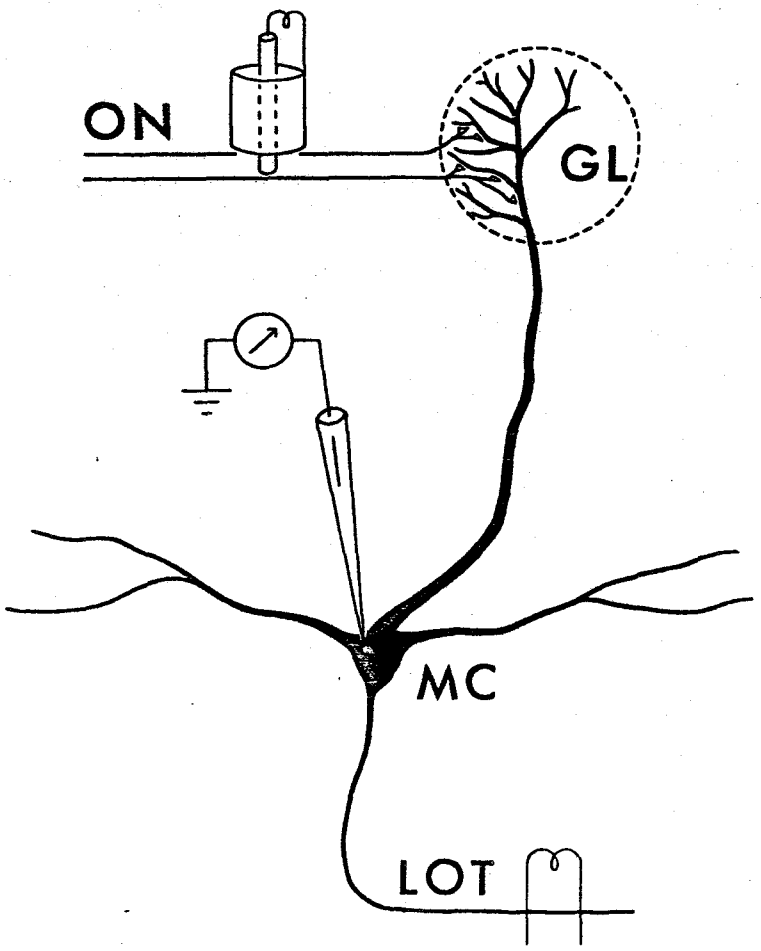


Fig. 4 Schematic drawing of the experimental arrangement and synaptic connections between the olfactory nerves and a mitral cell primary dendrite. Abbreviations: ON, olfactory nerve; GL, olfactory glomerulus; MC, mitral cell; LOT, lateral olfactory tract.

impalement and showed high frequency injury discharges, the data presented here have been derived from stable ~~neurons~~ recordings which showed, for 4 min to more than 2 h, spikes of more than 40 mV (41-60 mV) and no remarkable fluctuation of the membrane resting potential (which ranged from -50 to -64 mV).

## A-2 RESULTS

Fig. 5 shows an example of intracellular recordings from the mitral cells. Lateral olfactory tract stimulation elicited an antidromic spike which was followed by a long lasting hyperpolarization, as shown in Fig. 5A. An orthodromic response of this mitral cell to olfactory nerve stimulation is shown in Fig. 5B. A single spike was elicited on the rising phase of a small depolarization and this orthodromic spike was also followed by a long lasting hyperpolarization. If the antidromic spike was placed several milliseconds before the orthodromic spike, a discontinuity between a brief depolarizing potential (FPP) of about 9 mV and the rest of the spike appeared in the rising phase of the latter spike (Fig. 5C). In some cases, the FPP could be seen in isolation, as is shown in Fig. 5D, and when stimulus strength of the orthodromic volley was weakened, the FPP disappeared in an 'all-or-none' fashion. Superimposed tracings of the orthodromic spikes following the conditioning antidromic response are shown in Fig. 5E. When the interval between the conditioning antidromic spike and the testing orthodromic spike was decreased, the inflection of FPP and the rest of the test spike was accentuated, as oblique arrows on the traces of the two orthodromic spikes indicate, and, by further decreasing of the stimulus intervals, FPPs were isolated in two traces and finally the FPP also disappeared and only a small, slow depolarization could be seen. In rare cases an A-B inflection (Phillips, Powell & Shepherd, 1963) (the arrow with a star) appeared in the rising phase of the test spike with an amplitude of about 20 mV which had almost the identical height of the A-B inflection of the antidromic spike. Except for the presumed M-spike in a few cases, no FPP was observed in the rising phase of the antidromic spike when preceded by another antidromic or orthodromic spike. The FPPs of the orthodromic spikes were distinguishable from the M-spikes of the antidromic responses with respect to amplitude and time course. These results suggest that the FPPs are not generated in the initial segment or in the medullated axonal segment.

Fig. 6 shows another method of demonstrating the existence of the

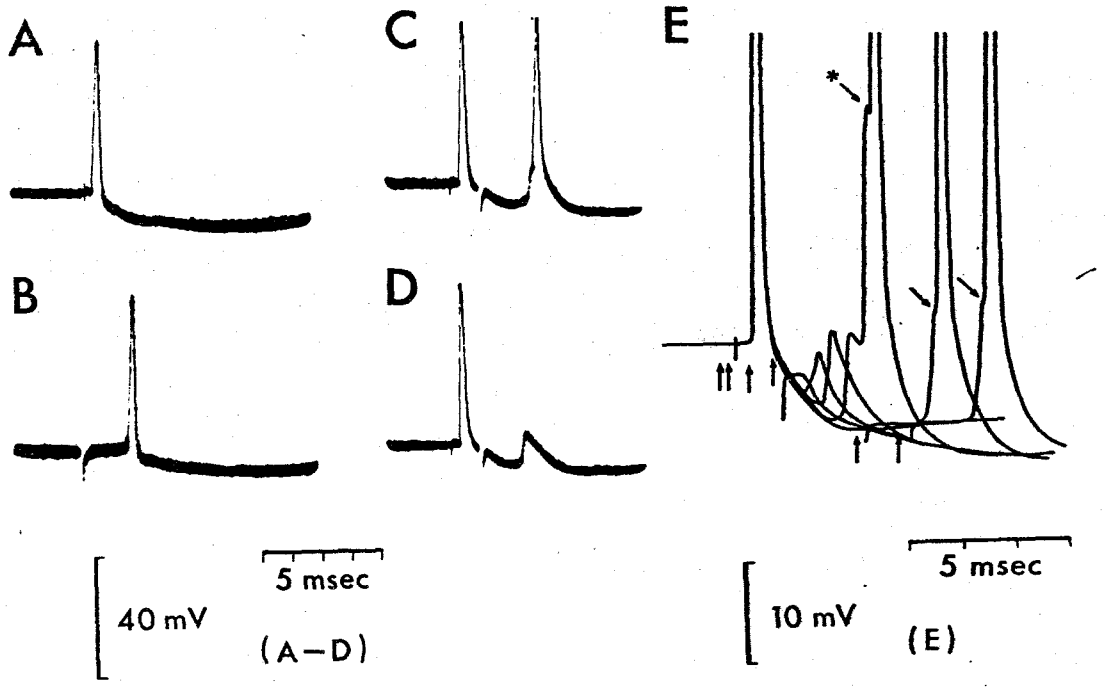


Fig. 5 FPPs on the rising phase of the orthodromic spike of a mitral cell revealed by conditioning lateral olfactory tract stimulation. A: an antidromic response produced by lateral olfactory tract stimulation. B: an orthodromic response produced by olfactory nerve stimulation. C and D: effects of the conditioning antidromic response upon the testing orthodromic spike. E: superimposed tracings of orthodromic spikes preceded by a conditioning antidromic response. Stimulus intervals are gradually decreased. The arrow with a star indicates the A-B inflection. Upwards arrows indicate the times of olfactory nerve stimulation. Voltage calibrations as indicated. Time scale: 5 msec/division.

FPPs. In Fig. 6A, the orthodromic spike of another mitral cell (upper middle trace) is shown just as in Fig. 5B. When the stimulus strength was weakened (lower middle trace), a very small, slow depolarization (which may be the EPSP produced in the olfactory glomerulus by olfactory nerve volley and spread electrotonically to the soma) could be seen, but FPPs were not seen in isolation. During the passage of a hyperpolarizing current (2.4 nA) to the soma, which presumably is the site of impalement, an inflection of FPP and the rest of the spike was seen (Fig. 6B), and when a little stronger current (2.6 nA) was applied, FPP appeared in isolation (Fig. 6C). This FPP disappeared only when very strong hyperpolarizing currents were applied. Fig. 6D shows superimposed tracings of the 3 orthodromic responses of another mitral cell during a hyperpolarizing current injection. An olfactory nerve volley elicited a full spike with an inflection (arrow) on the rising phase. This inflection coincides with the peak of FPPs sometimes elicited in isolation. The lower middle trace of a slow depolarization was obtained when stimulus strength was weakened to just subthreshold for FPP generation. The antidromic spikes never showed such a sequence (i.e., slow depolarization-FPP-full spike) but disappeared completely when a hyperpolarizing current was injected, just as when preceded by another antidromic spike. This also suggests that the FPPs are not generated in the axonal segment.

By hyperpolarizing current injections or by conditioning antidromic response, or by both, FPPs were clearly seen in 10 antidromically identified mitral cells out of 12 tested mitral cells and in two unidentified cells located in or near the dorsal mitral cell layer (judged by the extracellular field potential). Since the stimulating electrode was put on the dorsal bundle of the olfactory nerve, it was not possible to record orthodromic responses or to show the FPPs clearly in the mitral cells located in the ventral mitral cell layer, but spontaneous discharges of these cells often showed two modes of spike generation, i.e. the spikes on the rising phase of slow depolarizing potentials and spikes with the rapid depolarizing potentials (FPPs).

## A-3, DISCUSSION

As stated in the results, the FPPs are not likely to be of axonal origin. Furthermore, a very strong hyperpolarizing current was needed to eliminate the FPPs. The FPP generation site may be located in the dendrite rather far from the soma. Recently Pinching (1971) found

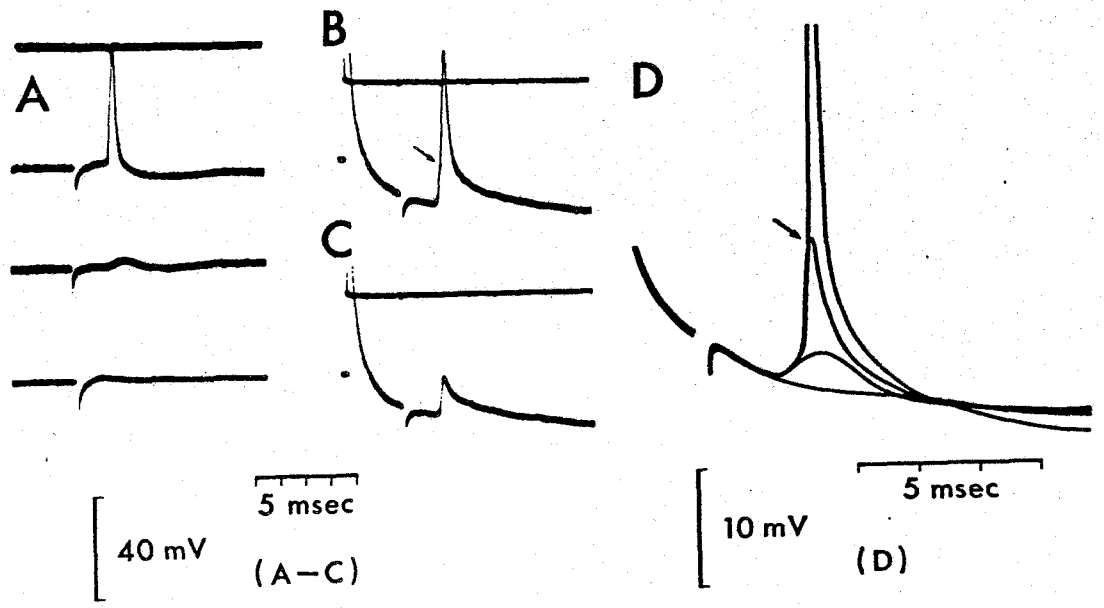


Fig. 6 FPPs appearing during hyperpolarizing current injections. A: an orthodromic response of an identified mitral cell to olfactory nerve stimulation (upper middle record), and response to subthreshold stimulation (lower middle record), and extracellular field potential with same stimulus strength as A (bottom record). In B and C, hyperpolarizing currents of 2.4 nA and 2.6 nA were injected, respectively. Uppermost traces in A, B and C are current monitors. An arrow indicates the inflection of the FPP and the rest of the spike in B. D: superimposed tracing of orthodromic response during a hyperpolarizing current injection. Note the correspondence of the inflection of a full spike with an isolated FPP. A slow depolarization (lower middle trace) was elicited by just subthreshold olfactory nerve stimulation for spike generation. Bottom trace is a recording without olfactory nerve stimulation. Voltage calibrations as indicated. Time scale: 5 msec/division.

that 'in the rat the portion of the mitral cell primary dendrite passing from the superficial part of the external plexiform layer through the periglomerular region up to the primary glomerular branching point is covered by several thin cytoplasmic lamellae of glial origin, and in the monkey, these dendritic segments have become myelinated'. This corresponds to our findings because the small amplitudes of the FPPs suggest that there exist an electrically inexcitable membrane area between the soma and the active membrane which is responsible for the FPP, as was already discussed on the apical dendrite of the hippocampal pyramidal neuron (Spencer & Kandel, 1961). Since the olfactory nerve synapses on the mitral cell primary dendrite exclusively within the olfactory glomerulus, it is highly probable that the active membrane responsible for the FPP is located within the glomeruli, where the primary dendrite arborizes.

## B. INHIBITORY POTENTIALS IN MITRAL CELLS AND DENDRODENDRITIC SYNAPTIC PATHWAYS BETWEEN MITRAL AND GRANULE CELLS

Antidromic stimulation of the lateral olfactory tract (LOT) produces a prolonged inhibition of mitral cell activity in the rabbit olfactory bulb (Green, Mancia & Baumgarten, 1962; Ochi, 1963; Phillips, Powell & Shepherd, 1963; Nicoll, 1969). Long lasting IPSPs have been demonstrated with intracellular recordings from mitral cells (Yamamoto, Yamamoto & Iwama, 1963; Phillips et al. 1963; Nicoll, 1969; Reese & Shepherd, 1972). Green et al. (1962) suggested that the axon collaterals of mitral cells had a direct inhibitory effect on the mitral cells. However, later physiological studies strongly supported the idea that an inhibitory interneuron, most probably a granule cell, is interpolated in the inhibitory pathway onto the mitral cell (Yamamoto et al. 1963; Phillips et al. 1963; Shepherd, 1963; Nicoll, 1969). Furthermore, a dendrodendritic pathway for synaptic excitation of granule cells through mitral cell dendrites has been postulated based on the theoretical analysis of field potentials in the olfactory bulb following LOT stimulation (Rall, Shepherd, Reese & Brightman, 1966; Rall & Shepherd, 1968; for a review see Shepherd, 1972). Electron-microscopical studies of the olfactory bulb have revealed reciprocal synapses between mitral cell dendrites and the peripheral processes of granule cells (Fig. 7B and C) (Hirata, 1964; Andres, 1965; Rall et al. 1966; Price & Powell, 1970a; Reese & Shepherd, 1972; Willey, 1973). Moreover, it has been reported that nearly all the synapses found on mitral cell dendrites and somata, except in or around the glomerular region, are reciprocal synapses with the peripheral processes of granule cells (Price & Powell, 1970b; Reese & Shepherd, 1972). To date, physiological analysis of the inhibitory mechanisms controlling mitral cell activity has been carried out largely by means of extracellular recordings. It was necessary to obtain intracellular recordings from olfactory bulb neurons in order to analyse directry the properties of the inhibitory mechanism.

The first objective of the present study was to clarify the properties of IPSPs of mitral cells following LOT stimulation in order to ascertain whether or not they have similar characteristics as the IPSPs of other central neurons. Secondly, to determine whether or not the inhibitory synapses are widely distributed on mitral cell dendrites. The third

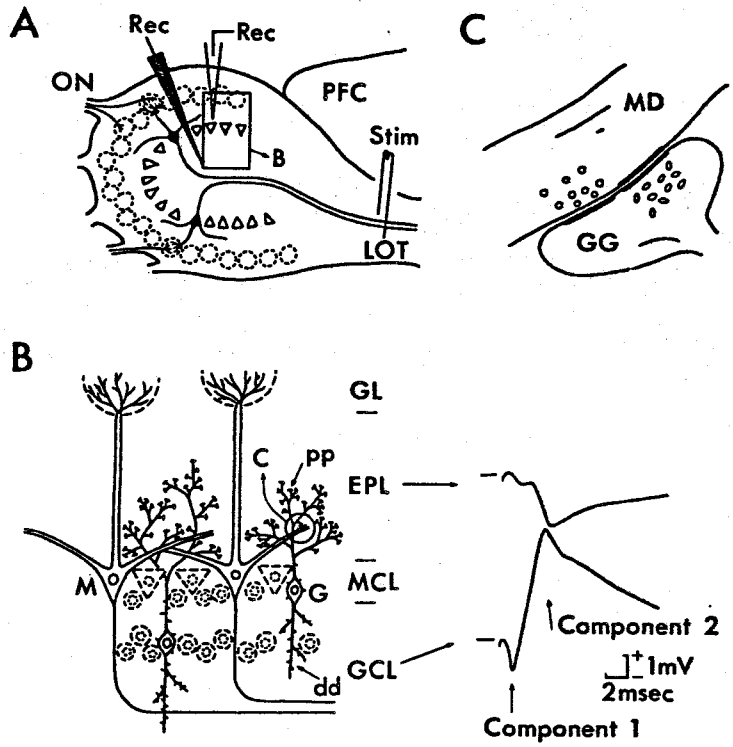


Fig. 7 A, Diagramatic illustration of the experimental arrangement showing a stimulating electrode placed in the lateral olfactory tract (LOT) and two types of recording electrodes, a tungusten microelectrode (black one) for recording the field potential in the middle area of the granule cell layer (GCL) and a glass microelectrode (white one) for intracellular recordings. ON, olfactory nerve; PFC, prefrontal cortex. B, The enlarged shematic illustration of the region enclosed in the rectangle in A (arrow with letter B). Histological layers are shown at right; GL, glomerular layer; EPL, external plexiform layer, MCL, mitral cell layer; GCL, granule cell layer. Only two types of neurons are shown in this diagram; mitral cells (M) and granule cells (G). pp, peripheral process of granule cell; dd, deep dendrite of granule cell. The traces on the right of the diagram are the extracellular field potentials recorded in the EPL (upper trace) and the GCL (lower trace) following LOT stimulation. The latter are composed of first negative wave (component 1) and the following large positive wave (component 2). C, enlarged illustration of the region enclosed in the circle in B showing dendrodendritic reciprocal synapses between mitral cell dendrite (MD) and the gemmule of a granule cell (GG).

objective was to test the hypothesis of dendrodendritic pathways for excitation of granule cells and subsequent inhibition of mitral cells.

## B-1. METHOD

### Preparations

Seventy-two albino rabbits weighing between 1.7 to 3.2 kg were anaesthetized by intraperitoneal injection of 20% urethane (1-1.2g/kg) or a mixture of 20% urethane (1g/kg) and 1% chloralose (5mg/kg) and later supplemented by intravenous injection of 10% urethane when needed. 15 animals were then immobilized with I.V. Flaxedil (gallamine triethiodide) (10mg/kg) and artificially ventilated through a tracheal canulla. A venous catheter was inserted into the saphenous vein. The animal was then mounted on a stereotaxic instrument (Narishige SN-3). Drainage of the cerebrospinal fluid at the atlantooccipital linkage was routinely carried out in order to minimize the pulsation of the brain. Openings were made in the dorsal cranium for introducing stimulating electrodes and in the bone overlying the dorsal surface of the olfactory bulb for inserting the recording electrodes. The exposed surface of the olfactory bulb was covered by a mixture of warmed mineral oil and white vaseline in order to reduce cooling and drying. The rectal temperature was monitored and kept within 35.5°C and 39°C by a heating pad.

### Stimulation

For stimulation of the LOT, bipolar electrodes of acupuncture needles (amalgam of silver, nickel and iron) insulated except for the tip were stereotaxically inserted into the LOT (Fig. 7A). The final position of the stimulating electrode was determined following small adjustments to obtain a low threshold antidromic field potential in the olfactory bulb. In 10 experiments, the left eye was enucleated and the lateral side of the cranium overlying the LOT was opened in order to place the stimulating electrode directly on the surface of the LOT under visual control. Single square pulses of 0.1 msec in duration were used for stimulating the LOT. Stimulation was usually at a frequency of 0.8/sec. At the end of the experiment, a small electrolytic lesion was made at the site of stimulation which was later checked histologically.

### Recording

The electrode placement is shown in Fig. 7A. For intracellular recording, micropipettes field with 2M K-Cl, 2M K-citrate or 2M K-acetate

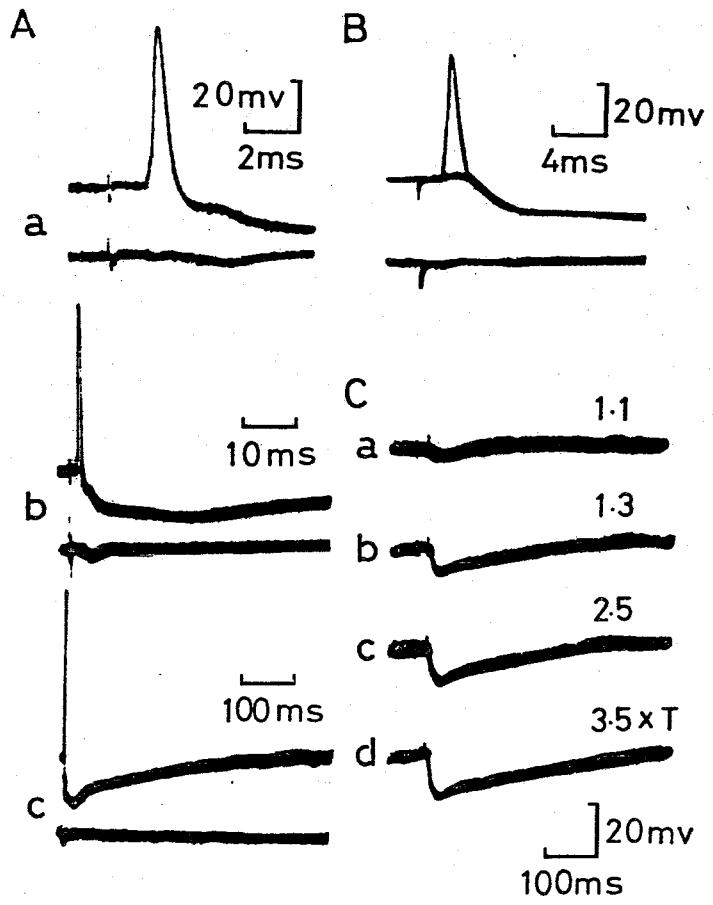


Fig. 8 Intracellular potentials of mitral cells evoked by single LOT stimulation. In A, an antidromic spike and a subsequent IPSP are shown at three different sweep speeds (upper traces). B shows mitral cell responses to just threshold stimulation for the antidromic activation of this cell. C, Intracellular responses of mitral cells to LOT stimulation at indicated stimulus intensities (multiples of the threshold stimulus strength (T) for eliciting the hyperpolarization). The latency of the antidromic spike of this cell was 2 msec, which was later disappeared due to the deteriolation. The lower traces in A and B show the extracellular field potentials recorded just outside of the impaled cell. Spikes retouched.

having 15-80 MΩ resistance were used. The micropipettes were driven vertically from the dorsal surface of the olfactory bulb by a conventional oil micromanipulator. Contact of the micropipette tip with the surface of the olfactory bulb was adjusted under direct vision using a binocular microscope. In addition, a tungusten electrode was inserted in the middle area of the GCL in the olfactory bulb for recording the field potential in the GCL. The microelectrode was connected to a preamplifier (Nihon-Koden MEZ 9001) designed for both recording and passing currents through single microelectrodes. The recorded signals were then amplified and displayed on an oscilloscope and photographed on X-ray film. The resting membrane potential was simultaneously monitored by a DC-pen recorder. A silver plate coated with silver chloride was placed on the temporal muscle as a reference electrode.

## B-2. RESULTS

### Identification of mitral cells

The micropipette was progressively advanced from the dorsal surface of the olfactory bulb (Fig. 7A) and extracellular field potentials evoked by LOT stimulation were recorded. The field potential has a characteristic pattern at each layer in the olfactory bulb so that the position of the micropipette can be determined accurately (cf. Phillips et al. 1963; Rall & Shepherd, 1968). For example, the second negative wave of the field potential in the external plexiform layer (EPL) reverses its polarity at or near the mitral cell layer and becomes a large positive wave in the GCL (Component 2 in Fig. 7B). Impaled cells at or near the mitral cell layer were identified as mitral cells when they were activated antidromically from the LOT (cf. Fig. 8A(a)). The latencies of the antidromic spike potentials of mitral cells varied from 1.0 to 2.1 msec (mean 1.7 ± 0.3 msec S.D., N=242) but the following observations on the properties of LOT-evoked IPSPs described in this communication were similary seen in mitral cells with different antidromic activation latencies. The data presented here have been derived from stable recordings which showed no remarkable fluctuation of the resting membrane potential. The level of spontaneous discharges of these mitral cells were usually less than 5 impulses/sec and the resting membrane potentials ranged from -45 to -72 mV. The recording times ranged from 4 minutes to more than 2 hours.

### Inhibitory postsynaptic potentials of mitral cells

In almost all mitral cell (238 out of 240 mitral cells) recordings, stimulation of the LOT produced a large and prolonged hyperpolarization in addition to an antidromic spike potential, as shown in Fig. 8A(b) and (c). This hyperpolarization was clearly distinguished from an after-hyperpolarization of the antidromic spike by the following two observations: first, when the stimulus strength was adjusted to just subthreshold for antidromic activation of the cell, the hyperpolarization could be evoked without antidromic spike invasion (Fig. 8B); second, the hyperpolarization remained even in those cells in which the spike generating mechanism was damaged (Fig. 8C). The inhibitory effects of the hyperpolarization could be seen as depression of spontaneous activity and as interference with synaptic activation from olfactory nerve input (cf. Mori & Takagi, 1975). In addition, intracellular application of hyperpolarizing current reduced the amplitude of the hyperpolarizing potential and eventually converted it into a depolarization (cf. Fig. 10). These observations indicate that the hyperpolarization is an inhibitory postsynaptic potential (IPSP) similar to that found in spinal motoneurons (Commbs, Eccles & Fatt, 1955) and other nerve cells (cf. Eccles, 1964). Fig. 8C shows the finely graded nature of the IPSPs in relation to the intensity of LOT stimulation. As the stimulus strength was increased, both the amplitude and duration of the IPSPs gradually increased. Supramaximal LOT stimulation (i.e. stimulus strength adjusted so that an increase would not further augment the evoked potentials) produced large and prolonged IPSPs whose peak amplitudes ranged from 5 to 21 mV (mean 14 ± 4 mV S.D., N=173). However, the amplitudes were influenced by the level of the membrane potential (cf. Fig. 10). IPSPs in mitral cells had slow rise times, attaining their flat peak 10 to 32 msec (mean 19 ± 4 msec S.D., N=159) after LOT stimulation, and having a much slower decay time. The total duration of IPSPs varied among the recordings from different mitral cells whthin the range of 60 msec to 650 msec (mean 300 ± 140 msec S.D., N=64).

Conductance changes of the mitral cell membrane during IPSPs

The conductance changes of the mitral cell membrane during the IPSPs were measured by a similar method to that used by Pollen & Lux (1966) for studying the conductance increase in cortical neurons and by Tsukahara & Fuller (1969) in red nucleus neurons. Mitral cell IPSPs evoked by LOT stimulation have slow time courses similar to those of cortical neurons and red nucleus neurons. A slow time course is advantageous for measuring

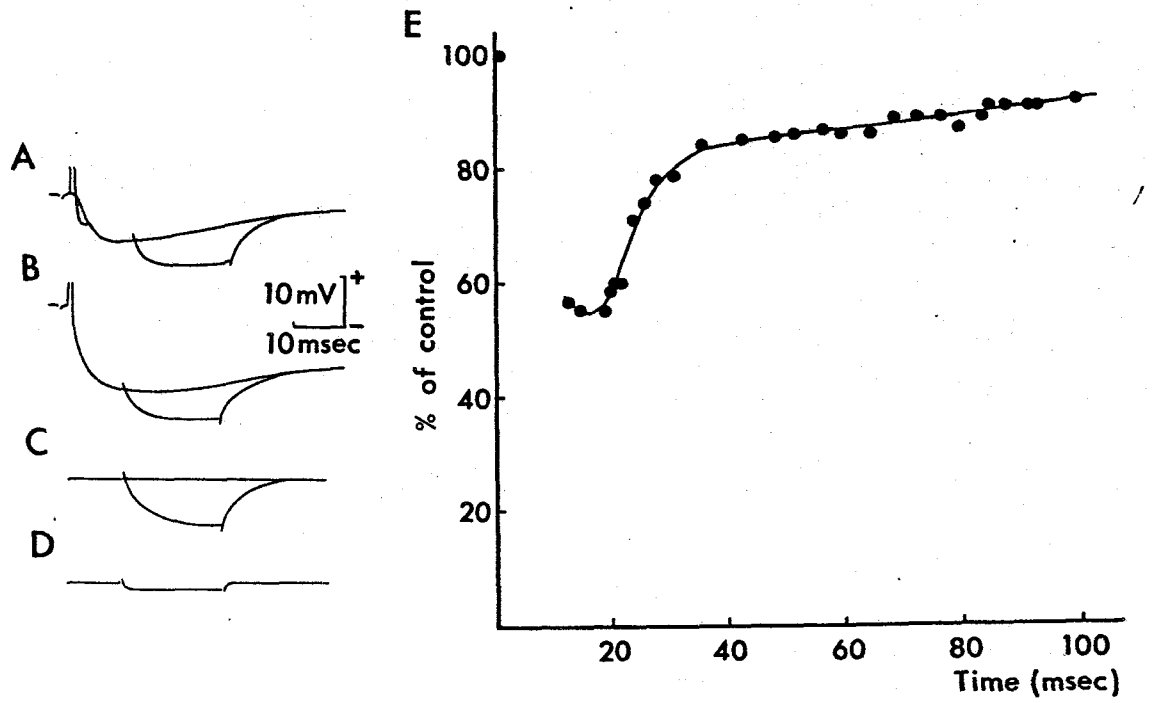


Fig. 9 Membrane conductance changes of a mitral cell during IPSPs evoked by LOT stimulation.

A, Mitral cell responses to just threshold (a) and supramaximal (b) stimulation for antidromic activation of this cell. In addition, hyperpolarizing current pulses (19 msec duration, 7 x $10^{-10}$A) were applied through the recording electrode during the IPSPs and voltage drops produced by the pulses were measured. Fig. A c and d are the control intracellular (c) and extracellular (d) voltage drop produced by the same current pulse without conditioning LOT stimulation. B, Plot of relative amplitudes (a percentage of the control) of voltage drops produced by test constant current pulses at various times after conditioning LOT stimulation.

the conductance changes by applying current pulses of relatively long durations. Fig. 9A(a) is a superimposed tracing of the IPSP in a mitral cell elicited by just threshold stimulation for antidromic activation together with the voltage drop produced by a hyperpolarizing current pulse during the falling phase of the IPSP. When this voltage drop was compared with that produced by the same current without the conditioning LOT stimulation (Fig. 9A(c)), the former had a smaller amplitude and a faster time course than the latter, indicating an increase in membrane conductance of the mitral cell during the IPSP. Using this method, conductance increase during IPSPs was observed in all 24 mitral cells examined. It can also be seen in Fig. 9A(a) that the occurrence of the antidromic spike, or afterhyperpolarization of the antidromic spike, had little effect on the testing voltage drop in this period.

When the stimulus strength was increased to supramaximal, as shown in Fig. 9A(b), the membrane conductance was seen to increase as well as the amplitude of the IPSP. The decrease in membrane resistance of mitral cells measured near the peak of IPSPs ranged from 20 to 45%. The amplitudes of voltage drops produced by current pulses at different phases of the IPSPs were measured in 12 mitral cells and plotted against the time after conditioning supramaximal LOT stimulation (Fig. 9B). The conductance of the mitral cell membrane increased maximally at or near the peak of the IPSPs and decreased rapidly thereafter. But, it could still be detected in the declining phase of the IPSPs (up to 100 msec in Fig. 9B).

Effects of hyperpolarizing current injection on mitral cell IPSPs

The IPSPs of mitral cells evoked by LOT stimulation were reduced in amplitude and then reversed in polarity by intracellular application of hyperpolarizing current. Fig. 10A(a) shows the control response of a mitral cell to supramaximal LOT stimulation which consists of an antidromic spike and a long lasting hyperpolarizing IPSP. When a hyperpolarizing current of 0.6 nA was applied internally (b), the antidromic spike was blocked and the IPSP was reduced in amplitude. Increase of the hyperpolarizing current reversed the initial part of the IPSP into a depolarization, while the later part persisted as a hyperpolarization (c and d), so that a complex positive-negative wave could be seen. Fig. A(e) and lower trace of B shows depolarizing IPSPs produced by the application of stronger hyperpolarizing current. Here, it can be seen that the depolarizing IPSPs have quite different time courses from the original hyperpolarizing potential,

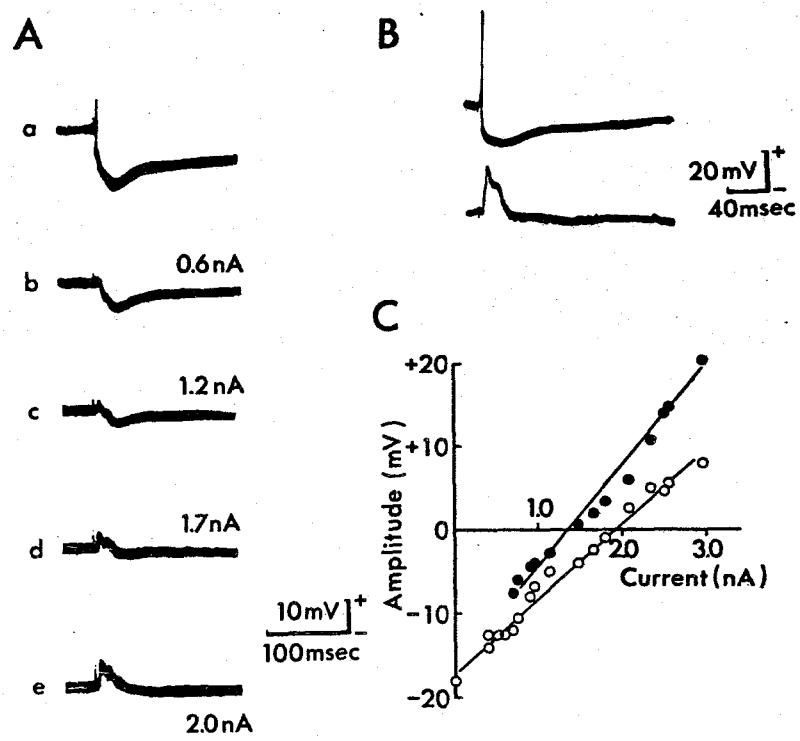


Fig. 10 Intracellular records of IPSPs from mitral cells during intracellular application of the hyperpolarizing current. Records A show the IPSPs evoked by LOT stimulation during application of progressively increasing hyperpolarizing currents. The control mitral cell response composed of an antidromic spike and a subsequent IPSP is shown in a (The antidromic spike was truncuated). In b to e, the decrease in amplitude of the IPSP and then reversal of that occured when the hyperpolarizing currents were applied through the impaling microelectrode. The number on the right shoulder of each trace indicates the amount of the applied current. Records in B show an IPSP in another mitral cell elicited by LOT stimulation (upper trace) and a reversed IPSP during application of a hyperpolarizing current ($2.9 \times 10^{-9}$A). C; Plot of the amplitude of the IPSP at a latency of 6 msec (filled circles) and 20 msec (open circles) following LOT stimulation (ordinate) against the intracellulary applied currents (abscissa), from the same cell as B. Spikes retouched.

the former always having shorter time course than the latter. For example, the average latency of the peak of reversed IPSP was 7 msec while that of the original hyperpolarizing IPSP was 19 msec. This asymmetrical reversal suggests that the IPSP may be produced by an aggregation of inhibitory synapses with different sensitivities to the hyperpolarizing current, which was presumably applied in the soma. In order to compare the vulnerability of the early part of the IPSP to hyperpolarizing current with that of the later part, the amplitude of the IPSP at a latency of 7 msec (near the peak of the reversed IPSP, filled circles) and at the latency of 20 msec (near the peak of original IPSP, open circles) are plotted against the injected current in Fig. 10C. It can be seen that the early part of the IPSP (filled circles) is affected more strikingly than the later part by the hyperpolarizing current. For example, the current at the reversal point of the IPSP at a 7 msec latency was approximately 1.3 nA whereas at a latency of 20 msec it was approximately 1.9 nA. These observations may be explained by the hypothesis that the inhibitory synapses responsible for the mitral cell IPSPs are not localized on the soma but are distributed widely on the dendrites, and that the early part of the IPSP is mainly produced by the inhibitory synapses located at or in proximity to the soma, while those located on distal dendrites are responsible for the later part of the IPSP.

Latency of mitral cell responses

Fig. 11A shows the antidromic spike potential in a mitral cell elicited by LOT stimulation (middle trace) together with the simultaneously recorded field potential in the GCL (upper trace). The field potential in the GCL consists of an early negative wave with onset latency from 0.9 to 1.6 msec and duration of about 1 msec (component 1) which was followed by a large positive wave (component 2) (cf. Fig. 7B). The interval between the onset time of component 1 (dotted line in Fig. 11A) and that of the antidromic spike (upward arrow) was measured in 136 mitral cells and the frequency distribution of the time interval was plotted in Fig. 11C. As shown by the blank columns, the range was 0.0-1.0 msec (mean 0.5 ± 0.2 msec S.D., N=136) indicating that component 1 corresponds well in time with the occurrence of antidromic activation of mitral cells. This observation confirms the postulate that component 1 can be attributed to the antidromic spike potentials of mitral cell somata (Rall & Shepherd, 1968). In Fig. 11B, the superimposed tracings of the normal IPSP and the reversed IPSP produced

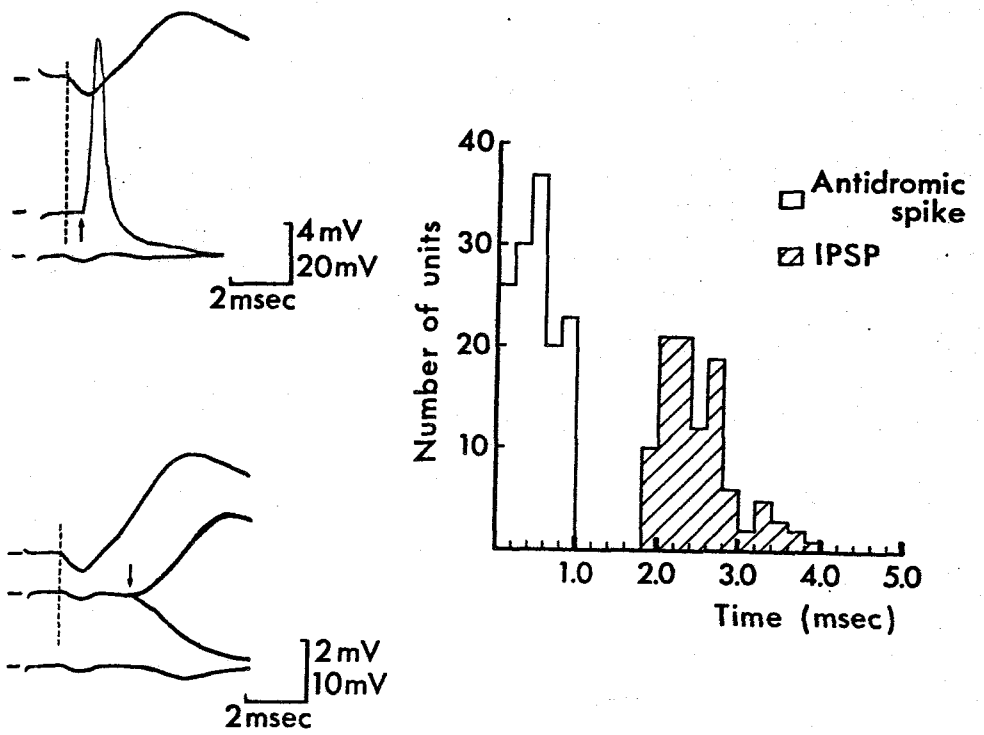


Fig. 11 Responses of mitral cells to LOT stimulation. A, Intracellulary recorded potential change in a mitral cell (middle trace) together with the field potential in the GCL (upper trace). The onset of the antidromic spike is marked by an upward arrow. B, superimposed tracings of the original hyperpolarizing IPSP in another mitral cell and the reversed IPSP during passage of the hyperpolarizing current of $2 \times 10^{-9}$A (middle traces). A downward arrow marks the diverging point of the above two traces. The dotted lines mark the onset of the component 1 of the field potential in GCL in A and B. The lower traces in A and B show the extracellular field potential recorded just outside of the impaled cell. C, Frequency distribution of the time interval between onset of component 1 and that of the antidromic spike (blank columns) or the IPSP (shadowed columns). In this figure and Fig. 6, 7, 8 and 9, upper voltage calibrations are for the field potentials in the GCL. Lower ones are for intracellular potentials and extracellular potentials just outside the impaled cells.

by application of the hyperpolarizing current (middle traces) are shown together with the field potential in the GCL (upper trace). The onset time of the IPSP was determined as the divergence point of these two tracings (marked by an downward arrow). When hyperpolarizing current injection was not successful in reversing the polarity of the IPSPs, the onset time was determined as the divergence point of the superimposed tracings of the hyperpolarizing IPSP and the extracellular field potential recorded just outside of the cell. The onset latency thus measured ranged from 3.0 to 5.5 msec (mean 3.9 ± 0.6 msec S.D., N=105). This latency contains, however, the conduction time of the antidromic spike from the stimulating site along the mitral cell axon to the soma of the mitral cell. This conduction time had considerable variation from experiment to experiment, because of difference in the distance from the stimulating to the recording site, and also because of the relatively slow conduction velocity of mitral cell axons (about 10 m/sec; Mori & Takagi, unpublished observation). In order to exclude this conduction time, the interval between the onset time of the component 1, which signals the arrival of the antidromic spike in the somata of the mitral cells with fastest axonal conduction velocities, and the onset time of the IPSP elicited by supramaximal LOT stimulation was measured. This time interval ranged from 1.8 to 3.9 msec in 102 mitral cells (mean 2.4 ± 0.4 msec S.D.) (shaded columns in Fig. 11C), indicating that mitral cell IPSPs are not produced monosynaptically, but there may be inhibitory interneurons responsible for the IPSPs. As will be shown later in Fig. 13, the onset latency of the mitral cell IPSP was progressively decreased as the intensity of LOT stimulation was increased. This also suggests that interneurons may be interpolated in the inhibitory pathway.

Responses of GCL neurons to LOT stimulation

When a microelectrode was in the GCL, it often penetrated cells whose responses to the LOT stimulation were entirely different from those of mitral cells. Many of the recordings from these GCL cells showed an element of damage due to micropipette penetration as evidenced by a rapid decrease in the resting membrane potential. The following observations were derived from comparatively stable recordings from 63 GCL cells with resting membrane potentials from -40 to -64 mV. An example of the responses of a GCL cell is shown in Fig. 12A(b) together with the simultaneously recorded field potential in the middle area of the GCL (a). Supramaximal

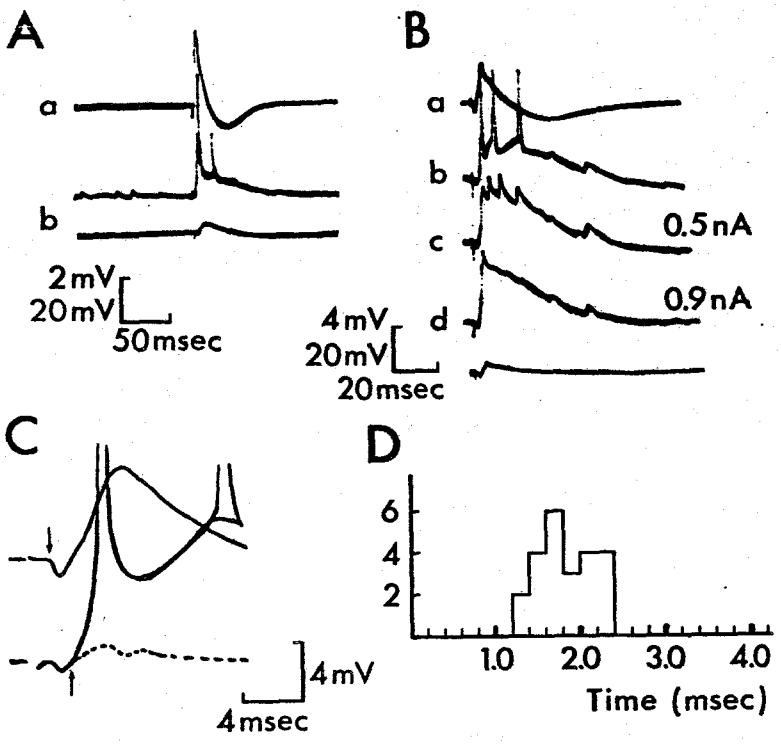


Fig. 12 EPSPs in GCL cells produced by the LOT stimulation. A, Intracellular potentials in a GCL cell (b) together with the simultaneously recorded field potential in the middle area of the GCL (a). B, Changes in the intracellular potentials in another GCL cell produced by the application of hyperpolarizing current. EPSPs and superimposed spikes were induced by supramaximal LOT stimulation in (b). The simultaneously recorded field potential in the middle area of the GCL is shown in a. Hyperpolarizing current of $0.5 \times 10^{-9}$A and $0.9 \times 10^{-9}$A was applied in c and d respectively. The lowest traces in A and B are the field potentials taken just after withdrawal. C. Superimposed tracings of the intracellular and just extracellular (interrupted line) recordings from the other GCL cell (lower traces) together with the field potential in the middle area of the GCL (upper trace). Upward arrow indicate the diverging point of the above two traces. Hyperpolarizing current of $0.2 \times 10^{-9}$A was applied in order to increase the amplitude of the EPSP. D, Frequency distribution of the time interval between onset of the component 1 and that of the EPSP in GCL cell. Spikes retouched.

LOT stimulation elicited a slow depolarization with superimposed spikes. This depolarization corresponded in time to component 2 of the GCL field potential although the depolarization lasted longer than component 2. Such a depolarizing responses was a common feature of GCL cells and no antidromic spikes were recorded from them following LOT stimulation.

Fig. 12B are the records from another GCL cell showing a depolarization of about 14 mV amplitude and 60 msec duration with three superimposed spikes (b). When a hyperpolarizing current of 0.5 nA was applied intracellularly (c), the amplitude of the depolarization increased to about 20 mV, indicating that this depolarization is not produced by a disinhibitory mechanism but rather by an activation of the excitatory synapses on the GCL cell. It can also be seen in (c) that the full spikes were blocked and only the partial spikes remained. Increase of the hyperpolarizing current to 0.9 nA (d) augumented the amplitude of the excitatory postsynaptic potential (EPSP) and blocked the partial spikes except the first one.

In Fig. 12C, the EPSP was recorded together with the field potential in the middle area of GCL with faster sweep speed in order to measure the time interval between the onset of component 1 (downward arrow) and the onset of the EPSP (upward arrow). As shown in D, the time interval ranged from 1.2 to 2.3 msec (mean 1.8 $\pm$ 0.3 msec S.D., N=23) indicating that the onset of the EPSP in GCL cells is about 0.6 msec earlier than that of the IPSP in mitral cells (cf. Fig. 11).

Dendrodendritic synaptic pathways

It has been suggested that granule cells are the inhibitory interneurons mediating mitral cell inhibition (e.g. Shepherd, 1963) deep in the olfactory bulb. Furthermore, Rall & Shepherd (1968) postulated that antidromic activation of mitral cell dendrites cause synaptic excitation of the peripheral processes of granule cells through mitral-to-granule dendrodendritic excitatory synapses, and that component 2 of the field potential is produced by the flow of extracellular current from the deep dendrites of the granule cells radially outward to the synaptically depolarized peripheral processes of the granule cells in the EPL. If the above hypotheses are corect, the EPSP of the granule cell and component 2 of the field potential in the GCL should show a parallel behavior under all conditions and both of them should have a positive correlation with the IPSP in the mitral cell.

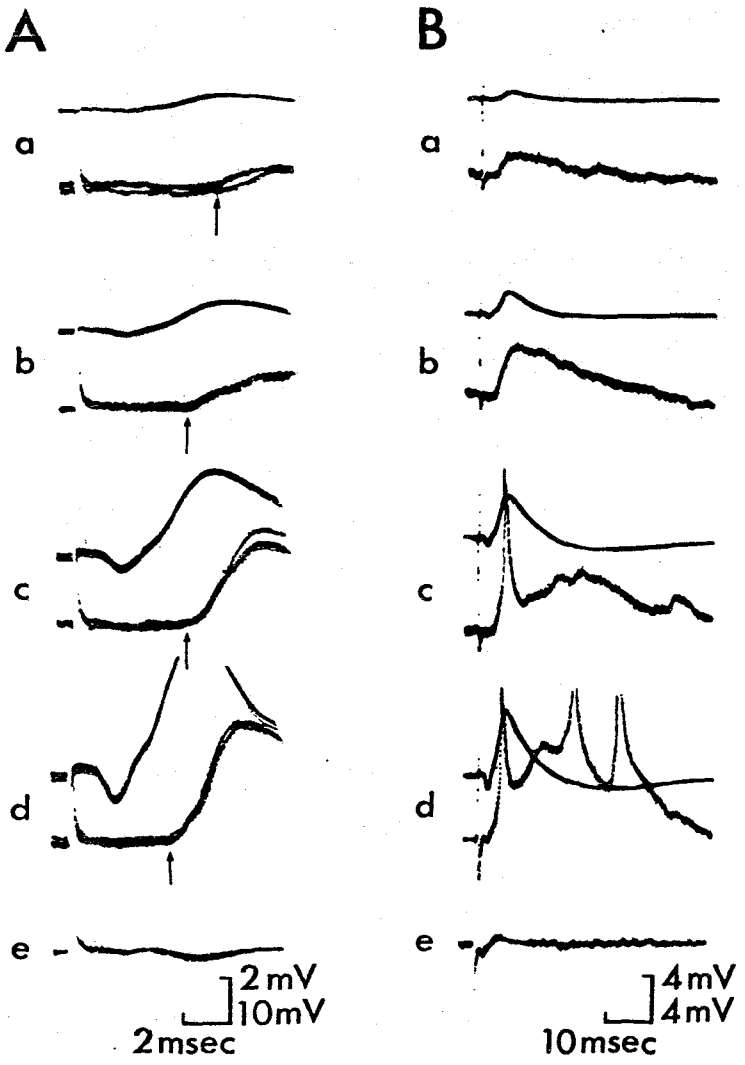


Fig. 13 Comparison of intracellular potentials and field potentials elicited by LOT stimulations at various intensites. A, a-d, Reversed IPSPs in a mitral cell (lower traces) together with the simultaneously recorded field potentials in the middle area of GCL (upper traces). Hyperpolarizing current of about 5 x $10^{-9}$A was applied internaly throughout these recordings. The onsets of the reversed IPSPs were indicated by the upward arrows. e, Extracellular field potential recorded just after withdrawal. B, a-d, EPSPs in a GCL cell (lower traces) together with the field potential in the middle area of GCL (upper traces). e, Extracellular field potential recorded just outside of the cell. The stimulus intensities were indicated by the multiples of the threshold strength (T) for eliciting the component 2 the field potential in the GCL. Spikes retouched.

In order to test the above hypotheses two experiments were performed. First the intensities of LOT stimulation were graded while the field potential in the GCL and the synaptic potentials in the mitral or GCL cells were recorded simultaneously. Graded stimulation of the LOT caused graded IPSPs in the mitral cells and graded field potentials in the GCL. An example of simultaneous recordings of them is shown in Fig. 13A, where the IPSPs were reversed in polarity by the hyperpolarizing current. The threshold strength for eliciting the field potential in the GCL was almost equal to that for eliciting the mitral cell IPSP (a). As LOT stimulation was strengthened the amplitude of the IPSP increased in parallel with that of the field potential (both component 1 and 2). It can also be seen in Fig. 13A that the latency of the IPSP progressively decreased (from 5.8 msec to 4.2 msec in this figure) as the stimulus intensity was increased. Not only is the amplitude of the IPSP in the mitral cell correlated with that of the field potential in the GCL, but also the amplitude of the EPSP in the GCL cell. This is demonstrated in Fig. 13B, where the upper traces show the field potentials in the GCL and the lower traces are intracellular records from a GCL cell. As the intensity of LOT stimulation was gradually increased from subthreshold strength, the field potential and the EPSP appeared simultaneously at an almost equal threshold intensity (a) and then varied together in amplitude (b-d).

The second experiment to test the hypothesis of the dendrodenritic pathways for activation of the granule cells and subsequent inhibition of mitral cells was to use paired LOT volleys of equal intensity. A conditioning LOT stimulation elicits large IPSPs in the mitral cells, which would prevent test antidromic spikes from invading the mitral cell somata or dendrites. If the granule cells are activated through the mitral-to-granule dendrodendritic pathway, conditioning LOT volleys would thus depress the test EPSPs in the granule cells. On the other hand, if the granule cells are activated through an axon collateral pathway, the test EPSPs in granule cells should not be depressed by the conditioning LOT stimulation because the axon collateral pathway would not be blocked by the IPSPs in the mitral cell somata or dendrites. In most of the GCL cells (23 out of 26 cells), the EPSP responses to test LOT stimulation were markedly depressed by the conditioning LOT stimulation, as shown in Fig. 14A (middle trace). In Fig. 14B, the relative amplitudes of the test

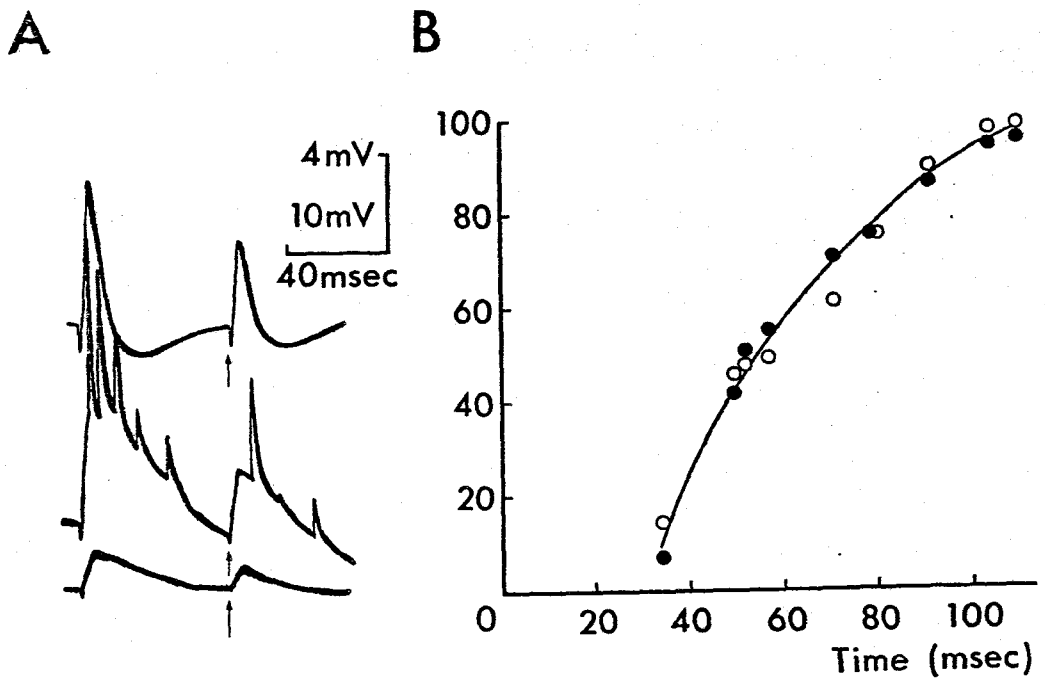


Fig. 14 Intracellular records from a GCL cell. A, EPSPs and superimposed partial spikes evoked by the paired LOT shocks of equal intensity (middle trace) together with the simultaneously recorded field potential in the middle area of the GCL (upper trace). The lowest trace shows the extracellular field potential recorded just after withdrawal. The time of test stimuli was indicated by the upward arrows. B, Plot of relative amplitudes of the EPSPs in the same cell as in A (open circles) and field potentials in the GCL (filled circles) elicited by the test LOT volley (ordinate) against the interval between the conditioning and test stimulus (abscissa).

LOT-evoked EPSPs in the GCL cells (indicated by open circles) and of the test LOT-evoked field potentials (component 2) in the GCL (indicated by filled circles) following conditioning LOT stimulation are plotted against the interval between the conditioning and test stimulus. In this experiment, the intensity of conditioning stimulation was equal to that of the test stimulation. It can be seen in this figure that the depression curves have quite similar time courses.

Fig. 15A shows the mitral cell responses to paired LOT stimulation. When the interval between the conditioning and test stimulation was decreased, the antidromic spikes of the test volleys were blocked and the test IPSPs were markedly reduced in amplitude which confirms Nicoll's results (1969). In B, reversed IPSPs in a mitral cell are shown together with the field potentials in the GCL elicited by the paired LOT volleys. It can be seen in this figure that the amplitudes of both the test IPSPs and the GCL field potentials were depressed in almost equal degree. The relative amplitudes of the test IPSPs (open circles) and those of the test field potentials (component 2, filled circles) were plotted against the intervals between the conditioning and test stimuli (C). As seen in C, the depression curves had similar time courses, just as those of the EPSPs in GCL cells and the GCL field potentials (Fig. 14B) under conditions of paired LOT stimuli of equal intensity. It should be noted that this depression of test LOT-evoked IPSPs were observed in all the 46 mitral cells which were examined by paired LOT volleys. These observations thus strongly support the hypothesis of the dendrodendritic pathways for activation of granule cells and subsequent inhibition of the mitral cells.

## B-3. DISCUSSION

### Mitral cell IPSPs

The present results have confirmed the previous observations that LOT stimulation causes large amplitude IPSPs in the mitral cells (Yamamoto et al. 1962; Phillips et al. 1963; Nicoll 1969; Reese & Shepherd, 1972). These IPSPs had essentially similar characteristics as the IPSPs of the other neurons i.e. they were accompanied by a conductance increase of the mitral cell membrane (cf. Nicoll, 1969) and were decreased in amplitude and then reversed in polarity by intracellular application of hyperpolarizing current. A characteristic feature of the mitral cell IPSPs is their long

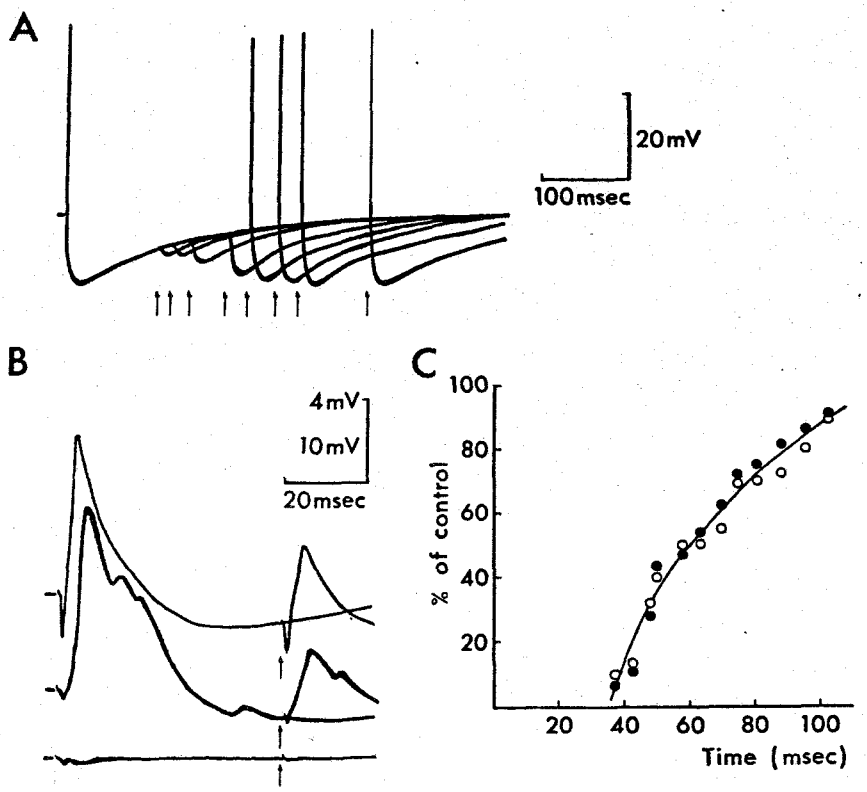


Fig. 15 Intracellular records from mitral cells. A, Paired shocks of equal intensity were delivered to the LOT at various intervals between conditioning and test stimulus. Eight traces of responses were superimposed. B, Reversed IPSPs elicited by the paired LOT shocks of equal intensity during hyperpolarizing current application ($4 \times 10^{-9}$A) (middle traces) together with simultaneously recorded field potential in the GCL (upper traces). K-1 electrode. Two traces with and without test stimuli were superimposed. The lowest trace indicate the extracellular field potential recorded just after withdrawal. The times of test stimulus were indicated by upward arrows in A and B. C, plot of relative amplitudes of the reversed IPSPs (open circles) and field potentials in the GCL (filled circles) evoked by the test LOT stimulation (ordinate) against the interval between the conditioning and test stimulus (abscissa). From the same cell as in B.

duration, which is comparable to those of hippocampal pyramidal cells (e.g. Kandel & Spencer, 1961) cortical pyramidal cells (e.g. Phillips, 1959) and thalamic neurons (e.g. Purpura & Cohen, 1962). It should also be noted that the conductance increase of the mitral cell membrane lasted up to 100 msec during the IPSPs when supramaximal stimulation was applied to the LOT.

An asymmetrical reversal of the IPSPs by intracellular injection of hyperpolarizing current has been observed in cerebellar Purkinje cells following parallel fiber stimulation (Eccles, Llinás & Sasaki, 1966). This has been ascribed to the distribution of inhibitory synapses both on the somata and dendrites of the Purkinje cell. In the present experiment, the reversed IPSPs of the mitral cells produced by hyperpolarizing current application were found quite asymmetrical in shape compared to the original IPSPs, the time course of the former being always much shorter than that of the latter. If as seems likely (see below) the inhibitory synapses on the mitral cell are not localized on the soma but distributed widely both on the soma and dendrites, then the asymmetrical reversal of the IPSPs may be interpreted as follows; the hyperpolarizing current application may produce a non-uniform change in the membrane potential of the mitral cell. Thus, the IPSPs produced by the synapses located near the soma may be easily reversed in polarity by the hyperpolarizing current application because the soma is the presumed site of current injection. On the other hand, the IPSPs produced by the synapses on distal dendrites may not be reversed due to insufficient potential change of the subsynaptic membrane. Comparison of the sensitivity to an applied current between the early part and the later part of the mitral cell IPSPs suggested that the former may be mainly produced by the inhibitory synapses located on the soma or proximal dendrites while the latter by those located on the remote dendrites. It is known from a number of electronmicroscopical investigations that granule cell synapses are not localized solely on the somata of the mitral cells but distributed widely on both soma and dendrites (e.g. Price & Powell, 1970b). Most of the synapses are in fact located on mitral cell dendrites with relatively small diameters. Furthermore, neary all the synapses found on mitral cell dendrites and somata are reciprocal synapses with the gemmules of granule cell peripheral processes, except in or around the glomerular region (Price & Powell, 1970b; Reese & Shepherd, 1972). Using immunocytochemical methods, it has also been

reported that glutamate decarboxylase (GAD), the enzyme that synthesizes the neurotransmitter γ-aminobutyric acid, is located in the gemmules of granule cells and that, in some instances, the GAD-positive gemmules appeared to line up adjacent to the secondary dendrites of the mitral cell (Ribak, Vaughn, Saito, Barber & Roberts, 1977).

Responses of granule layer cells to LOT stimulation

According to histological studies, there exist two types of neuronal somata in the GCL; many granule cells (cf. Fig. 7B) and a smaller number of short-axon cells. Thus, microelectrodes may encounter short-axon cells as well as granule cells. If the short-axon cells receive excitatory inputs from axon collaterals of the mitral cells or centrifugal fibers running in the LOT, they may also show EPSPs following LOT stimulation. Because of the axon collateral pathway (or centrifugal fiber pathway), the test LOT-evoked EPSPs in these short-axon cells should not be depressed by the conditioning LOT stimulation. In fact, a few GCL cells were encountered which did not show depression of test LOT-evoked responses following conditioning LOT stimulation (Type 2 GCL cell, unpublished observations). In the present study, such cells were excluded and all the GCL cells presented in this communication showed clear depression of test LOT-evoked EPSPs by the conditioning LOT stimulation (Type 1 GCL cell). Furthermore, these Type 1 GCL cells showed the following responses which would be expected in granule cells:

1) The EPSPs elicited by LOT stimulation corresponded in time with component 2 of the field potential in the GCL which appears to be produced by depolarization of granule cells.

2) When the intensity of LOT stimulation was increased from a subthreshold strength for activating mitral cell axons, the amplitude of the EPSPs progressively increased in parallel with that of the GCL field potential (both component 1 and 2).

3) The test LOT-evoked EPSPs were depressed not only by conditioning LOT stimulation but also by conditioning stimulation of the anterior commissure (Mori & Takagi, 1978a) or deep-lying structure of the prepiriform cortex (Mori & Takagi, unpublished observations), both of which cause IPSPs in the mitral cells.

4) Moreover, the depression of the test LOT-evoked EPSPs following conditioning stimulation of one of these sites is similar in time course to the depression of the component 2 of the field potential elicited by the test

LOT stimulation (cf. Mori and Takagi, 1978b).

These observations strongly suggest that the GCL cells described in this study are the granule cells which receive excitatory synaptic input from the mitral cell dendrites. Because of the lack of the morphological identification of the impaled GCL cells, we, nevertheless, cannot rule out the possibility that impaled GCL cells are a type of deep short-axon cell, if the dendrites of such cells should have reciprocal synaptic interactions with the mitral cells. However, there are as yet no anatomical reports of such reciprocal synapses between the dendrites of mitral cell and short-axon cells.

The time interval between the onset of the field potential produced by the antidromic spike potentials of mitral cell somata and the onset of the EPSPs in presumed granule cells ranged from 1.2 to 2.3 msec (mean 1.8 msec). This time interval may contain not only the synaptic delay from a mitral cell dendrite to the presumed granule cell but also the time required for active or passive depolarization of the mitral cell dendrites by the invasion of antidromic spike potentials. In the theoretical model of the mitral cell presented by Rall & Shepherd (1968), depolarization of the mitral cell dendrites occurs late in period I and during period II (see Fig. 7 of Rall & Shepherd, 1968) i.e., depolarization of the mitral cell dendrites sufficient for activation of the dendrodendritic synapse occurs presumably about 1 msec after the onset of component 1 of the field potential in the GCL. Thus the time interval between the onset of component 1 of the field potential and that of the EPSPs in presumed granule cells is compatible with the postulate that the granule cells are monosynaptically excited by the mitral-to-granule dendrodendritic synapses following LOT stimulation; the time interval may include the time for depolarization of mitral cell dendrites (about 1 msec) and that for a synaptic delay from the mitral cell dendrites to the granule cells (about 0.8 msec).

It is well known that the granule cells in the olfactory bulb are axonless neurons analogous to the amacrine cells in the retina (Cajal, 1955). The presumed granule cells in this study showed two types of spike potentials, large amplitude spikes and small partial spikes. Similar types of spike potentials have been reported in mudpuppy amacrine cells, in which large and small spikes are assumed to be somatic and dendritic impulse activity respectively (Miller & Dacheux, 1976). The large amplitude spikes in presumed granule cells are much more easily blocked

by intracellular application of a hyperpolarizing current than small spikes (cf. Fig. 12B), which suggests that the large spikes may be elicited in the somata or proximal dendrites while the small spikes may be produced in the peripheral processes. It has been suggested by Rall & Shepherd (1968) that at the dendrodendritic synapses between the mitral and granule cells, synaptic activation would not require a presynaptic action potential; the depolarization of the presynaptic membrane itself could activate the dendrodendritic synapse. Such a depolarization produced at individual gemmules would cause sufficient electrotonic depolarization in the neighbouring gemmules of the same granule cell for activating the dendrodendritic inhibitory synapses. However, it can be assumed that there would be a considerable damping of the electrotonically spread depolarization at the gemmules located far from the synaptically depolarized gemmules. The spike activity of the peripheral process of granule cells may function as a booster for depolarizing the remote gemmules of the same cell.

The excitatory nature of dendrodendritic synapses from the mitral to the granule cells and the inhibitory nature of those from the granule to the mitral cells are consistent with the morphology of the reciprocal synapses between the two cells (Fig. 7C); the mitral-to-granule synapse has an asymmetrical synaptic thickening and spheroidal synaptic vesicles, while the granule-to-mitral synapse has a symmetrical synaptic thickening and flattened vesicles (Rall et al. 1966; Price & Powell, 1970a).

## C, ALTERNATING RESPONSES AND INDUCED WAVES

A dendrodendritic reciprocal synaptic interaction between mitral cell dendrites and peripheral processes of granule cells has been postulated by the theoretical analysis of field potentials in the olfactory bulb following lateral olfactory tract (LOT) stimulation (Rall & Shepherd, 1968; Rall et al. 1966). Subsequent electrophysiological investigations (Mori & Takagi, 1977a; 1978a; Shepherd, 1969; Westecker 1970b; Nicoll, 1969) have supported this hypothesis of dendrodendritic synaptic pathways. Furthermore, it has been reported (Shepherd, 1969; Westecker, 1970a, b) that, during repetitive LOT stimulation, successively evoked potentials in the olfactory bulb showed a characteristic alternating behavior over wide simulus frequencies (Fig. 16B), suggesting the widespread synaptic interactions between mitral cells and granule cells.

In the present investigation we have obtained intracellular recordings from mitral cells and granule layer cells in order to determine, firstly, whether synaptic potentials of these bulbar neurons show similar alternating behavior during repetitive LOT stimulation and, secondly, if so, whether their behavior is explainable by the hypothesis of dendrodendritic pathways for granule cell activation and subsequent mitral cell inhibition following LOT stimulation. The results presented here are an extension of our research dealing with synaptic mechanisms controlling mitral cell excitability (Mori and Takagi, 1975; 1977a).

### C-1 METHOD

Experiments were performed on adult albino rabbits. The animals were anesthetized with urethane (ethylcarbamate) or a mixture of urethane and α-chloralose and then immobilized with gallamine triethiodide (Flaxedil) and artificially ventilated. Stimulation of LOT was performed by means of a bipolar silver electrode. Tungsten microelectrodes were used for recording the field potential in the granule cell layer (GCL) of the olfactory bulb. Intracellular records were obtained with glass micropipettes filled with 2M KCl or 2M potassium citrate and ranged in resistance from 15 to 80 MΩ. Olfactory stimuli were delivered through cannulae inserted into the nostrils.

## C-2, RESULTS

### Alternating responses

Fig. 16A shows the extracellular field potential in the GCL of the olfactory bulb elicited by a single LOT stimulation. It consists of the initial negativity (component 1) and succeeding large positivity (component 2). The distribution of the antidromically evoked field potentials at various layers in the olfactory bulb has been intensively studied (Nicoll, 1969; Phillips et al. 1963; Rall & Shepherd, 1968; Rall et al. 1966). The detailed theoretical analysis of them (Rall & Shepherd, 1968) showed that the component 1 is caused by the antidromic spike invasion to mitral cell bodies and the component 2 is best explained by a depolarization of the peripheral processes of granule cells. In agreement with previous investigations (Shepherd, 1969; Westecker 1970a, b), repetitive LOT stimulation caused the alternation of amplitudes of successively-evoked potentials (both component 1 and 2) as shown in Fig. 16B .

Mitral cells were identified by the following two criteria. Firstly, they were located in or near the mitral cell layer (which was determined by the reversal of the second negative wave of the LOT-evoked field potential to a positive wave). Secondly, they showed antidromic spike potential with latencies less than 2 msec upon LOT stimulation. The resting membrane potential of mitral cells ranged from -50 to -70 mV. Intracellular records from a representative mitral cell during repetitive LOT stimulation are illustrated in Fig. 16C-E. At low stimulus frequencies (11 cps, Fig. 16C), this cell showed an antidromic spike and a subsequent IPSP with an almost constant amplitude to each LOT shock (arrows). When the stimulus frequency was increased to 27 cps, the antidromic spike invasion was often blocked and an alternation of the IPSP amplitude was clearly seen, as shown in Fig. 16D. The complex patterns of the alternation of mitral cell IPSPs were also observed at higher stimulus frequencies (Fig. 16E). The alternating behavior of IPSPs was observed clearly in 25 out of 33 mitral cells over wide stimulus frequencies (from about 10 cps to over 60 cps).

Intracellular recording of the cells in the GCL was tried, and the recording of their responses to repetitive LOT stimulation was so far successful in only 5 cells presumably because of their small size. The resting membrane potential in these granule layer cells ranged from -48 to -64 mV. The middle trace of Fig. 17A shows a large EPSP and superimposed spikes elicited by a single LOT stimulation in one of these cells which

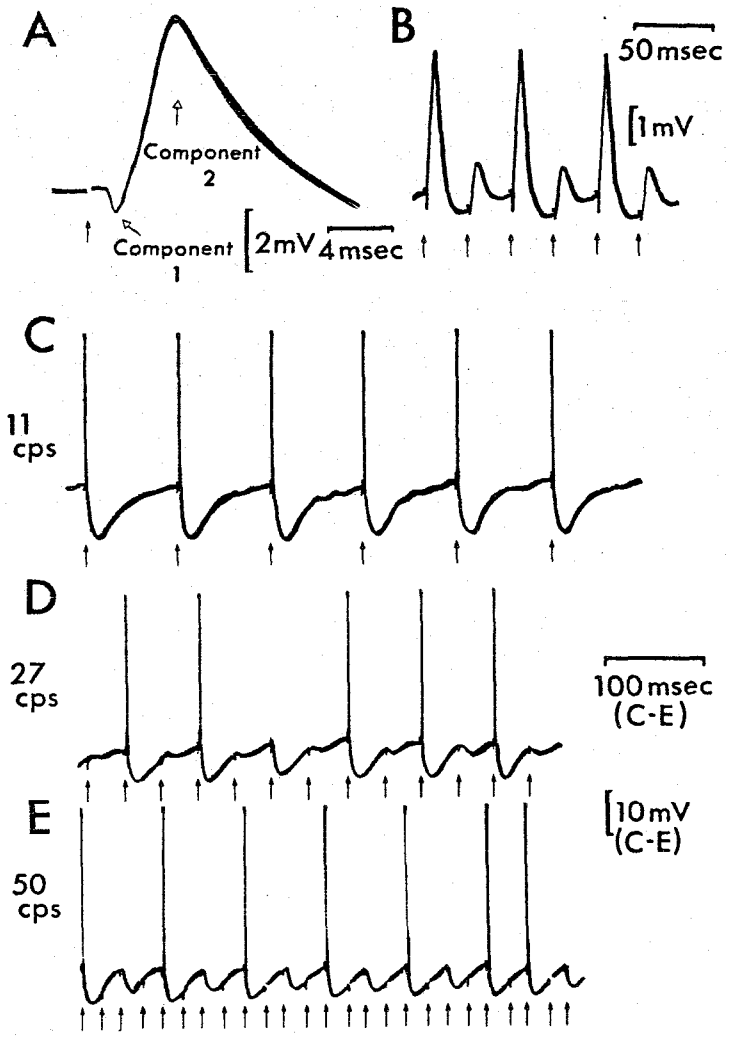


Fig. 16 Alternating responses in the olfactory bulb cells to repetitive LOT stimulation. A and B: extracellular field potential in the granule cell layer elicited by a single (A) or repetitive (B) LOT stimulation. C-E: intracellular recordings from a mitral cell (the antidromic spike potential had a latency of 1.5 msec; resting membrane potential was-- 55 mV). Stimulus frequencies were indicated at the left of each trace. The time of LOT stimulation was indicated by arrows in this figure and Fig. 2.

was located in the GCL near the ventral mitral cell layer. When repetitive LOT stimulation was applied, all the impaled granule layer cells showed alternation of the amplitude of the EPSPs. The lower trace of Fig. 17B shows such a phenomenon in the intracellular potentials of the same cell as in Fig. 17A. The amplitude of the field potential just outside of this cell was relatively small (less than 2 mV) during repetitive (40 cps) LOT stimulation, indicating that most of the intracellular potentials were true membrane potentials. The upper trace of Fig. 17B shows the field potentials recorded simultaneously in the middle area of the GCL (In this area, much larger field potentials can be recorded than the potentials just outside of the impaled cell located in the GCL near the mitral cell layer). The alternating behavior of the EPSPs was found to be synchronous with that of the component 2 of the simultaneously recorded field potential. The synchronized alternation was also found between the mitral cell IPSPs and the field potentials of the granule cell layer during repetitive LOT stimulation (Fig. 17C).

## C-3 DISCUSSION

It should be noted that the alternating behavior of the antidromic spikes and the IPSPs in mitral cells and EPSPs in the granule layer cells can be explained by the hypothesis of dendrodendritic synaptic interactions between mitral and granule cells (Fig. 18). It was postulated by Rall et al.(Rall & Shepherd, 1968; Rall et al. 1966; Shepherd, 1972) that a single LOT volley causes the antidromic depolarization of mitral cell bodies and dendrites, which activates the mitral-to-granule dendrodendritic excitatory synapses (white arrows marked with E in Fig. 18). This in turn depolarizes the peripheral processes of the granule cell and activates the granule-to-mitral dendrodendritic inhibitory synapses (black arrows with I in Fig. 18). This action hyperpolarizes the mitral cells and inhibits their activity.

If we stimulate the LOT when mitral cells are hyperpolarized by a preceding LOT volley, the antidromic spikes would not be able to invade the mitral cell bodies and thus fail to depolarize the dendrites, being therefore unable to activate mitral-to-granule dendrodendritic excitatory synapses. This would cause the depression of the EPSPs in the granule cells. Because of the failure of the granule cell depolarization, the granule-to-mitral dendrodendritic inhibitory synapses would not be activated, resulting in the depression of the IPSPs in the mitral cells. Thus, the membrane potential of mitral cells may recover from hyperpolarization.

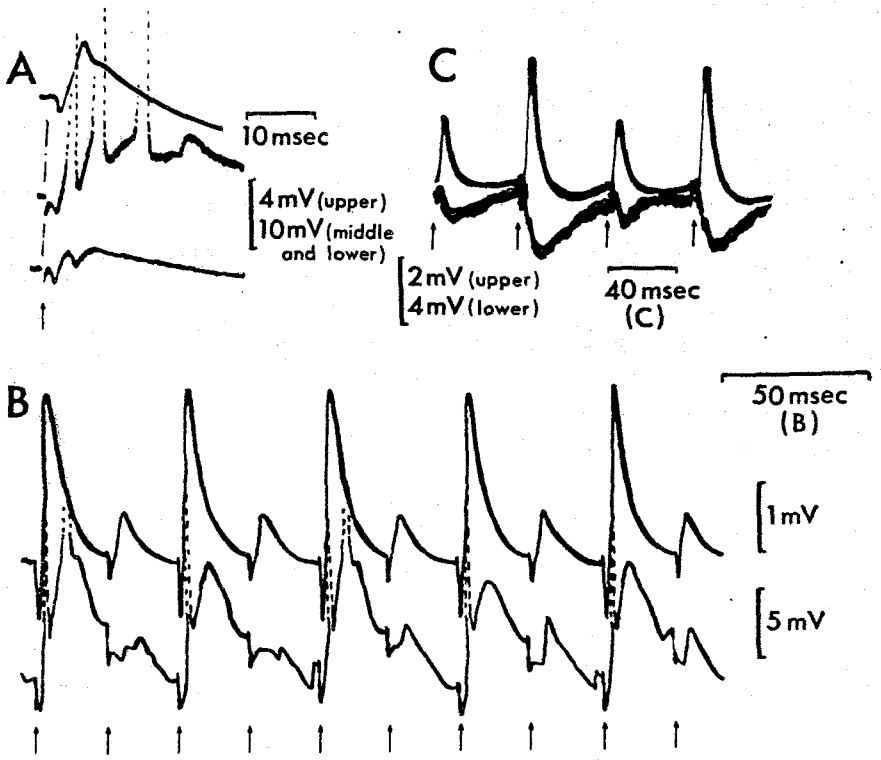


Fig. 17 Synchronized alternating behavior of intracellular potentials of a mitral or a granule layer cell and extracellular field potentials. A and B: intracellularly recorded potential from a granule layer cell with resting membrane potential of -60 mV (middle trace in A and lower trace in B) and simultaneously recorded field potentials in the middle area of the granule cell layer (upper traces). A single and repetitive (40 cps) LOT stimulation were applied in A and B respectively. Superimposed spikes (dotted lines) are seen on the intracellular potentials in A and B. The bottom trace in A shows an extracellular field potential recorded just outside the impaled cell. C: intracellularly recorded potentials from a mitral cell (lower trace) (the antidromic spike potentials had a latency of 1.9 msec; resting membrane potential undetermined). Simultaneously recorded field potentials in the granule cell layer (upper trace).

Consequently, the next LOT stimulation again causes the antidromic spike invasion to mitral cell bodies and then depolarizes the dendrites, resulting in the activation of the mitral-to-granule dendrodendritic excitatory synapses. In this way, alternation of the antidromic spike invasion and the amplitudes of IPSPs in mitral cells and those of EPSPs in granule cells may occur. The manner of the observed alternating behavior of mitral and granule layer cells in addition to the field potentials in the olfactory bulb were coincident with the above interpretation.

There are two types of neuronal somata in GCL of the olfactory bulb, many granule cells and a lesser number of deep short-axon cells (Cajal, 1955). It is unlikely that the impaled granule layer cells are the deep short axon cells which may receive excitatory input from axon-collaterals of mitral cells or centrifugal fibers running in the LOT, because the conditioning LOT stimulation always suppressed the test LOT-evoked EPSP in these granule layer cells.

Westecker (1970a, b) analyzed evoked responses in the olfactory bulb to repetitive LOT stimulation and provided the detailed experimental basis to support the hypothesis that alternating responses reflect the widespread synaptic interconnections between the mitral and granule cell dendrites, so that large numbers of mitral and granule cells undergo blockage and recovery in unison (Shepherd, 1969, 1972). Simultaneous recording of the field potential and the granule layer cell or the mitral cell potential (Fig. 17B and C) almost always showed a synchronized behavior between them during alternation. This suggests that the alternating response requires participation of large numbers of mitral and granule cells. In this context, it should be noted that mitral cells have extraordinarily long secondary dendrites (Scheibel & Scheibel, 1975) which are in contact with many granule cell peripheral processes, and that almost all the synapses found on mitral cell secondary dendrites are reciprocal synapses with the peripheral processes of granule cells (Price & Powell, 1970; Reese & Shepherd, 1972).

In conclusion, the findings of alternating behavior of olfactory bulb neurons during repetitive LOT stimulation give a further support to the hypothesis of dendrodendritic synaptic interactions between mitral cell dendrites and granule cell peripheral processes. In addition, our results of simultaneous recordings of field potentials in the GCL and the individual olfactory bulb neurons provide experimental evidence which supports the hypothesis that these synaptic interactions are quite widespread,

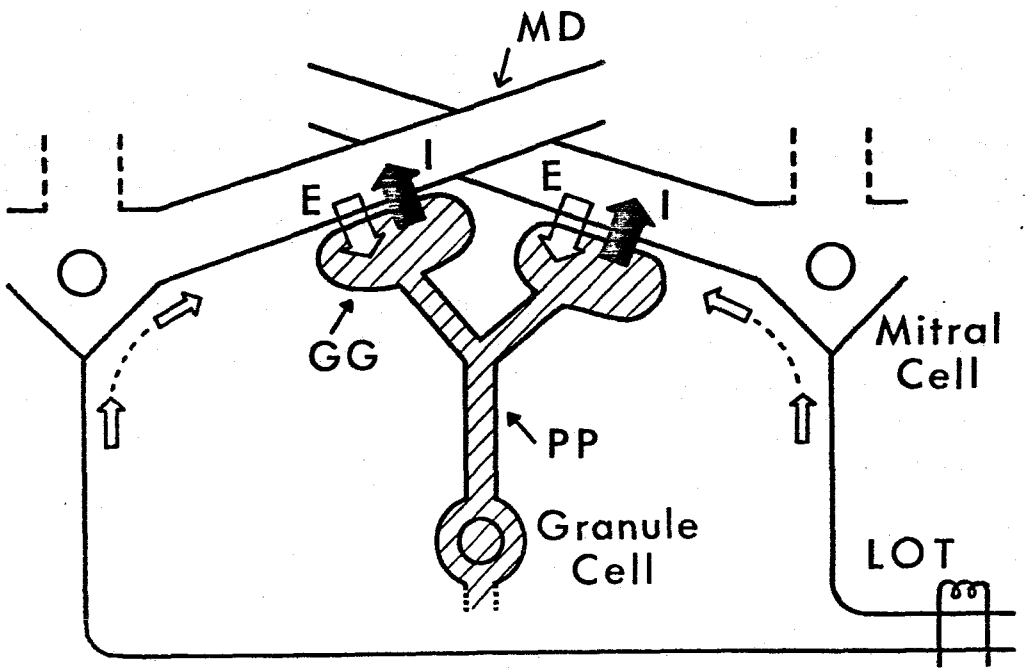


Fig. 18 Diagrammatic representation of the dendrodendritic synaptic pathway for generating the alternating response. MD, mitral cell dendrite; GG, granule cell gemmule; PP, peripheral process of the granule cell; LOT, lateral olfactory tract.

so that many mitral and granule cells undergo synchronous blockage and recovery.

## Induced waves

A characteristic feature of the electric activity in the olfactory bulb is the regular rhythmic oscillations of field potentials (the "induced waves") during olfactory stimulation (Adrian, 1950; Baumgarten et al. 1962). In intracellular recordings from mitral cells, similar rhythmic oscillations of the membrane potential were observed during odor stimulation (amyl acetate in the case of Fig. 19), as shown in Fig. 19A. In some cells, full spikes, usually one discharge per wave, were elicited rhythmically. The rhythmic oscillations of the membrane potential were observed also in the presumed granule cell (Fig. 19B). During odor stimulation, the membrane potential of this cell depolarized and oscillated sinusoidally and spikes occurred with a rhythmic discharge pattern. When tracings of the two cycles of oscillations of the induced waves in the GCL and the simultaneously recorded membrane potential in the presumed granule cell were superimposed as in Fig. 20B, a clear correlation between them could be seen. In Fig. 20, the bottoms of the induced waves in GCL were chosen as the starting points for traces, and two cycles of the induced waves from those points and corresponding intracellular potentials were traced. The membrane transients in the presumed granule cell were fairly well in phase with the induced waves in GCL, e.g., the positive wave of the induced waves in GCL was associated with the depolarization of the presumed granule cell. Since the induced waves in GCL are 180° out of phase with those in EPL (Baumgalten et al. 1962), depolarization of the presumed granule cell occurs during the negative wave in the induced waves in EPL. This suggests that during rhythmic oscillations, depolarization of the presumed granule cell may be produced by excitatory synapses located on the peripheral processes in the EPL. Figure 20A shows the superimposed tracings of the mitral cell membrane potential together with the induced waves in the GCL during olfactory stimulation. The sinusoidal oscillations of mitral cell membrane potentials were a little in advance of the induced waves in phase.

These observations may give support to the hypothesis discussed in the paper of Rall and Shepherd (1968) that the dendrodendritic interactions between mitral and granule cell populations provide a mechanism for

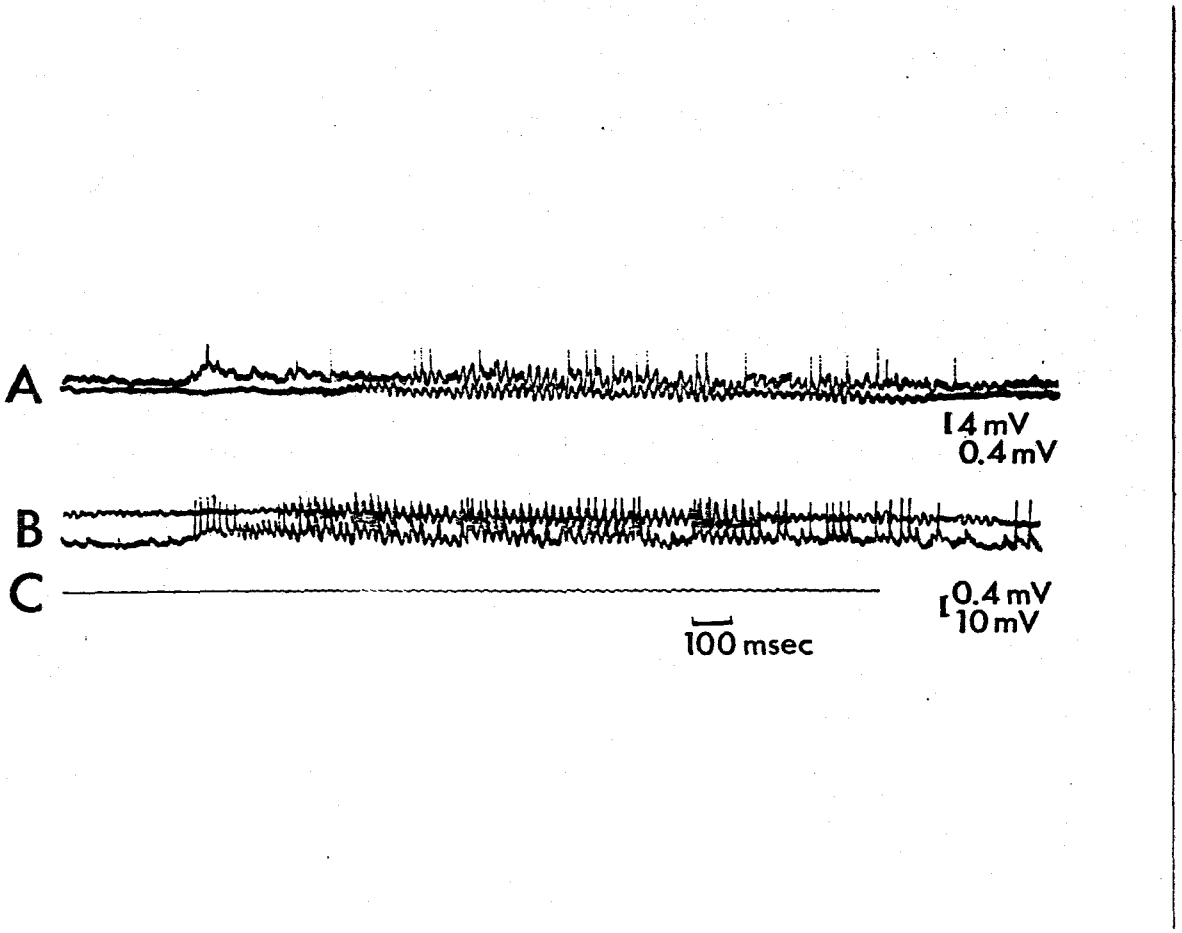


Fig. 19 Simultaneous recordings of intracellular potentials and field potentials in the GCL during odor stimulation (amyl acetate). A: intracellular responses of a mitral cell (upper trace). B: intracellular responses of a granule layer cell (lower trace). C: extracellular field potential recorded just outside the cell in B during the same odor stimulation.

generating rhythmic activity. The depolarization of many mitral cells elicits synaptic depolarization of granule cell peripheral processes through mitral-to-granule dendrodendritic excitatory pathway which causes a negative swing of induced waves in the EPL and a positive swing in GCL. The depolarized granule cells inhibit the activity of mitral cell populations by granule-to-mitral dendrodendritic inhibitory synapses, resulting in the depression of the activity of the mitral-to-granule synapses. The depression of the activity of the mitral-to-granule synapses diminishes the depolarization of granule cell peripheral processes and causes a positive swing in the induced waves in EPL and a negative swing in GCL. When the depolarization of the granule cell peripheral processes diminishes, inhibition of mitral cells by granule-to-mitral inhibitory synapses is reduced and mitral cell activities again increase. In this way, rhythmic oscillations of membrane potentials of both mitral cells and granule cells develop. The depolarization of mitral cells precedes the depolarization of granule cells, which then causes mitral cell hyperpolarization as in Fig. 20A-B. Further works based on statistical analysis on many mitral cell and granule cell populations are needed to clarify more the details of the mechanism of generating the rhythmic waves.

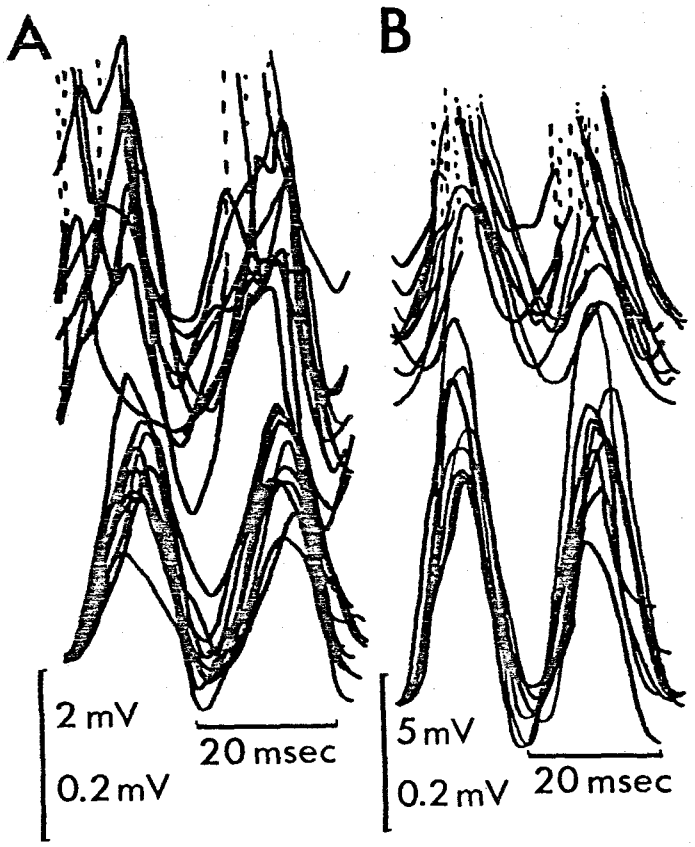


Fig. 20 Superimposed line drawings of induced waves recorded in the GCL (lower traces) and corresponding intracellular records (upper traces) from a mitral cell (A) and a granule layer cell (B).

## D, ANTERIOR COMMISSURE INPUT TO OLFACTORY BULB

In the preceeding chapter, it was shown that lateral olfactory tract (LOT) stimulation activated presumed granule cells in the olfactory bulb through mitral-to-granule dendrodendritic excitatory synapses and that mitral cell IPSPs seemed to be mediated by these granule cells (Mori & Takagi, 1978a). Since the inhibition of the mitral cell activity can be produced not only by stimulation of LOT but also by stimulation of anterior commissure (AC) (Baumgarten, Green & Mancia, 1962; Ochi, 1963; Yamamoto, Yamamoto & Iwama, 1963), it was desirable to extend the previous study of the inhibitory mechanisms controlling mitral cell activity by analysing the responses of olfactory bulb neurons to AC stimulation. In the early part of the present chapter, intracellularly recorded responses of mitral cells and of neurons in the granule cell layer (GCL cells) to AC stimulation will be described and they will be compared to their responses to LOT stimulation. In the later part, the effect of the AC stimulation upon the LOT-evoked EPSPs in GCL cells and LOT-evoked IPSPs in mitral cells will be described. The results presented here support the hypothesis that the granule cells which receive excitatory inputs from mitral cell dendrites are also activated by the AC stimulation through axo-dendritic or axo-somatic excitatory synapses located on the deep dendrites and soma of granule cells. The activated granule cells in turn inhibit the mitral cell activity through the granule-to-mitral dendrodendritic inhibitory synapses (cf. Shepherd, 1972).

### D-1, METHODS

Twenty-nine albino rabbits weighing between 1.7 to 3 kg were used. The general experimental procedures were the same as those described in the preceding chapter. In this experiment, bipolar electrodes of acupuncture needles insulated except the tips were used to stimulate the anterior commissure. These electrodes were inserted into the anterior commissure in the contralateral forebrain about 1 mm lateral from the midline. The final position of the electrode tips was such as to obtain the maximum AC-evoked field potential in the GCL of the olfactory bulb. A small electrolytic lesion was made at the site of stimulation at the end of the experiment and the location of the electrode tip was

subsequently checked histologically. The unitary and potential wave responses recorded in the olfactory bulb to AC stimulation ceased completely after sectioning the AC at the midline or in the ipsilateral forebrain caudal to the anterior olfactory nucleus.

## D-2, RESULTS

### Field potentials in the olfactory bulb elicited by AC stimulation

It has been demonstrated by several authors that stimulation of the AC elicits a large negative-going potential in the GCL of the olfactory bulb (Kerr, 1960; Ochi, 1963; Callens, 1965; Dennis & Kerr, 1968; Nicoll, 1970). Nicoll (1970) showed that this negative going potential reverses its polarity near the mitral cell layer (MCL) and becomes a smaller positive wave in the external plexiform layer. In the first step to analyse the responses of olfactory bulb neurons to AC stimulation, it was important to reinvestigate the depth profile of the AC-evoked field potential in the olfactory bulb and to compare it with the depth profile of the LOT-evoked field potential because the latter has been analysed most extensively by several investigators (Phillips, Powell & Shepherd, 1963; Rall, Shepherd, Reese & Brightman, 1966; Rall & Shepherd, 1968; Nicoll, 1969).

Fig. 21B shows the AC-evoked field potentials recorded at various depths in the olfactory bulb. In this series of experiments, the field potentials evoked by LOT stimulation were also recorded at the same depths as above (Fig. 21A). The amplitudes of the potentials were measured at the point of 6 msec after the LOT stimulation in column A (which is near the peak of component 2 of the field potential, cf. Mori & Takagi, 1978) and 25 msec after AC stimulation in column B. The depth profiles are shown graphically in Fig. 21C. As is well known (e.g. Rall & Shepherd, 1968), component 2 of the field potential evoked by LOT stimulation is a large positivity in the middle area of the GCL (g-j in Fig. 21A) and a large negativity in the external plexiform layer (EPL) (b-d in Fig. 21A). Thus, there is a flow of extracellular current from the GCL to EPL. Rall & Shepherd (1968) showed that this current flow could be reconstructed by assuming that there is a strong membrane depolarization of the peripheral processes of granule cells in the EPL: the negativity in the EPL is due to this depolarization and the positivity in the GCL is due to the extracellular current flow from deep dendrites or cell bodies of granule

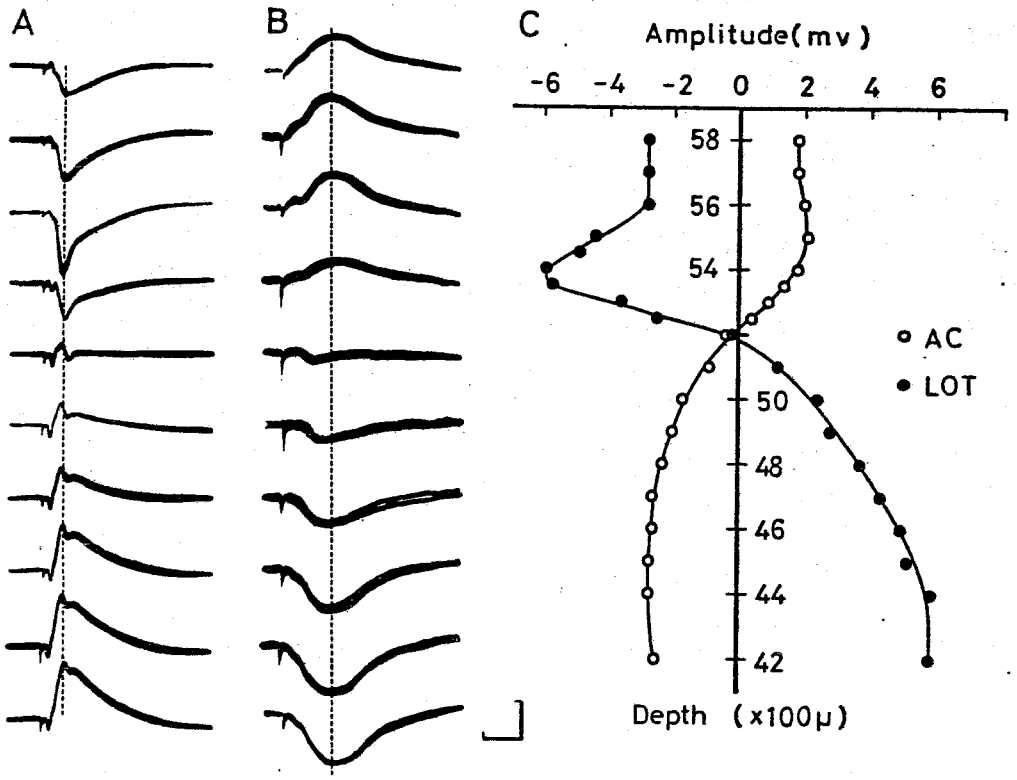


Fig. 21 A comparison of the field potentials in the olfactory bulb evoked by LOT and AC stimulation. A, Field potentials evoked by LOT stimulation were recorded at varying depths. The amplitudes of the field potentials (component 2) as measured at a latency of 6 msec (vertical broken line) are plotted against depth in C (filled circles). B, Field potentials elicited by AC stimulation. The amplitudes of the field potentials were measured at a latency of 20 msec (vertical broken line), which are also plotted against depth in C (open circles). The depth of the recording electrode in the olfactory bulb is indicated at the left of the each row. The records were obtained from the ventral side of the olfactory bulb. Vertical bar: 4 mV for A; 2 mV for B. Horizontal bar: 10 msec for A; 20 msec for B. Positivity is up.

cells to the depolarized peripheral processes of granule cells. On the other hand, the AC-evoked field potential was a large negativity in the middle area of the GCL (g-j in Fig.21B). It reversed its polarity at the MCL and became a positive wave in the EPL (b-d in Fig. 21B). This indicates a flow of extracellular current with opposite direction to that caused by LOT stimulation: a current flow from the EPL to GCL. These observations suggest that the flow of extracellular current caused by AC stimulation may be mainly produced by the depolarization of deep dendrites or cell bodies of granule cells in the GCL: the negativity in the GCL may be due to this depolarization while the positivity in the EPL may be due to the corresponding current source.

Responses of mitral cells to AC stimulation

Volleys in the anterior commissure cause a hyperpolarization of the mitral cell membrane (Yamamoto et al. 1963). Fig. 22 (a) (b) and (c) demonstrates such membrane hyperpolarizations of a cell located at the MCL which were elicited by AC stimulation with one, two and three shocks respectively. This cell was identified as a mitral cell by antidromic activation through the LOT (Fig. 22B). The latency of the hyperpolarization evoked by a single AC volley was 8 msec. In other cells, this latency ranged from 7 to 11 msec. The amplitude of the hyperpolarization increased when the additional volleys were applied at short intervals (Fig. 22Ab and Ac). In some instances, double shocks evoked hyperpolarizations in mitral cells even when the stimulus strength was weakened so that a single AC stimulation failed to elicit them. When responses to strong AC volleys (three shocks with 30 volts and 0.1 msec duration) were examined in 55 antidromically identified mitral cells, all the mitral cells showed the hyperpolarization. The resting membrane potential of these mitral cells ranged from -45 to -70 mV. As shown in Fig. 3A, the amplitude of the AC-evoked hyperpolarization was decreased and then reversed in polarity when increasing hyperpolarizing currents were applied intracellularly. This observation indicates that this AC-evoked hyperpolarization is the IPSP produced by the inhibitory synapses on the mitral cell. From the fact that the onset latencies of the IPSPs evoked in the mitral cells by AC stimulation were relatively long compared with those of the extracellular field potentials recorded in the GCL, and that a single weak shock to AC was sometimes ineffective in producing the IPSPs, it may be postulated that the IPSPs in the mitral cells are not produced monosynaptically by AC

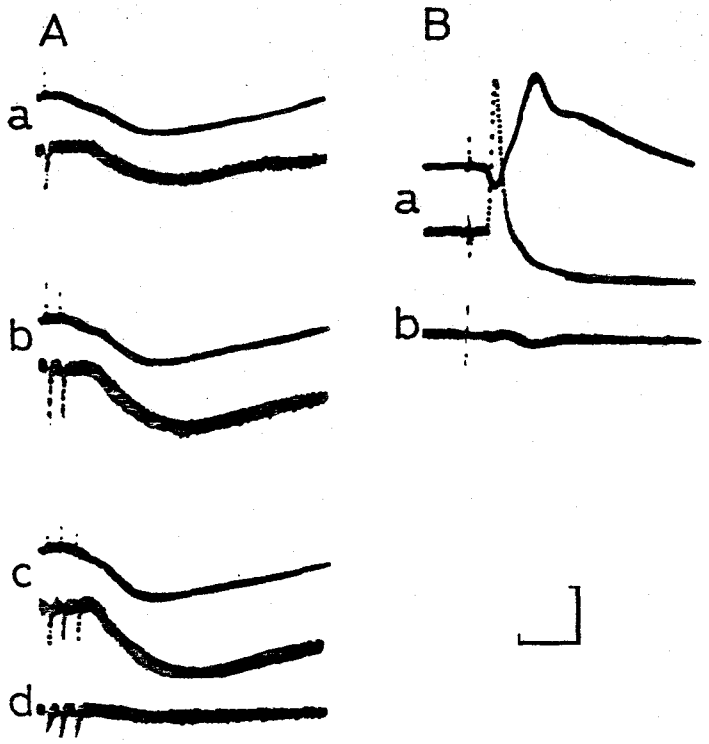


Fig. 22 Intracellular potentials of a mitral cell evoked by AC and LOT stimulation. A, Mitral cell responses to AC stimulation (lower traces of a, b and c) together with the simultaneously recorded field potential in the GCL (upper traces). In a, b and c, AC was stimulated once, twice and three times respectively. B, The response to LOT stimulation (lower trace of a) obtained from the same mitral cell as A. The upper trace of a shows the simultaneously recorded field potential in the GCL. The extracellular field potentials recorded just after withdrawal are shown in A d and B b. Vertical bar: 4 mV for uppertraces of A a, b, c and B a; 10 mV for lower traces of A a, b, c and d; 20 mV for lower trace of B a and b. Horizontal bar: 10 msec for A; 4 msec for B.

stimulation, but there may be inhibitory interneurons responsible for the AC-evoked IPSPs in the mitral cells. It can also be seen in Fig. 22A and B that the AC-evoked IPSPs have a much slower rising phase than the LOT-evoked IPSPs in mitral cells.

In Fig. 23A (b-f) are shown the comparison of the effects of internally applied currents upon the AC-evoked IPSP and the LOT-evoked IPSP in a mitral cell. In this figure the trace in b shows a response of a mitral cell to AC stimulation (indicated by three dots) and then a response to LOT stimulation (indicated by the upward arrow). When a hyperpolarizing current was applied intracellularly, the amplitude of the AC-evoked IPSP decreased in parallel with the amplitude of the LOT-evoked IPSP (c and d). Further increase of the hyperpolarizing current reversed both IPSPs into depolarizing responses (e and f). In e it can be seen that the reversal of the AC-evoked IPSP could be produced by almost the same amount of current required for reversal of the LOT-evoked IPSP. Furthermore, the reversed IPSPs elicited by AC volleys during application of hyperpolarizing current were quite asymmetrical in shape with the original hyperpolarizing IPSP (Fig. 23B) as is the case in the LOT-evoked IPSPs (Mori & Takagi, 1978a). These observations suggest that the inhibitory synapses responsible for the AC-evoked IPSP are also distributed widely on the soma and dendrites of the mitral cell. Fig. 23Ca shows the IPSP recorded in another mitral cell following AC stimulation (lower trace) and simultaneously recorded field potential in the GCL (upper trace). During this IPSP, a hyperpolarizing current pulse of 0.9 nA was applied intracellularly (Fig. 23Cc). When the voltage drop produced by this hyperpolarizing current pulse was compared with that produced by the same current pulse without conditioning AC stimulation (Fig. 23Cd), the former had a smaller amplitude and a faster time course than the latter. This indicates that the IPSPs of mitral cells caused by AC stimulation were accompanied by an increase in the conductance of the mitral cell membrane.

Responses of granule layer cells to AC stimulation

In the preceeding chapter (Mori & Takagi, 1978a) it has been shown that type 1 GCL cells (presumably granule cells) receive an excitatory input from mitral cell dendrites. In addition to this, the analysis of the field potentials elicited by AC stimulation and of the AC-evoked IPSPs in mitral cells suggests that granule cells may receive an excitatory input from the AC. It therefore seemed important to record the responses of type 1 GCL

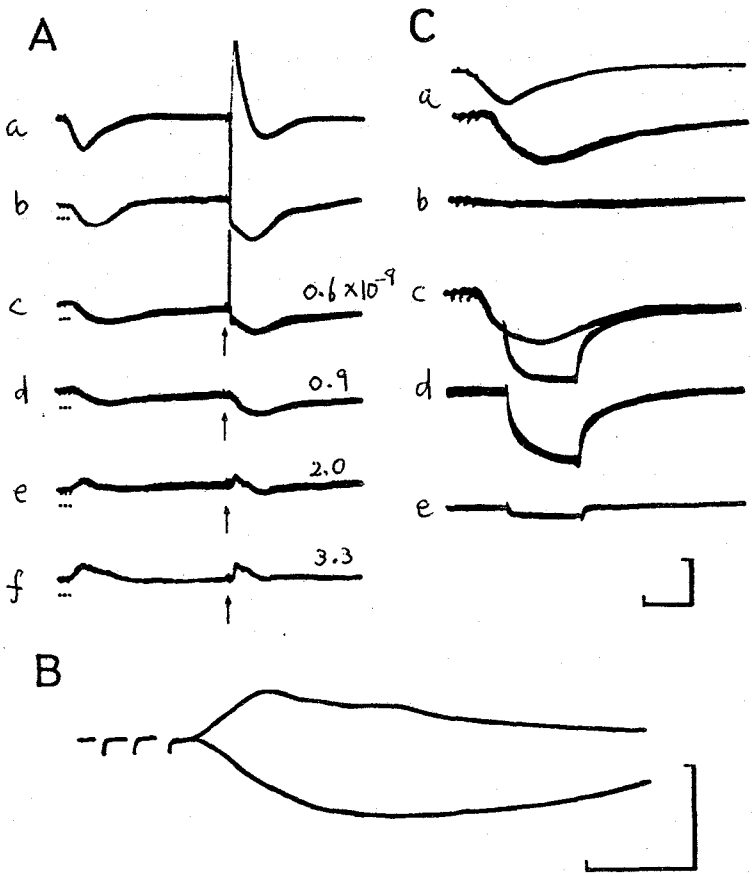


Fig. 23 Intracellular records of IPSPs from mitral cells. In A, both AC (three dots) and LOT (arrows) were stimulated with a interval of 120 msec in one sweep. Trace a shows the field potential recorded in the middle area of the GCL. The intracellular potentials from a mitral cell are shown in b-f. In c-f, hyperpolarizing currents were applied intracellularly. The amount of the applied currents is indicated on the right shoulder of each trace. B shows the superimposed tracings of the original hyperpolarizing IPSPs elicited by anterior commissure stimulation and the reversed IPSPs caused by the internal application of the hyperpolarizing currents ($3.0 \times 10^{-9}$A). C, IPSPs of another mitral cell elicited by AC stimulation (lower-trace of a) are shown together with the simultaneously recorded field potential in the GCL (uppertrace of a). The trace in b is the field potential recorded just after withdrawal of the microelectrode. In C, a hyperpolarizing current pulse of $9 \times 10^{-10}$A was sometimes applied through the recording electrode during the IPSP. Control intracellular and extracellular voltage drop produced by the same current pulse without conditioning AC stimulation are shown in d and e respectively. Vertical bar in A; 4 mV for a and 20 mV for b-f. Horizontal bar in A; 40 msec. Vertical bar in B; 10 mV. Horizontal bar in B; 10 msec, Vertical bar in C; 4 mV for upper trace of a, 10 mV for lower trace of a and b-e. Horizontal bar in C; 20 msec. Spikes retouched.

cells to AC volleys in order to elucidate whether or not there is convergence on the same type 1 GCL cells of excitatory inputs from both the mitral cell dendrites and the AC. Fig. 24C shows an EPSP in a type 1 GCL cell elicited by LOT stimulation. This cell was classified as a type 1 GCL cell because EPSPs in this cell evoked by test LOT stimulation were markedly depressed by the conditioning LOT stimulation (cf. Mori & Takagi, 1978a). When a single volley was applied to the AC, this cell showed an EPSP with onset latency of about 5 msec. This EPSP increased in amplitude when additional shocks were applied to AC at short intervals (Fig. 24Ab and c). Since the extracellular field potential just outside the impaled cell was large, the time course of the true membrane potential was determined by subtracting the extracellular field potential from the intracellularly recorded potential (Fig. 24B). It may be noted in Fig. 4B (and also in Fig. 6B) that the onset time and duration of the AC-evoked EPSP corresponds with those of the negative wave of the GCL field potential. The responses to AC stimulation were examined in 30 type 1 GCL cells with resting membrane potential of -40 to -64 mV and clear EPSPs were seen in 27 cells. Thus, most of the type 1 GCL cells receive excitatory inputs both from mitral cell dendrites and from the AC. It is interesting to note that AC stimulation failed to elicit spike activity in most of the type 1 GCL cells which showed an EPSP with superimposed spikes following LOT stimulation (Fig. 24 and Fig. 26).

Effects of conditioning AC stimulation upon the responses of mitral cells or GCL cells to test LOT stimulation

It was shown in the preceding chapter (Mori & Takagi, 1978a) that conditioning LOT stimulation caused the depression of test LOT-evoked EPSPs in type 1 GCL cells and test LOT-evoked IPSPs in mitral cells. These results were ascribed to the blocking of antidromic activation of mitral cell somata and dendrites by the preceding IPSPs in mitral cells which were elicited by the conditioning LOT stimulation. Since strong AC stimulation causes large IPSPs in mitral cells (cf. Fig. 22), they may also block the antidromic activation of mitral cell somata and dendrites following LOT stimulation. Thus, one might expect that conditioning AC stimulation also depresses the test LOT-evoked EPSPs in Type 1 GCL cells and test LOT-evoked IPSPs in mitral cells, if the dendrodendritic pathways should be responsible for activatation of the type 1 GCL cells and the subsequent inhibition of mitral cells. Fig. 25A shows the superimposed tracings of

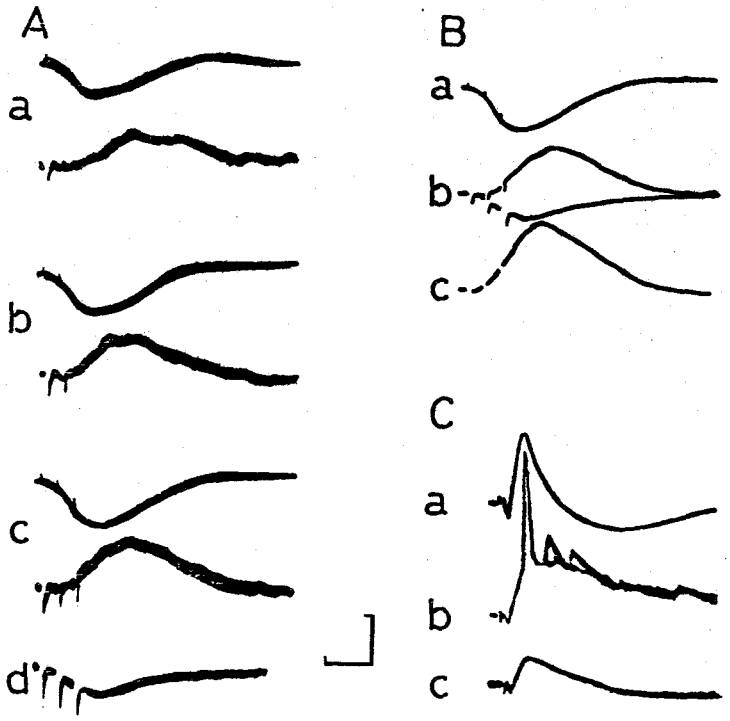


Fig. 24 Responses of GCL cells to AC stimulation. A, Intracellular potentials from a GCL cell (lower traces in a-c) and simultaneously recorded field potentials in the GCL (uppertrace in a-c). In d is shown the field potential recorded just outside the recorded GCL cell. B, a is the field potential in the middle area of GCL. Superimposed tracings of the intracellular potential from a GCL cell (upper trace) and just extracellular potential (lower trace) are shown in b. The true membrane potential (c) was obtained by subtracting the just extracellular potential from the intracellular potential. C, Response of the same GCL cell as A to LOT stimulation (b) together with the field potential in GCL (a). Extracellular field potential recorded just after withdrawal is shown in c. Vertical bar: 4 mV for upper traces of A a-c, B a and C a; 10 mV for the other traces. Horizontal bar; 20 msec for A and B; 10 msec for C. Spikes retouched.

intracellular records from a mitral cell (lower traces) together with the records of the simultaneously elicited field potentials in the middle area of GCL (upper traces). Conditioning AC stimulation (three shocks in the extreme left) caused IPSPs in the mitral cell and a negative-going extracellular potential in the GCL. Following the conditioning AC stimulation, the responses of this cell to test LOT stimulation were examined at various conditioning-test intervals. It can be seen in A that there was a clear depression of IPSPs in the mitral cell and of the field potentials in the GCL evoked by the test LOT stimulation. In C, the relative amplitudes of the conditioned test IPSPs in the mitral cell (open circles) and those of the test field potentials in the GCL (filled circles) in percent of their unconditioned control values were plotted against the conditioning-test interval. When the time course of the depressions of the test IPSPs in mitral cells and that of the test field potentials in GCL were compared with that of the IPSP evoked by a conditioning AC stimulation, clear correlation could be seen between them (Fig. 25B and C): the depressions of the test IPSPs in mitral cells and test field potentials in the GCL were maximal when the time of the test LOT stimulation coincided with the peak of the IPSP evoked by a conditioning AC stimulation. Such a depression of the test IPSPs by a conditioning AC stimulation was observed in most of the impaled mitral cells (22 out of 24 cells examined).

Fig. 26 shows an intracellular recording of a type 1 GCL cell together with the recording of the simultaneously elicited field potentials in the middle area of GCL. This cell showed a large EPSP with superimposed spikes following LOT stimulation (Fig. 26Ab) and AC stimulation also caused a large EPSP (Fig. 26Bb). Next, the effect of conditioning AC stimulation was studied upon the EPSPs caused by test LOT stimulation (C-H). As the interval between a conditioning and a test stimulation was decreased, the test EPSPs were depressed markedly (C-F). However, when the conditioning-test intervals were further decreased, as in Fig. G and H, the test EPSPs were restored and summated with the EPSP elicited by the conditioning AC stimulation. In Fig. 27B, the relative amplitudes of the EPSPs and the field potentials in the GCL elicited by the test LOT stimulation are shown in percent of their unconditioned control values against the conditioning-test interval. It can be seen in this figure that the depression of test EPSPs in type 1 GCL neurons has similar time course as that of the test field potential in the GCL. One of the possible explanations for this

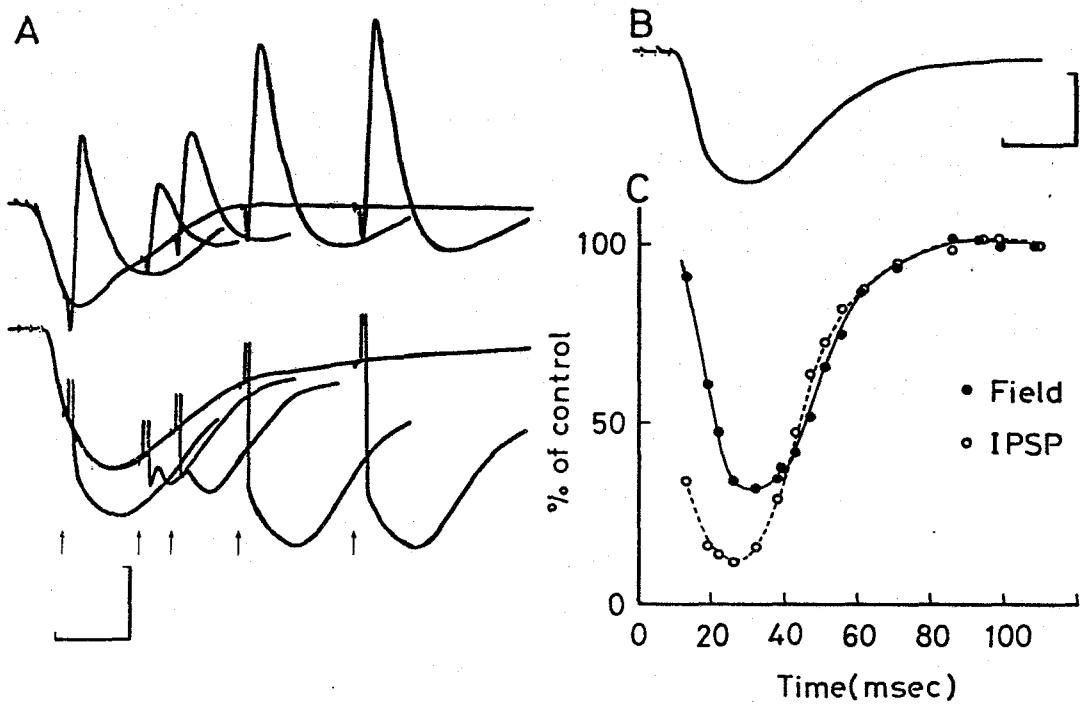


Fig. 25 The effect of conditioning AC stimulation on mitral cell IPSPs evoked by test LOT stimulation. A. Superimposed tracings of the intracellular records from a mitral cell (lower traces) and the field potentials in the GCL (upper traces). The times of the test LOT stimulation were indicated by arrows. B, The IPSP elicited by the conditioning AC stimulation is shown with the same time scale as in C. C, Plot of relative amplitudes of the mitral cell IPSPs (white circles) and field potentials in the GCL (filled circles) evoked by the test LOT stimulation (ordinate) against the interval between the conditioning and test stimulus (abscissa). From the same cell as in A. Calibrations, A, Vertical bar; 2 mV for upper traces; 5 mV for lower traces. Horizontal bar; 20 msec. B, Vertical bar; 5 mV. Horizontal bar; 20 msec.

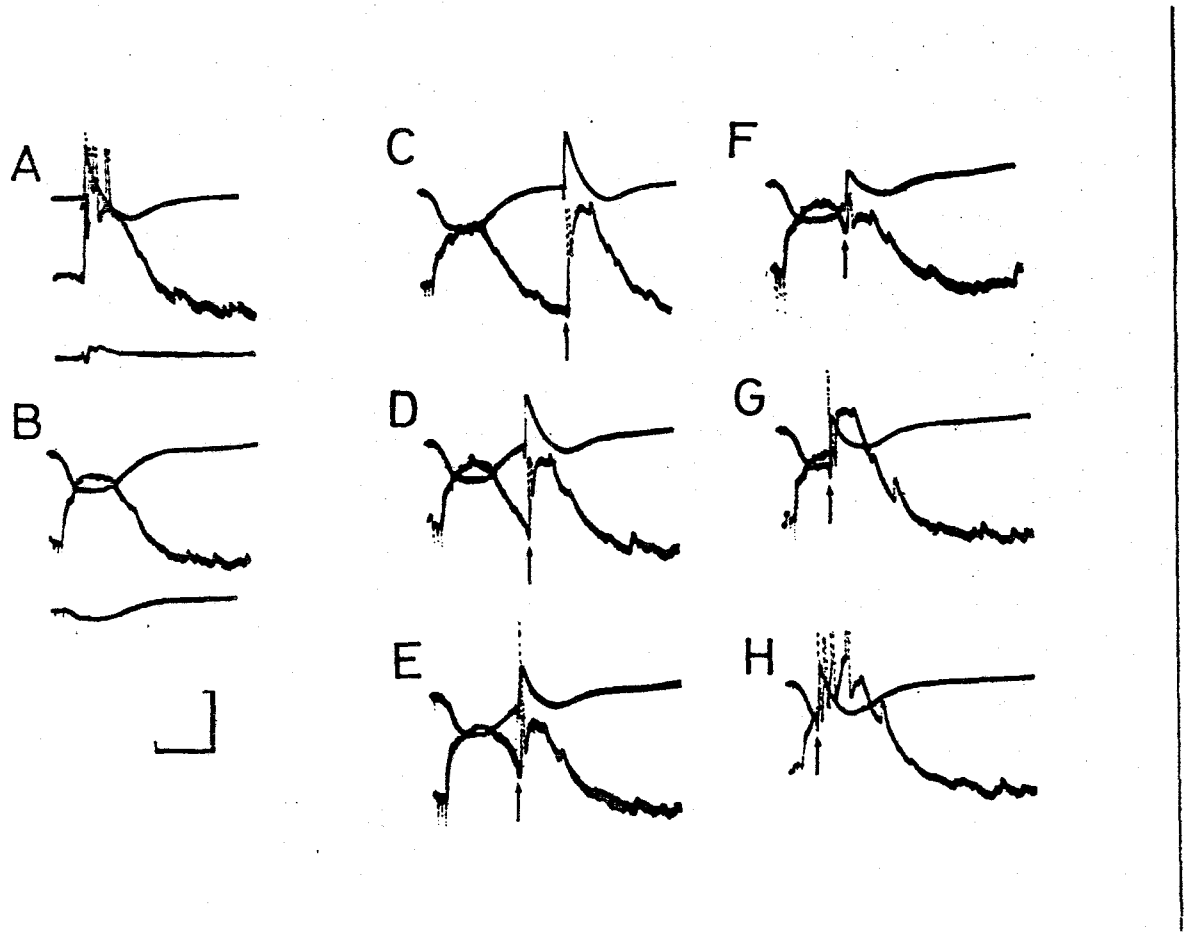


Fig. 26 The effect of conditioning AC stimulation on EPSPs in a GCL cell evoked by test LOT stimulation. A, Intracellularly recorded response of a GCL cell to LOT stimulation (b) and simultaneously recorded field potential in the middle area of the GCL (a). B, Intracellularly recorded response of the same GCL cell to AC stimulation (b) and the field potential in the GCL (a). A c and B c show the extracellular field potential recorded just outside of the impaled GCL cell. C-H, Suppression of the test LOT-evoked EPSPs in the GCL cell (lower traces) and that of the test field potential in the GCL (upper traces) by the conditioning AC stimulation. The time of test LOT stimulation was indicated by an upward arrow in each trace. Vertical bar; 4 mV for field potentials in the GCL (upper traces); 10 mV for intracellular potentials (A b, B b and lower traces in C-H) and just extracellular potentials (A c and B c). Horizontal bar; 40 msec. Spikes retouched.

depression of the test LOT-evoked EPSPs by the conditioning AC stimulation may be that it is caused by an increase in membrane conductance of the GCL neurons due to IPSPs elicited by the conditioning AC stimulation (cf. Yamamoto et al. 1963). In fact, AC stimulation sometimes elicited a hyperpolarization following large EPSPs in the type 1 GCL cells (Fig. 26Bb and Fig. 27Aa). However, the time course of the depression in Fig. 27B does not follow this hyperpolarization (compare Fig. 7Aa and Fig. 7B). Furthermore, strong conditioning AC stimulation nearly completely depressed the test LOT-evoked EPSPs in type 1 GCL cells (Mori & Takagi 1977a). This observabion cannot be explained by a conductance increase of the postsynaptic membrane because there would have to be infinite conductance in order to depress the test LOT-evoked EPSPs completely. On the other hand, when the plot of the depression of the test LOT-evoked EPSPs (Fig. 27B) and the shape of the AC-evoked IPSPs in mitral cells are compared, it can be seen that they have similar time courses. For example, in the case of Fig. 27B, the amplitudes of both test LOT-evoked EPSPs in the GCL cell and the test field potential in the GCL decreased maximally with conditioning-test interval of 40- to 60- msec. At this time, the IPSPs elicited in many mitral cells by AC stimulation were also maximal in amplitude, if the stimulus intensity was equal to that used for the conditioning AC stimulation in Fig. 27B. Though such a comparison was obtained in only 5 cases, the time course of the depression of test LOT-evoked EPSPs in type 1 GCL cells was similar to that of the AC-evoked IPSPs in mitral cells in all cases. These results are in good agrement with the hypothesis that IPSPs in mitral cells elicited by conditioning AC stimulation block the antidromic activation of mitral cell somata or dendrites and thereby prevent the activation of mitral-to-granule dendrodendritic excitatory synapses, resulting in the depression of test LOT-evoked EPSPs in granule cells and test LOT-evoked IPSPs in mitral cells (cf. Nicoll, 1969).

## D-3, DISCUSSION

### Properties of IPSPs in mitral cells elicited by AC stimulation

In nearly all mitral cell recordings, stimulation of the anterior commissure showed (possibly disynaptic and polysynaptic) IPSPs. These IPSPs showed the following characteristics as compared with LOT-evoked IPSPs;

I. The AC-evoked IPSPs had a much slower rising phase than the LOT-evoked IPSPs.

II. Conditioning LOT stimulation had little effect on the test AC-evoked

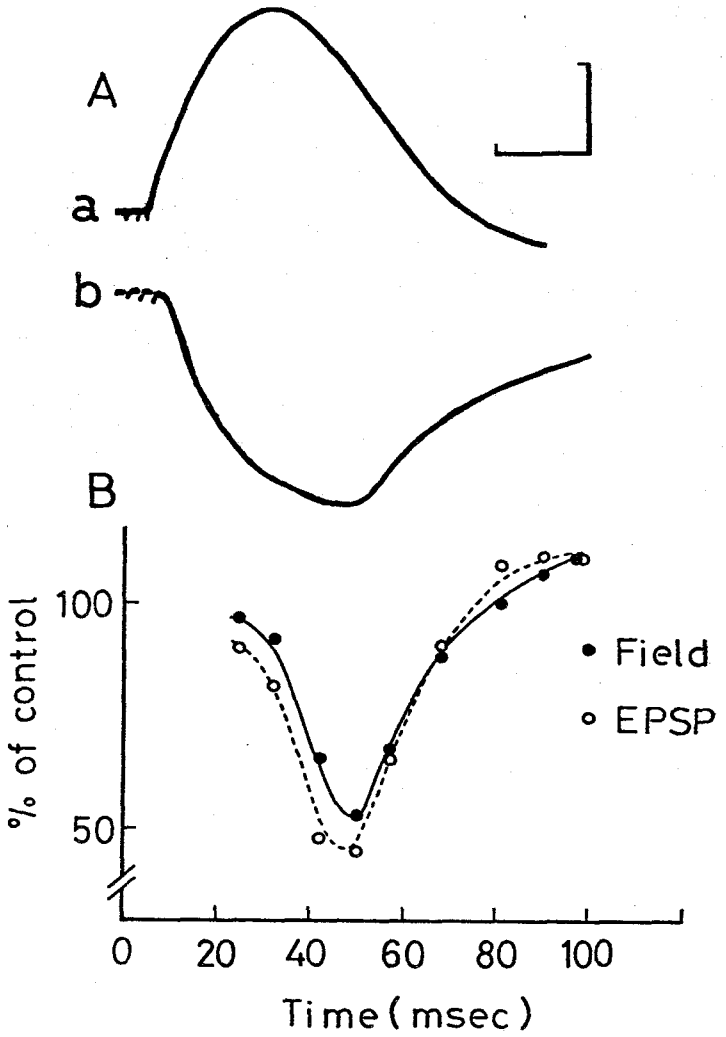


Fig. 27 The time course of the depression of the test LOT-evoked EPSPs in a GCL cell and the test LOT-evoked field potential in the GCL after a conditioning AC stimulation. A, An intracellular response of the same GCL cell as in Fig. 6 (a) and that of a mitral cell (b) to AC stimultation with the same time scale as in B. Both of them were recorded in the course of a single microelectrode penetration. B, Relative amplitudes of the EPSPs in the same GCL cell as in Fig. 6 (white circles) and the field potentials in the GCL (filled circles) evoked by the test LOT stimulation after a conditioning AC stimulation are calculated and shown in percent of their unconditioned control values (ordinate). The interval between the conditioning and the test stimulations is shown in abscissa. Vertical bar; 5 mV. Horizontal bar; 20 msec.

IPSPs, while it markedly depressed the test LOT-evoked IPSPs.

III. Paired or repetitive AC stimulation augmented the amplitudes of AC-evoked IPSPs, while LOT-evoked IPSPs were usually depressed by the preceding strong AC stimulation.

From electronmicroscopical observations that almost all synapses found on mitral cells (except in or around the glomerular region) are reciprocal synapses with peripheral processes of granule cells (Price & Powell, 1970c; Reese & Shepherd, 1972), and that AC fibers terminate on the granule cells (Price & Powell, 1970b), one can assume that granule cells are the inhibitory interneurons responsible for the AC-evoked IPSPs in mitral cells. If this is true, it is important to elucidate whether the granule cells are common interneurons responsible for both AC-evoked IPSPs and LOT-evoked IPSPs in mitral cells, or if there are two subgroups of granule cells, one mediating the AC-evoked IPSP, the other mediating the LOT-evoked IPSP. One of the methods to test the above alternative was to compare the sensitivity of the AC-evoked IPSPs to internally applied current with that of LOT-evoked IPSPs. If the locations of inhibitory synapses responsible for AC-evoked IPSPs on the mitral cell are quite different from those for LOT-evoked IPSPs, AC-evoked IPSPs and LOT-evoked IPSPs would be expected to show different sensitivity to the internally applied current. The AC-evoked IPSPs in mitral cells, however, had similar sensitivity as the LOT-evoked IPSPs to the internally applied current; the reversal of both of the IPSPs occured at the same time during passage of the progressively increasing hyperpolarizing current. Furthermore, AC-evoked IPSPs showed quite asymmetrical reversal during application of hyperpolarizing current, suggesting that the inhibitory synapses responsible for the AC-evoked IPSPs are also distributed widely on mitral cell soma and dendrites, just as those responsible for LOT-evoked IPSPs. These results suggest that the granule cells may be common inhibitory interneurons mediating both AC-evoked IPSPs and LOT-evoked IPSPs in mitral cells. If this hypothesis is correct, one may expect a penetrating microelectrode to encounter interneurons in the granule cell layer, which have the following characteristics. These points were inferred from the studies of the AC-evoked IPSPs and LOT-evoked IPSPs in mitral cells:

I. Monosynaptic excitation from LOT.

II. Excitation by a volley in AC.

III. The AC-evoked EPSPs have a much slower rising phase than the LOT-evoked

EPSPs.

IV. Conditioning LOT or AC stimulation markedly depresses the test LOT-evoked EPSPs.

V. Paired or repetitive AC stimulation augments the amplitude of the EPSPs.

Activation of type 1 GCL cells by AC volley

The results reported here and in the preceding chapter (Mori & Takagi 1978a) show that most of the type 1 GCL cells exhibited all the properties listed above (cf. Fig. 24 and Fig. 26). For example, excitatory input to the type 1 GCL cells from the anterior commissure was found in 27 out of 30 type 1 GCL cells. These results suggest that the type 1 GCL cells may be the granule cells which mediate both LOT-evoked IPSPs and AC-evoked IPSPs in mitral cells. Furthermore, the analysis of the field potential in the olfactory bulb elicited by AC stimulation indicates that an AC volley activates the excitatory synapses located on the deep dendrites and somata of granule cells. These conclusions are in good agreement with electronmicroscopical observations by Price & Powell (1970b), who found that the fibers of the anterior commissure terminate upon spines and varicosities of the deep dendrites and upon somatic spines of granule cells. Since the AC-evoked EPSPs in the type 1 GCL cells are long lasting, it is possible that AC stimulation causes not only monosynaptic but also disynaptic (or polysynaptic) activation of granule cells. One of the possible interneurons may be the neurons in the ipsilateral anterior olfactory nucleus because their axons enter the olfactory bulb and terminate upon the granule cells (Price & Powell 1970b) and they were activated by AC stimulation (Mori & Takagi, unpublished observations).

The neuronal pathway of mitral cell inhibition following AC or LOT stimulation

The results presented here and in the preceding chapter confirm the hypothesis proposed by Rall et al. (1966) and Rall & Shepherd (1968) that LOT-evoked IPSPs in mitral cells are mainly mediated by dendrodendritic reciprocal synapses between mitral cell dendrites and peripheral processes of granule cells. In Fig. 28 is shown a schematic diagram of the neuronal pathways of LOT-evoked and AC-evoked IPSPs in mitral cells, based largely on a comparison of the anatomical investigations (Cajal, 1955; Rall et al. 1966; Price & Powell, 1970a, b, c) and previous (Rall & Shepherd, 1968, Nicoll, 1969) and present electrophysiological investigations. According to this diagram, the pathway of mitral cell inhibition following LOT or

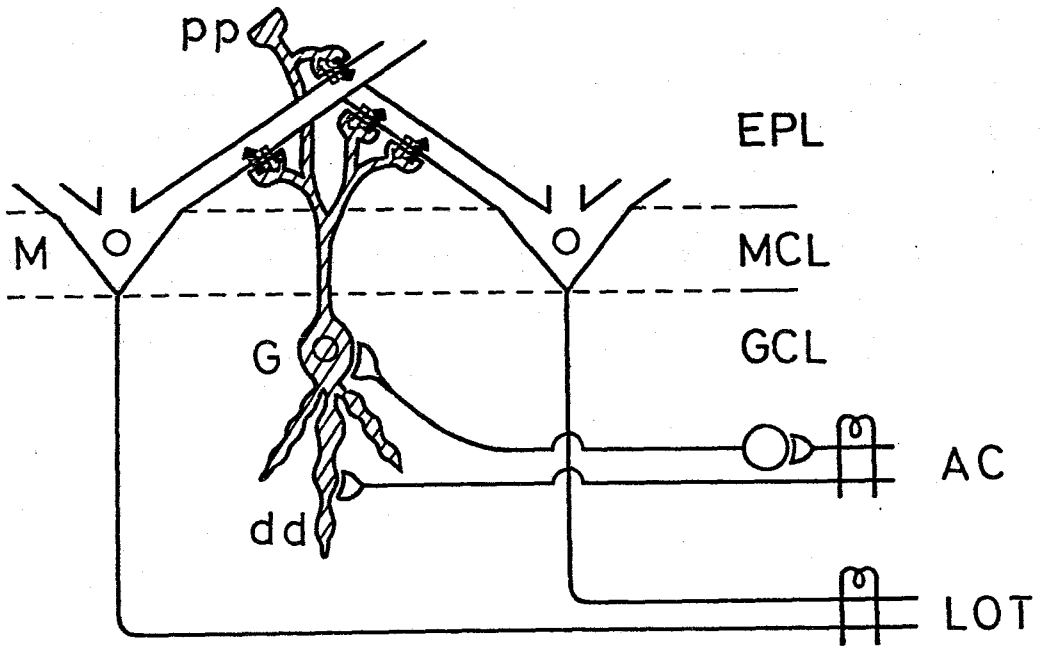


Fig. 28 Schematic diagram of the synaptic pathways in the deep layers of the olfactory bulb. EPL; external plexiform layer, MCL; mitral cell layer, GCL; granule cell layer. M; Mitral cell, G; granule cell, pp; peripheral process of granule cell. dd; deep dendrite of granule cell. AC; anterior commissure, LOT; lateral olfactory tract.

AC stimulation may be explained as follows; LOT stimulation causes synchronous antidromic activation of mitral cell somata and dendrites and activates the peripheral processes of granule cells through the mitral-to-granule dendrodendritic excitatory synapses (open arrows). The activated peripheral processes in turn hyperpolarize the mitral cell dendrites through the granule-to-mitral dendrodendritic inhibitory synapses (closed arrows). On the other hand, AC stimulation causes monosynaptic EPSPs (and possibly disynaptic EPSPs via neurons in the anterior olfactory nucleus) in the deep dendrites and somata of granule cells. The depolarization of these sites in the granule cells causes negative field potential in the GCL (Fig. 21B). The activated granule cells then inhibit mitral cell activity through the granule-to-mitral dendrodendritic inhibitory synapses (closed arrows). Since conditioning LOT or AC stimulation causes IPSPs in mitral cells, test LOT stimulation would fail to activate the somata and dendrites of the mitral cells. Thus, test LOT-evoked EPSPs in granule cells would be depressed by the conditioning LOT or AC stimulation (Fig. 26). Furthermore, the depression of the test LOT-evoked EPSPs in granule cells should have similar time courses as those of the IPSPs elicited in the mitral cells by the conditioning stimulation, because the number of mitral cells which are activated antidromically by a test LOT volley would be inversely proportional to the amplitude of IPSPs in the mitral cells caused by the conditioning volley. These explanations are in good agreement with the results reported here and in the preceding chapter.

Functional significance

The present study provides evidence for the convergence of excitatory inputs from the mitral cell dendrites and from the anterior commissure on a common inhibitory interneuron (presumably granule cell). Thus, the activities of granule cells may be regulated not only by the input from the mitral cell dendrites but also by that from the anterior commissure. This indicates that the main relay neurons (mitral cells) in the olfactory bulb are influenced by impulses in anterior commissure fibers indirectly via the granule cells. In fact, it has been reported that repetitive electrical stimulation of the anterior commissure inhibits the spontaneous discharges of mitral cells and the characteristic wave activity ("induced waves") in the olfactory bulb (Kerr & Hagbarth, 1955; Baumgarten et al. 1962; Yamamoto et al. 1963). It is interesting that the granule cells receive, in addition to the intrinsic synaptic input, various kinds of

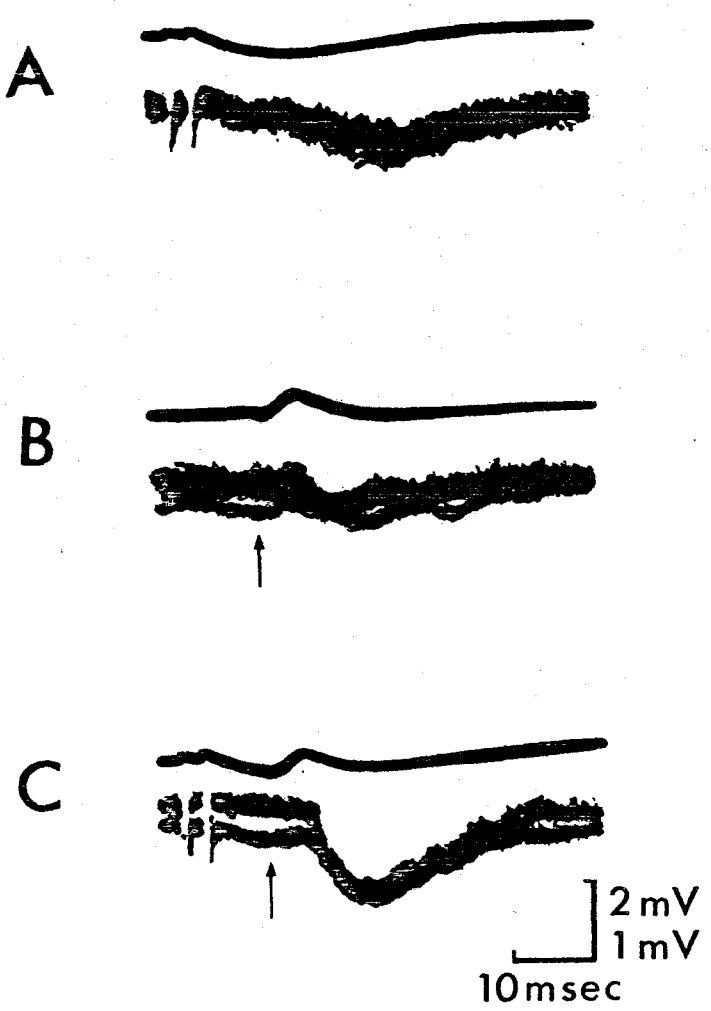


Fig. 29 Facilitation of transmission in the dendrodendritic synaptic pathway between mitral and granule cells by anterior commissure volley. Upper traces are extracellular field potential recorded in the middle area of granule cell layer. Lower traces are intracellular recordings from a mitral cell. A, Stimulation of anterior commissure (AC). B, Stimulation of lateral olfactory tract (LOT). Stimulus strength was adjusted to just above threshold for evoking the mitral cell IPSP in A and B. C, Stimulation of both AC and LOT. Arrows indicate the time of LOT stimulation.

extrinsic fiber inputs; in addition to fibers from the anterior commissure are also centrifugal fibers running in the LOT and fibers from the ipsilateral anterior olfactory nucleus (Price & Powell, 1970b). One of the possible functions of these extrinsic fiber inputs might be to modulate the dendrodendritic synaptic interactions between the mitral and granule cells. For example, when the granule cells are depolarized by AC fibers, there could be facilitation of transmission of the dendrodendritic negative feedback pathways. Thus the mitral cell activity would cause more effective lateral- and selfinhibition of the mitral cells. In fact, the amplituds of the LOT evoked IPSPs in mitral cells were augumented by weak AC stimulation as shown in Fig. 29. On the other hand, when the granule cells are not depolarized, due to the absence of AC inputs, excitatory input from mitral cell dendrites might fail to activate a large number of granule-to-mitral dendrodendritic inhibitory synapses, resulting in more limited lateral or selfinhibition of the mitral cell activity.

## E. CENTRIFUGAL EFECCTS ON OLFACTORY BULB ACTIVITY

The olfactory bulb receives various kinds of centrifugal fibers from the basal rhinencephalon (Broadwell & Jacobowitz, 1976; Dennis & Kerr, 1976; Price & powell, 1970). Electrophysiological investigations, using summed evoked potential method, demonstrated that centrifugal effects on the activity of the olfactory bulb can be elicited from an extensive portion of the basal rhinencephalon in the cat (Dennis & Kerr, 1968), in the ferret (Dennis & Kerr, 1975) and in the rat (Callens, 1965). Furthermore, it has been reported that stimulation of the centrifugal fibers from the basal rhinencephalon usually elicited a negative going potential in the granule cell layer (GCL) and that they depressed both unitary and wave activity in the olfactory bulb (Callens, 1965; Kerr & Hagbarth, 1955). Electron microscopical investigations have shown that the peripheral processes of the granule cell make reciprocal synapses with secondary dendrites of the mitral cell in the external plexiform layer (EPL) and that the granule cell receives various kinds of inputs from the telencephalon. Thus, it has been suggested that the granule cell is an interneuron interposed between the extrinsic fibers from the telencephalon and the mitral cells.

The purposes of the present investigation are:

1. to clarify the regions exerting centrifugal influences on the olfactory bulb activity in the rabbit by recording summed evoked potentials in the GCL of the olfactory bulb.
2. to analyse the intracellular responses of the mitral cells and the GCL neurons in order to clarify the modes of the centrifugal effects on the bulbar neurons.

### E-1, METHOD

#### Evoked potential study

The present experiments were performed on 42 adult rabbits, weighing 2.0-3.0 kg. The animals were anesthetized intravenously with ethyl carbamate (Urethane, 1.2g/kg), supplemental doses being administrated when necessary to maintain the surgical anesthesia. The animals were fixed in a conventional stereotaxic apparatus. The routine tracheotomy and cisternal drainage were performed to minimize the brain movement due to the cardio-vascular and respiratory influences. The rectal temperature was maintained

between 37°C and 39°C by intermittent heating. With a dental drill, craniotomy openings were made in the right side over the dorsal surface of the olfactory bulb, the ipsilateral LOT and the stimulating sites of the rhinencephalon. Then, the dura over these parts was reflected. The exposed parts of the brain were covered with mixture of vaseline and mineral oil.

Recording electrodes made of ~~300μ~~ tungsten wire were used to observe field potentials. The d.c. registances of those electrodes were between 800 kΩ and 1 MΩ. The tip of the electrode was placed at a depth in the GCL of the olfactory bulb, where the typical evoked potential could be recorded by the LOT stimulation (Fig. 30A).

Stimulations ~~were~~ was also applied throughout the rhinencephalon and the neighbouring structures, situated posterior to the coronal section A-10 in the streotaxic atlas of Fifková and Maršala (Fig. 31). A steel wire was tapered and insulated except for the tip. This was used as a monopolar stimulating electrode. For stimulation, a single shock pulse of 0.1 msec and 300 μA to 400 μA was delivered. Stimulating currents were always monitered in order to supply adequate stimuli.

The several sites, stimulation of which evoked the field potentials in the GCL, were marked by anodal currents of about 30 μA for 30 sec. At the end of each experiment, the animal was perfused at first with normal saline and then with mixture of 10% formalin and 1% potassium ferrocyanide.

Frozen sections of 50 μ thick were cut in parallel with the stimulating electrode tracks in the coronal plain, and stained by Nissl Method. The prussian blue spots were examined in the sections microscopically.

Intracellular recording

Intracellular recordings were performed in 30 rabbits.

Bipolar stimulating electrodes made of acupuncture needles (amalgam of silver, nickel and iron) were stereotaxically inserted into the LOT, the anterior commissure (AC) and the regions which seemed to exert centrifugal influences on the bulb activity. The regions were preliminary determined by the evoked potential study. A single pulse lasting 0.1 msec or a train of such pulses were used for stimulation. At the end of each experiment, stimulation sites were examined histologicaly.

For intracellular recording, glass capillary microelectrodes filled with 2M K acetate were used. The d.c. resistance ranged from 30 to 50 MΩ. In addition, a tungsten electrode was placed in the GCL of the olfactory

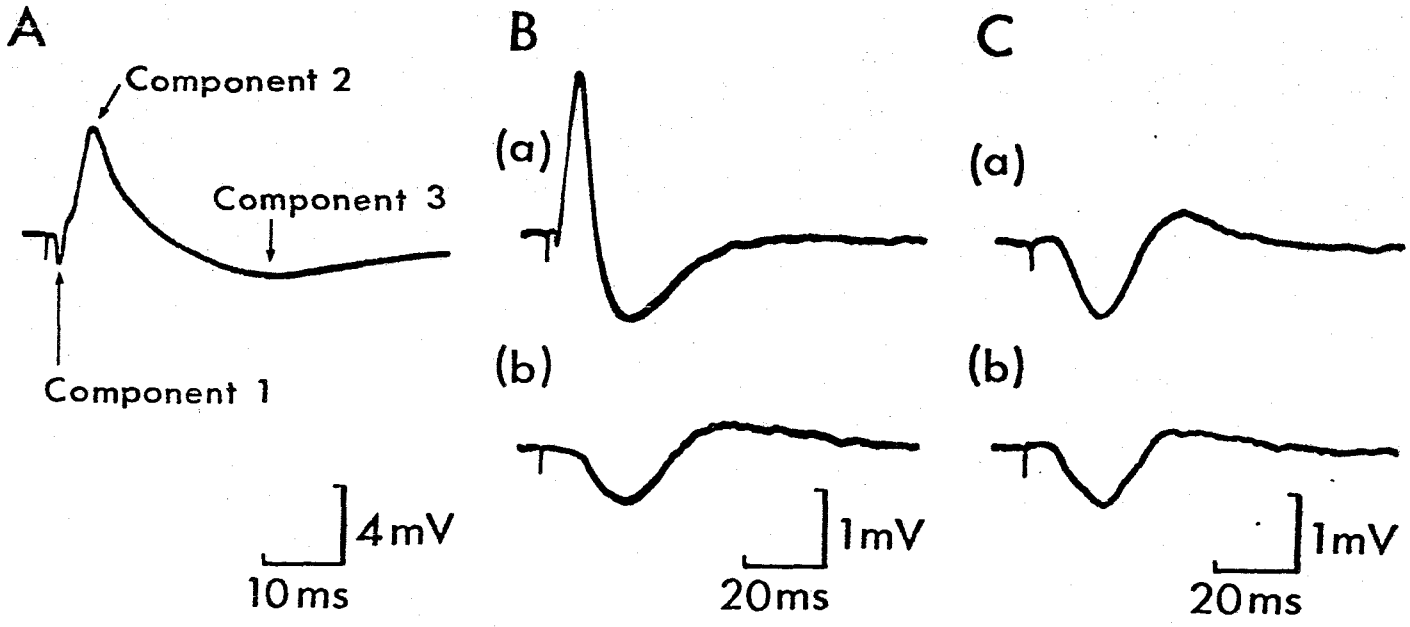


Fig. 30 A, A field potential in the granule cell layer (GCL) of the olfactory bulb elicited by LOT stimulation.
B, Field potentials recorded in the GCL elicited by stimulation of the superficial layer of the prepyriform cortex before (upper trace) and after (lower trace) sectioning the LOT.
C, Field potentials in the GCL of the bulb evoked by stimulation of the deep lying structure of the prepyriform cortex (DPC) before (upper trace) and after (lower trace) sectioning the LOT. Positivity is upward in this Fig. and Figs. 32 to 36.

bulb for recording the field potential. A silver plate coated with silver-chloride was placed on the cut edge of the temporal muscle for a reference electrode.

Potentials from the glass microelectrode were led through a preamplifier (Nihon-Koden MEZ 9001), and displayed on an oscilloscope (Tektronix Model 565). The d. c. membrane potentials and stimulus currents were routinely displayed on the other beams of the oscilloscope and monitored. Data was photographed on 35-mm films.

## E-2, RESULTS

### LOT projection areas

It is well known that electrical stimulation of the LOT elicits a large triphasic field potential in the GCL of the olfactory bulb (Nicoll, 1970; Phillips et al 1963; Rall & Shepherd, 1968; Rall et al, 1966; Shepherd, 1972). As shown in Fig. 30A, it is composed of an initial brief negativity (component 1) and a large positivity (component 2) followed by a second long-lasting negativity (component 3). Rall and Shepherd (1968) have posturated that the component 1 and 2 of the field potentials is caused by stimulation of the mitral cell axons; antidromic impulses in the mitral cell axons cause synchronous activation of the mitral cell somata which is responsible for the component 1. The activated mitral cells then produce synaptic depolarization of the peripheral processes of the granule cells through the mitral-to-granule dendrodendritic excitatory synapses. This depolarization of the granule cells is responsible for the component 2 of the field potential. From this, one can expect that electrical stimulation of the areas where the mitral cell axons project, may elicit a similar field potential to the components 1 and 2 in the GCL of the olfactory bulb. Fig. 30B (a) shows a field potential in the GCL elicited by the stimulation of the superficial layer of the prepyriform cortex. It may be noted that this field potential was quite similar to that in A except that the amplitude of the component 3 is relatively larger than that in A. When the LOT was sectioned at about 9 mm rostral to the stimulating site, both components 1 and 2 were completely abolished (Fig. 30B (b)). In contrast to this, component 3 remained though it was reduced in amplitude. This result indicates that the components 1 and 2 and a small part of component 3 of the field potential are elicited by the activation of fibers passing through the LOT. This is in agreement with the hypothesis that the components 1 and

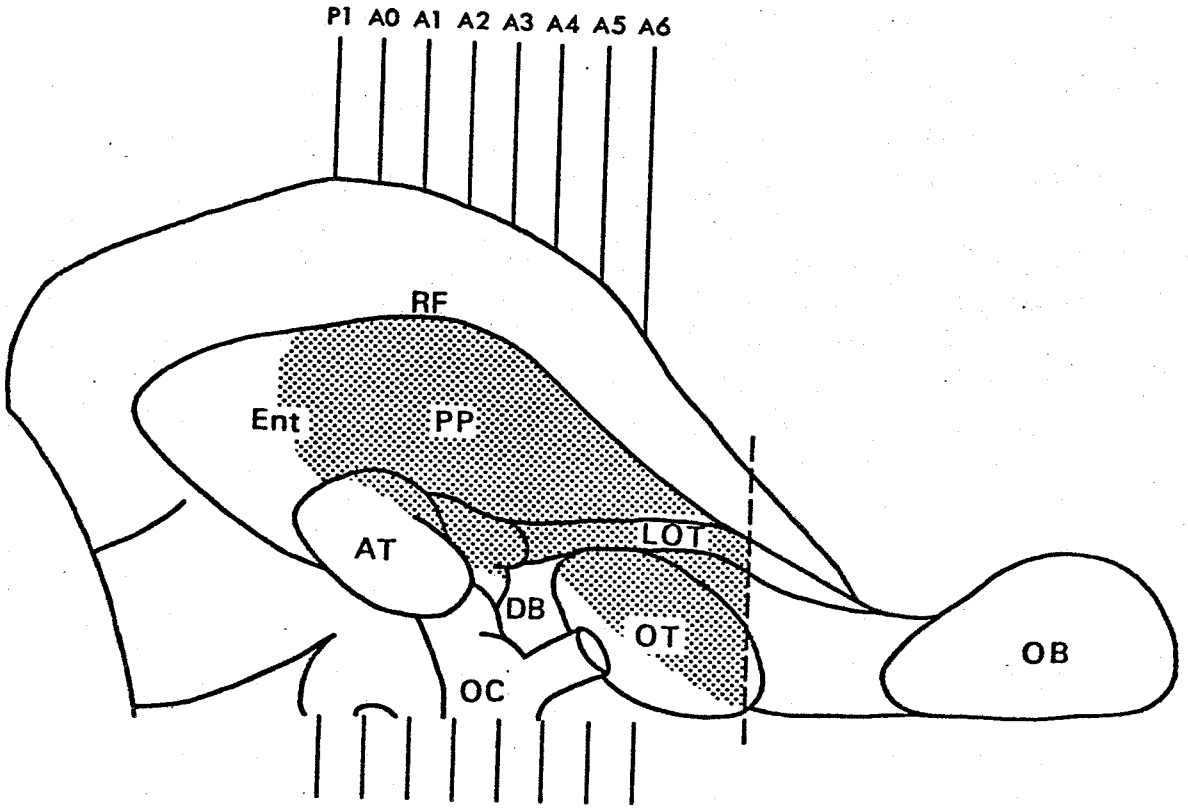


Fig. 31 Diagramatic representation of the LOT projection areas (the ventral riew of the rabbit brain). Shaded regions indicate the sites stimulation of which evoked the triphasic field potential in the GCL. The vertical lines nominated by A6 to P1 correspond to the coronal sections in the stereotaxic atlas of Fifková and Maršala. Mapping was performed in the areas caudal to the broken line. See abbreviations.

2 of the field potentials are caused by stimulation of the mitral cell axons.

The areas, stimulation of which caused similar field potential (components 1 and 2) in the rabbit olfactory bulb were essentially similar to those reported in the cat and in the ferret (Dennis & Kerr, 1968, 1975). As shown as dotted areas in Fig. 3, they contain superficial layers of extensive basal rhinencephalon; the prepiriform cortex, the olfactory tubercle (except its medial quadrant), the antero-lateral portion of the entorhinal cortex and the antero-lateral portion of the cortical amygdaloid nucleus. Though the retrobulbar areas (rostral to the broken line in Fig. 31) were not explored systematically in this experiment, stimulation of the superificial layer of the anterior olfactory nucleus also evoked large components 1 and 2 of the field potential in the ipsilateral olfactory bulb. When the caudal or medial part of the rhinencephalon which are distant from the LOT were stimulated, the amplitudes of the components 1 and 2 of the field potential were much smaller than those evoked by LOT stimulation. In particular the component 1 was often too small to be observed. This suggests that stimulation of these sites may activate only a small portion of the mitral (or tufted) cell axons.

Centrifugal projection to the olfactory bulb

Fig. 32B 3 shows the field potentials in the GCL of the olfactory bulb elicited by stimulation of each of the seven successive points along a single electrode track (track 3 in Fig. 32A) in the prepyriform cortex. The typical triphasic field potential was elicited by stimulation of the superficial layer (dotted area in Fig. 32) of the prepyriform cortex (the lowest trace). However, when the tip of the stimulating electrode reached the deep lying structure of the prepyriform cortex (shadowed areas with oblique lines in Fig. 32A) which was deeper than the pyramidal cell layer, both components 1 and 2 of the field potential disappeared but a pure negative potential remained (upper 5 traces). As shown in Fig. 30 C, this negative potential did not vanish after sectioning the LOT. This result indicates that the mitral cell axons or centrifugal fibers running in the LOT are not involved in the neuronal pathway for evoking this negative potential.

Similar pure negative potentials were elicited by stimulation of the deep lying structures of the other LOT projection areas; the olfactory tubercle, antero-lateral portion of the cortical amygdaloid nucleus and antero-lateral portion of the entorhinal cortex. Stimulation of deep

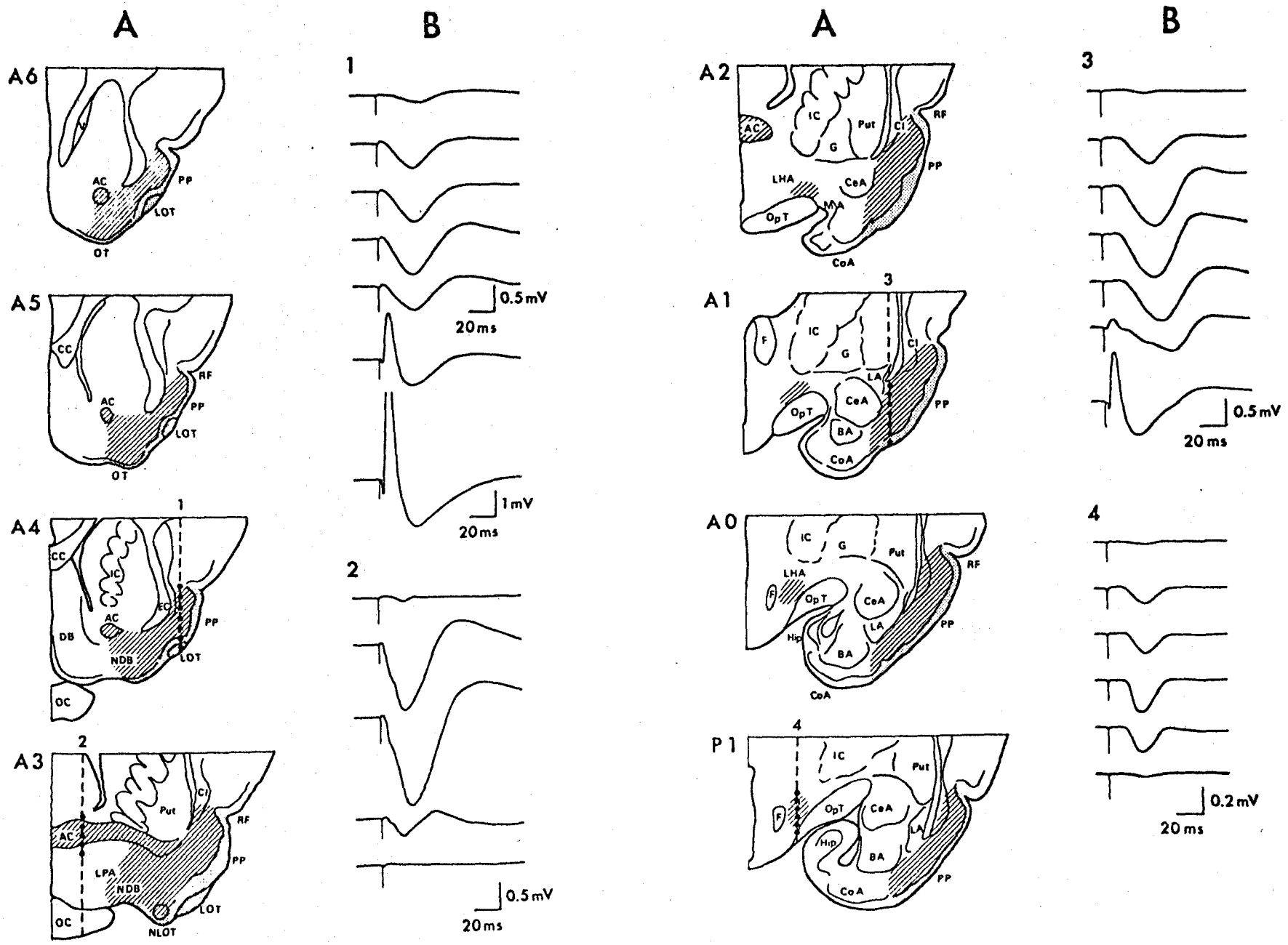
A
B
A6
AC
PP
LOT
OT
A5
CC
RF
AC
PP
LOT
OT
A4
1
CC
IC
EC
AC
PP
DB
NDB
LOT
OC
A3
2
Put
CI
RF
AC
PP
LPA
NDB
LOT
OC
NLOT
1
0.5mV
20ms
1mV
20ms
2
0.5mV
20ms
A
B
A2
IC
Put
CI
RF
AC
G
PP
LHA
CeA
MA
OpT
CoA
A1
3
F
IC
G
CI
LA
CeA
PP
OpT
BA
CoA
A0
IC
G
Put
RF
LHA
F
OpT
CeA
LA
PP
Hip
BA
CoA
P1
4
IC
Put
F
OpT
CeA
LA
Hip
BA
PP
CoA
3
0.5mV
20 ms
4
0.2mV
20 ms

Abbrevations used in section E

AC, anterior commissure; AON, anterior olfactory nucleus; AT, amygdaloid tubercle; BA, basal amygdaloid nucleus; CC, corpus callosum; CeA, central amygdaloid nucleus; CL, claustrum; CoA, cortical amygdaloid nucleus; DB, diagonal band of Broca; DPC, deep lying structure of the prepyriform cortex; EC, external capsule; Ent, entorhinal cortex; EPL, external plexiform layer; F, fornix; G, globus pallidus; GCL, granule cell layer; Hip, hippocampus; IC, internal capsule; LA, lateral amygdaloid nucleus; LHA, lateral hypothalamic area; LOT, lateral olfactory tract; LPA, lateral preoptic area; MA, medial amydgaloid nucleus; MFB, medial forebrain bundle; NDB, nucleus of the horizontal limb of the diagonal bund; NLOT, nucleus of the lateral olfactory tract; OB, olfactory bulb; OC, optic chiasma; ON, olfactory nerve; OpT, optic tract; OT, olfactory tubercle; PP, prepyriform cortex; Put, putamen; RF, rhinal fissure; V, ventricle.

Fig. 32 A, Coronal sections in A6 to P1 of the basal rhinencephalon of the rabbit. Shading by small dots indicates the areas, stimulation of which evoked the triphasic potential in the GCL. Shading by oblique lines shows the areas stimulation of which generate a purely negative potential in the bulb. Broken lines indicated by 1 to 4 show four examples of the tracks of the stimulation electrodes. The track 1 (broken line in A4) passes through the LOT, the track 2 (in A3) through the AC, the track 3 (in A1) through the prepyriform cortex and the track 4 (in P1) through the lateral hypothalamic area.
B, Traces in 1 to 4 indicate the field potentials evoked by stimulation of each dots along the broken lines 1 to 4 in A respectively.

lying structure of the anterior olfactory nucleus also produced a negative potential in the GCL (not illustrated). These negative potentials had various onset latencies, depending on the stimulating site. It ranged from about 4 msec to 7 msec when the deep lying structure of rostral prepyriform cortex was stimulated (A6-A4 in Fig. 4). On the other hand, stimulation of the deep structure of the caudal portion of the prepiriform cortex or the entorhinal cortex (A1-P1 in Fig. 4) elicited the negative potential with an onset latency of 14-22 msec. It has been shown that stimulation of AC fibers also evokes a negative potential in the GCL of the olfactory bulb. In Fig. 4B 2 are shown the field potentials in the GCL elicited by stimulation of each of the 5 successive points along a track which crosses the AC. It is clear that negative potentials were elicited only when the tip of the stimulating electrode was in the AC. No potential change was recorded in the olfactory bulb following stimulation of the point about 300 u ventral to the lower border of the AC (the lowest trace in Fig. 32B 2). This suggests that the stimulating current spead was not too extensive for our mapping procedure in the present experiment. Stimulation of either the anterior limb or the lateral limb of the AC elicited such negative potential. The onset latency of the potential ranged from 2 msec to 4 msec following stimulation of the AC in the ipsilateral basal forebrain. It can be seen in Fig. 32B 4 that stimulation of the medial forebrain bundle situated between the lateral hypothalamic area and the lateral preoptic area also evoked similar negative potential in the GCL of the olfactory bulb. The onset latency of the potential ranged from 12 msec to 15 msec with stimulation of the lateral hypothalamic area at A-0 in Fig. 32A.

Depth profile of the field potentials in the olfactory bulb

It has been established that the field potentials recorded at successive bulbar depth following LOT stimulation are highly correlated with the histological layers of the bulb (Phillips et al, 1963). Thus the position of the tip of the recording microelectrode can be accurately known by the shape of the LOT-evoked field potentials in the olfactory bulb. In Fig. 33A and B are shown respectively typical series of field potentials recorded at in dicated depths along a microelectrode track in the olfactory bulb which were elicited by stimulation of LOT and deep lying structure of the prepyriform cortex (DPC). The amplitudes of the field potentials were measured at points indicated by the vertical broken lines in A and

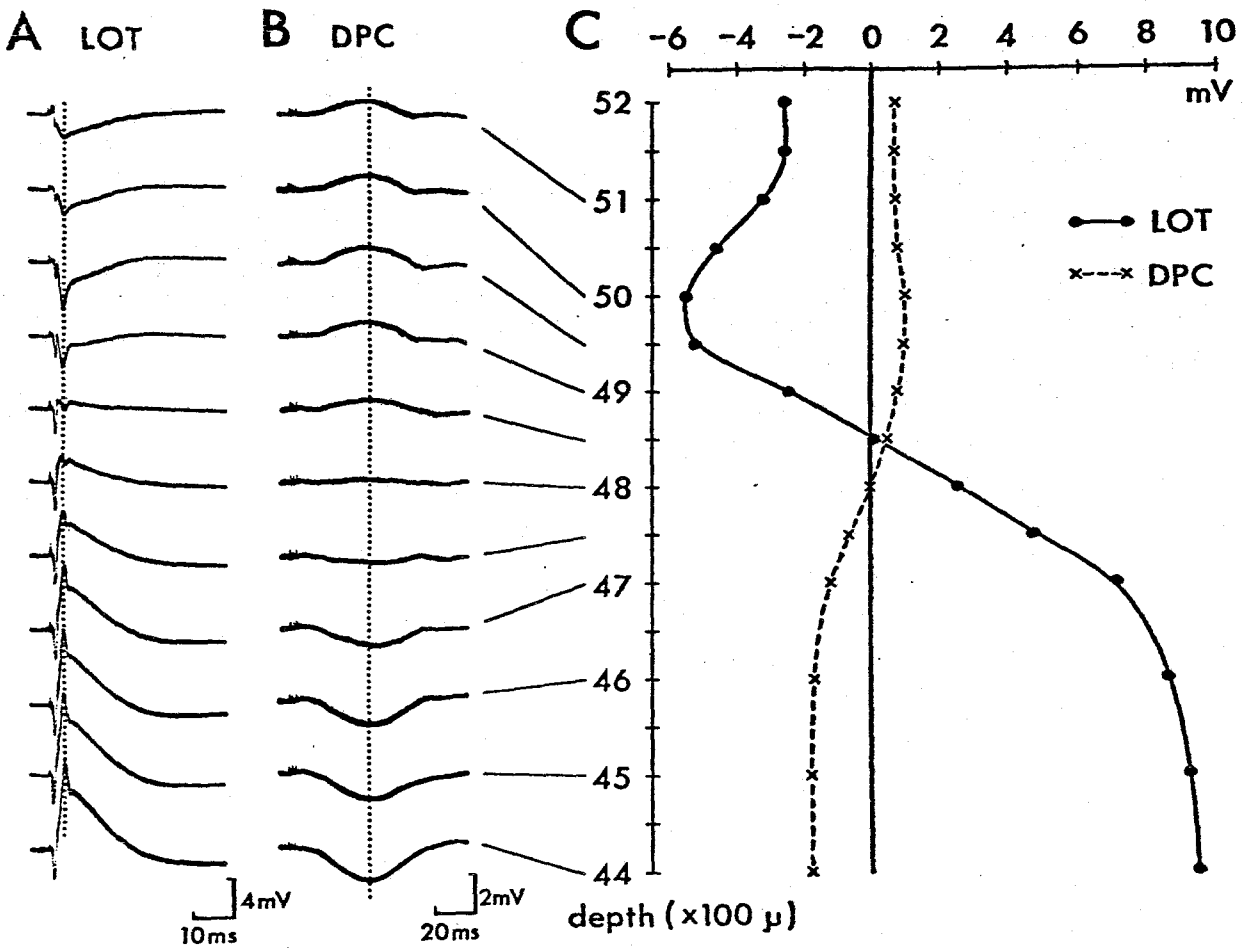


Fig. 33 A comparison of the field potentials in the olfactory bulb evoked by stimulation of LOT and DPC.
A, Responses to LOT stimulation recorded at varying depths in the olfactory bulb. Potentials from the top to the bottom were recorded in series from the ventral part (EPL) towards the central part (GCL).
B, Responses to DPC stimulation recorded in the same way as above.
C, The sizes in mV of the evoked potentials were measured at the vertical broken lines in A and B, and plotted against the depths. The depths were measured from the dorsal surface of the bulb.

B, which are then plotted against depth in C. In can be seen in C that the extracellular potential gradient along the depth of the bulb produced by stimulation of DPC is quite contrary to that produced by LOT stimulation: The LOT-evoked field potential has a large positivity in the GCL. It reverses its polarity near the mitral cell layer, and becomes to have a large negativity in the EPL. In contrast, DPC stimulation elicited a negative potential in the GCL. This potential also reversed its polarity near the mitral cell layer and became a positive potential in the EPL. This suggests that there is an extracellular current flow from the EPL to the GCL. As discussed in the theoretical analysis (Rall & Shepherd, 1968; Rall et al. 1966) of LOT-evoked field potentials in the olfactory bulb, the number of cells which generates this current flow should have a radial structure extending from the GCL to the EPL. The granule cells in the olfactory bulb have deep dendrites in the GCL and long peripheral processes in the EPL. Thus, they satisfy the requirement. It has been shown that stimulation of AC also produces extracellular potential gradient along the depth of the bulb (Mori & Takagi, 1978; Nicoll, 1970) which is quite similar to that elicited by stimulation of DPC.

Response of GCL neurons

It has been reported that AC stimulation produces EPSPs in the cells which are presumed to be the granule cells (Mori & Takagi, 1977a, 1978). It has also been suggested that the extracellular field potential elicited in the olfactory bulb by AC stimulation is mainly produced by the depolarization of the presumed granule cells (Mori & Takagi, 1978a; Shepherd, 1972). Since the field potential elicited by DPC stimulation is quite similar in the depth profile to the one elicited by AC stimulation (Fig. 33), one may expect that DPC stimulation also elicits EPSPs in the granule cells.

Fig. 34 shows intracellularly recorded responses of a neuron located in the GCL to LOT (A), AC (B) and DPC (C) stimulation (upper traces), together with the field potentials in the middle area of the GCL (lower traces). Resting membrane potential of this unit was -60 mV. Single supramaximal LOT stimulation produced a prolonged EPSP with a spike discharge in this GCL neuron. The onset latency and the peak amplitude of the EPSP were 2.4 msec and 8 mV respectively. This neuron was classified as a type 1 GCL neuron because conditioning LOT stimulation depressed the test LOT evoked EPSP (Mori & Takagi, 1978a). In this neuron, single shock to AC also caused an EPSP with an onst latency of 4 msec

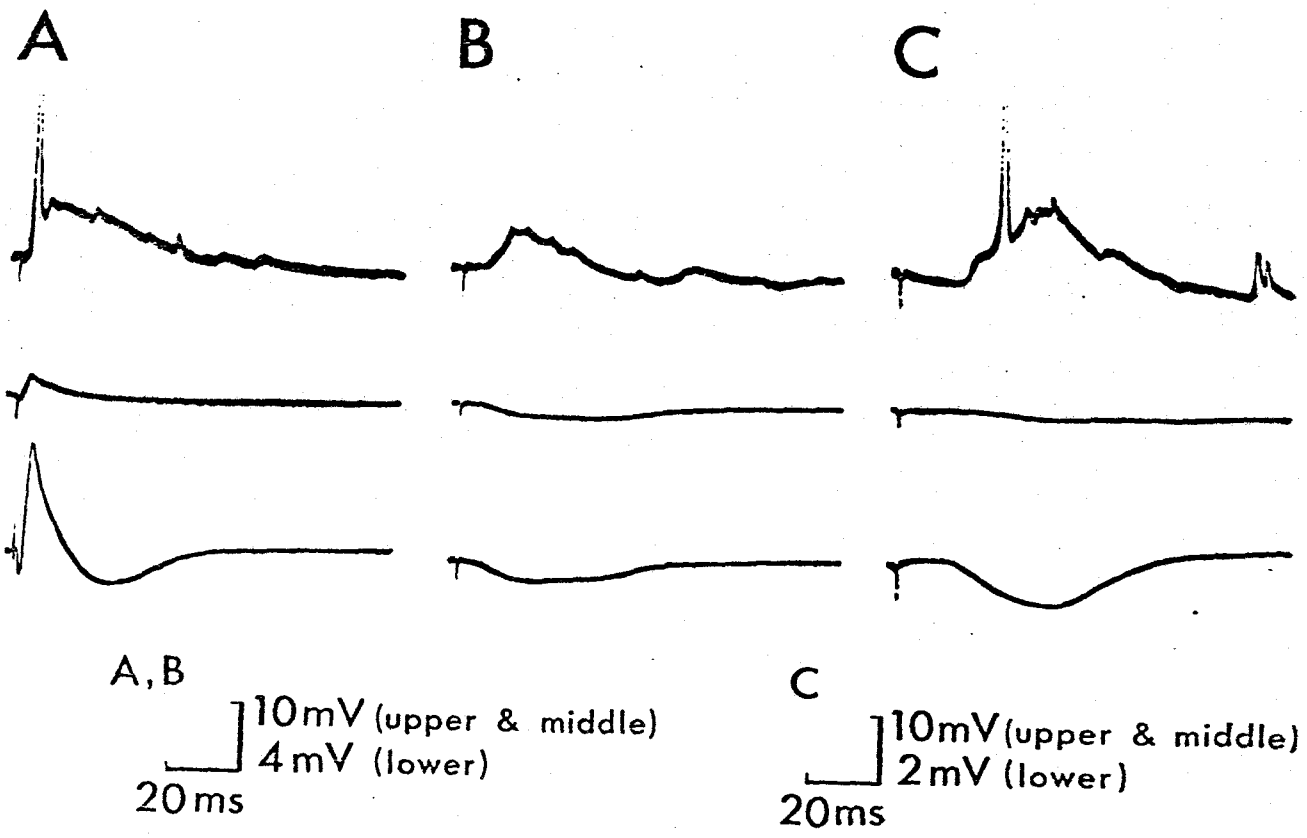


Fig. 34 Responses of a GCL neuron to LOT, AC and DPC stimulation. The top traces: Intracellularly recorded potentials. The middle traces: Extracellular field potentials just outside of the impaled cell. The lower traces: Field potentials in the GCL.
A, A spike discharge on a long-lasting EPSP elicited by LOT stimulation.
B, An EPSP elicited by AC stimulation.
C, An EPSP and a spike discharge elicited by a stimulus applied to DPC.

and a peak amplitude of 6 mV (B). It can be seen in Fig. 34C that a single shock to DPC also generated an EPSP with a spike discharge in this GCL cell. The EPSP had a relatively long onset latency (14 msec) and a slow rise time. The peak amplitude of the EPSP was 11 mV. Stable intracellular recordings were obtained from 18 type 1 GCL neurons with resting membrane potential from -40 mV to -70 mV. In all of these 18 neurons, both AC and DPC stimulation elicited EPSPs. Repetitive stimulation delivered to AC or DPC has summative effects on the EPSPs in the GCL neurons. It is interesting to note that LOT stimulation invariably elicited a single or train of spike superimposed on prolonged EPSPs in all 18 GCL neurons, while, out of these cells, spike generation occured in only one cell by AC stimulation and in only 3 cells by DPC stimulation. It can also be seen in Fig. 34B and C that EPSPs in the type 1 GCL cell correspond in time with the negative extracellular field potential in the GCL. This suggests that the negative wave elicited in the GCL by AC and DPC stimulation is mainly due to depolarization of the type 1 GCL cells (presumably the granule cells).

Response of mitral cells

When a micropippete was in the mitral cell layter (which was determined by the reversal of the polarity of component 2 of the LOT evoked field potential), it often penetrated one or two cells which showed an antidromic spike potential with latency of less than 2 msec following LOT stimulation. From the location of cell bodys and their axonal projection to LOT, these cells were identified as mitral cells. Fig. 35 shows intracellular responses of a mitral cell to LOT (A), AC (B) and DPC (C) stimulation (upper traces) together with the corresponding field potentials recorded just outside the cell (middle traces). The lower traces show simultaneously recorded field potentials in the middle area of the GCL. In agreement with previous studies (Mori and Takagi, 1975, 1977a, 1978a; Phillps et al. 1963; Yamamoto et al, 1963), an antidromic spike and a subsequent long lasting IPSP were elicited by LOT stimulation (A) and a slowly developing IPSP by AC stimulation (C). As shown in Fig. 35C, three shocks to DPC also produced a slowly developing IPSP in this mitral cell. The onset latency of the DPC-evoked IPSP from the initial shock was 23 msec which is much longer than that of the AC-evoked IPSP (9 msec in Fig. 35B). The peak amplitudes of DPC-evoked IPSP and AC-evoked IPSP were 8 mV and 9 mV, and the durations were 70 msec and 65 msec respectively. The amplitude of the DPC-evoked

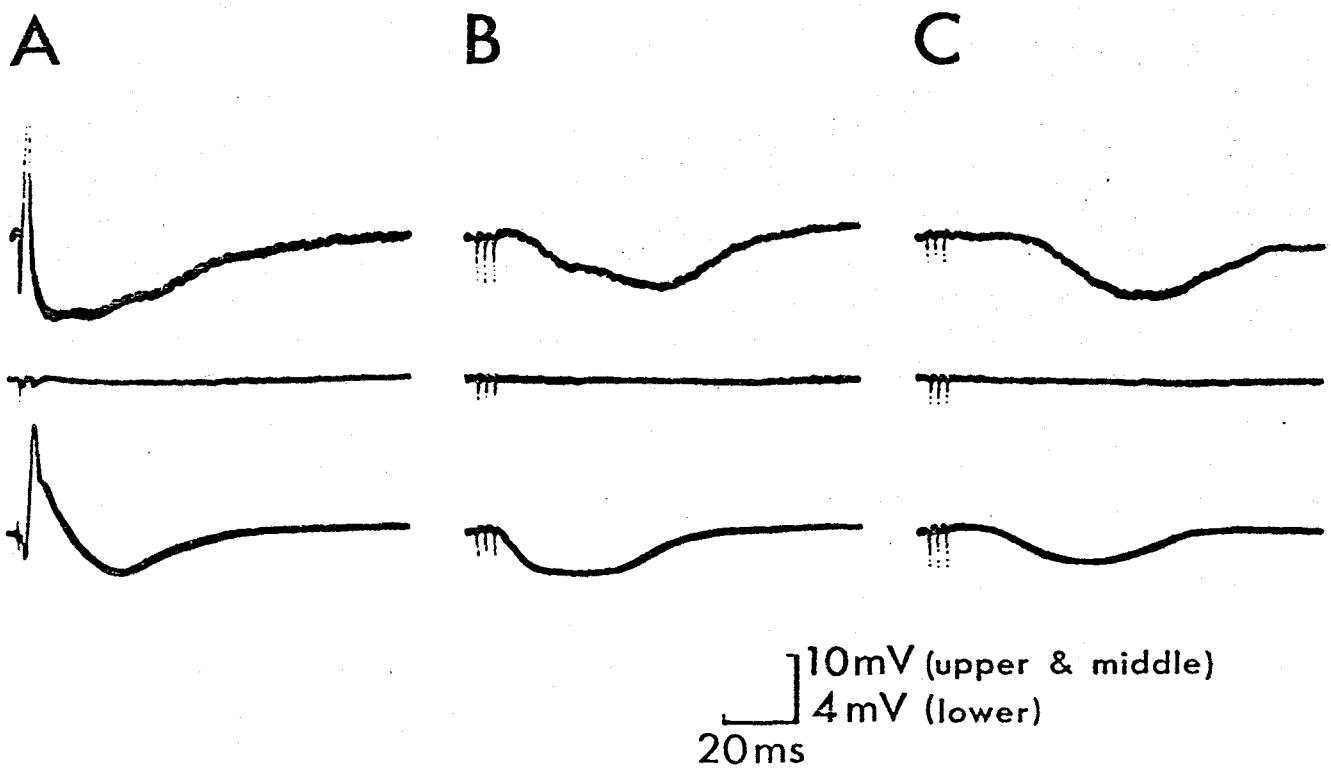


Fig. 35 Responses of a mitral cell to LOT, AC and DPC stimulation. The top traces: Intracellularly recorded potential of the mitral cell. The middle traces: Extracellular records just outside the impaled cell. The lower traces: Field potentials in the GCL.
A, An antidromic spike discharge followed by an IPSP elicited by LOT stimulation.
B, An IPSP evoked by three AC volleys.
C, An IPSP evoked by three stimuli delivered to DPC. Note that onsets of the IPSPs in B and C delayed for several milliseconds after those of the negative field potentials in the GCL.

IPSP grew when the number of shocks are increased just as the case for the AC-evoked IPSP.

When the intracellular response to DPC stimulation was checked in 23 antidromically identified mitral cells, clear IPSPs were found in all of them. In all of these 23 mitral cells, stimulation of AC also produced IPSPs. It can be seen in Fig. 35C that the onset of the DPC-evoked IPSP occured about 8 msec after the onset of the negative field potential in the GCL, suggesting that there may be inhibitory interneurons responsible for the mitral cell IPSP. A similar relationship was also seen between the onset of the AC-evoked IPSPs in the mitral cells and onset of the AC-evoked field potential in the GCL; for example in Fig. 7B, the former was about 6 msec later than the latter.

Fig. 36A shows a poststimulus-time histogram of an extracellularly recorded mitral cell activity following single DPC stimulation. The field potential in the GCL (B) and an intracellular response of another mitral cell are also shown with the same time scale as in A. In extracellular recordings, the mitral cells were identified by their spike potentials responding with a brief (less than 2 msec) and invariable latency to LOT stimulation. Though the rate of spontaneous discharges of mitral cells was quite low in our experimental conditions, the histogram which was constructed from 30 sweeps clearly shows an inhibition of the mitral cell spike activity for about 55 msec in the case of single DPC stimulation. Fig. 36A and B indicate that the onset of the inhibition occured about 10 msec later than that of the negative potential in the GCL. In contrast to this, Fig. 36A and C show that the inhibition of mitral cell activity corresponds well in time with the occurence of IPSPs in mitral cells. Following DPC stimulation, such an inhibition was seen in all of the 22 extracellularly recorded mitral cells. After this prolonged inhibition, rebound discharges appeared in about half of the mitral cells as shown in Fig. 36A.

IPSPs in the mitral cells were also found when the deep lying structures of the LOT projection areas other than the DPC (e.g. olfactory tubercle) were stimulated. In a few experiments, intracellular potentials of the mitral cells elicited by the lateral hypothalamic area stimulation were examined. Though the lateral hypothalamic area stimulation evoked a small negative field potential in the GCL, it failed to elicit detectable potential changes in the mitral cells. Presumably it is due to an insufficient

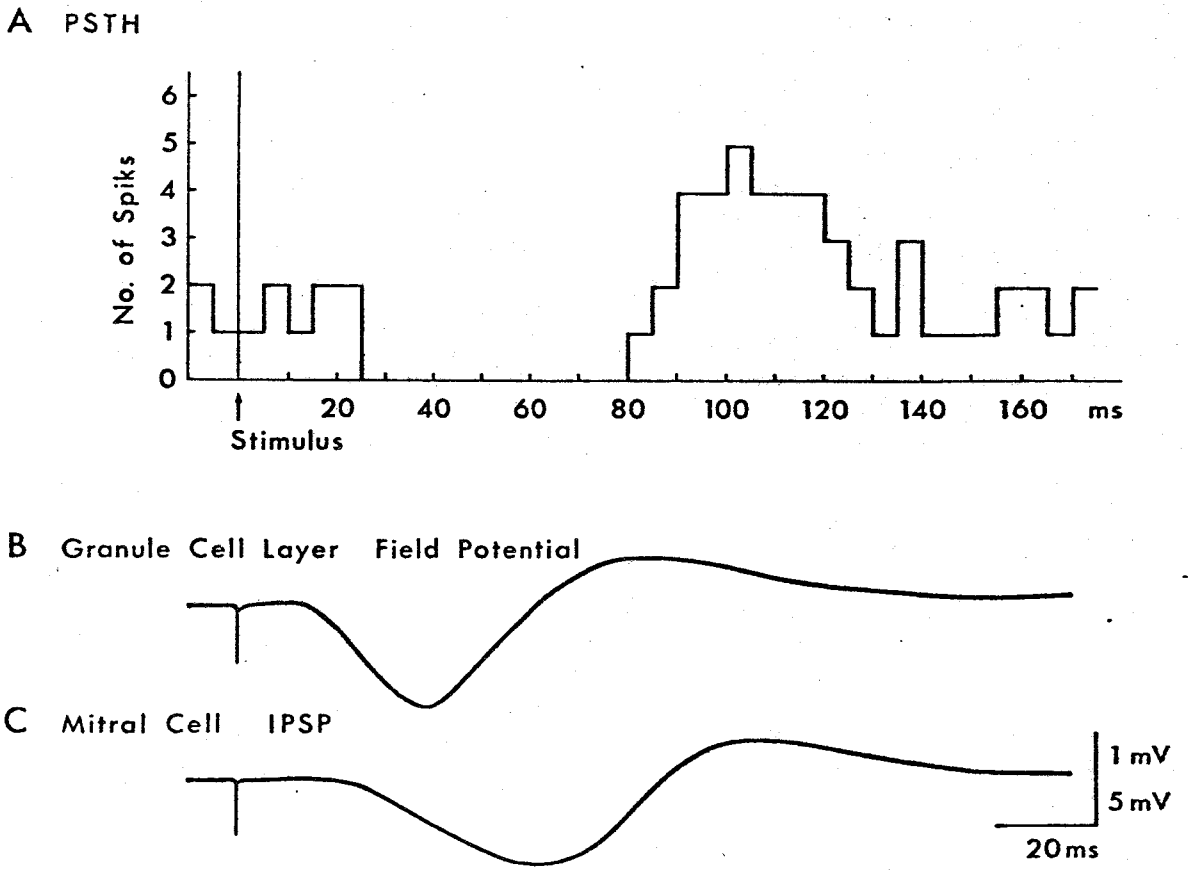


Fig. 36 A, Poststimulus-time histogram of extracellulary recorded spike discharges of a mitral cell. Stimuli were delivered to DPC (A0, L9). The histogram was made from the records of 30 sweeps.
B, A field potential in the GCL elicited by DPC stimulation.
C, An intracellular response of a mitral cell to DPC stimulation. A-C were recorded in the same rabbit.

depolarization of the inhibitory interneurons for activating their synapses on the mitral cells.

## E-3, DISCUSSION

The areas, stimulation of which caused the component 1 (antidromic activation of the mitral cells) and the component 2 (subsequent depolarization of the granule cells through mitral-to-granule dendrodendritic synapses) of the field potential in the rabbit olfactory bulb (Fig. 31) are in agreement with the projection areas of the mitral (and tufted) cell axons reported in the anatomical investigations (Broadwell, 1975; Heimer, 1968; Scalia, 1966; Scalia & Winans, 1975). These areas are the superficial layers of; the anterior olfactory nucleus, the entire prepyriform cortex, mediolateral surface of the olfactory tubercle, the antero-lateral half of the cortical amygdaloid nucleus, and the anterolateral portion of the entorhinal cortex. It should be noted that the components 1 and 2 of the field potential could be elicited only when the superficial layers of these basal rhinencephalons were stimulated. Stimulation of the deep lying structures of the same areas failed to activate the mitral cells antidromically. This result supports the anatomical observations that bulbar efferent fibers terminate predominantly in the superficial layer (layer IA) of the olfactory cortex (Broadwell, 1975; Price, 1973).

A negative field potential was elicited in the GCL of the olfactory bulb by DPC stimulation. In contrast to the components 1 and 2, the mitral (or tufted) cell axons are not involved in the neuronal pathway for evoking the negative field potential. In agreement with the previous investigations in the cat and the ferret, stimulation of the deep lying structures of all the LOT projection areas elicited similar negative field potentials in the GCL of the olfactory bulb. Stimulation of AC or lateral hypothalamic area also elicited a negative field potential in the GCL. Price and Powell (1970) reported three types of extrinsic fibers from the telencephalon to the olfactory bulb. The first is the fibers of the AC that end upon the deep dendrites and somata of the granule cells. The second is the fibers from the ipsilateral anterior olfactory nucleus that end upon the peripheral processes, somata and deep dendrites of the granule cells. The third is the centrifugal fibers which arise from the ipsilateral nucleus of the horizontal limb of the diagonal band, run fowared in the LOT and terminate upon the peripheral processes of the granule cells. In addition to these fibers, recent histological investigations, using the horseradish peroxidase

method, reported the origins of other centrifugal fibers to the olfactory bulb; i.e. the anterior prepyriform cortex, the far lateral preoptic area and the rostral hypothalamic area in the rabbit (Dennis & Kerr, 1968) and the anterior olfactory cortex and the olfactory tubercle in the cat (Dennis & Kerr, 1976). However, their routes to the bulb and the sites of termination in the bulb have not been reported yet.

It has been postulated that the AC stimulation elicits EPSPs in the somata and deep dendrites of the granule cells and these EPSPs are responsible for the negative field potential in the GCL (Mori & Takagi, 1977, 1978b). The following observations reported in this paper suggest that stimulation of DPC also elicits synaptic depolarization in the somata and dendrites of the same populations of granule cells in the GCL, i.e.

1. DPC stimulation produced a series of potentials in the different depths of the olfactory bulb which were quite similar in the shape and polarity to those produced by AC stimulation (negative potential in the GCL and positive one in the EPL), suggesting that there may be a synaptic depolarization in the GCL following DPC stimulation.
2. DPC stimulation produced EPSPs in the type 1 GCL cells (presumably the granule cells) in which AC stimulation also produced EPSPs. Furthermore, the DPC-evoked EPSPs usually corresponded in time with the occurrence of the negative field potential in the GCL. This suggests that there is a synchronous depolarization of many granule cells following DPC stimulation and the negative potentials in the GCL may be due to the depolarization of the granule cells.

Since stimulation of the deep lying structures of all the LOT projection areas other than the DPC produced extracellular potentials in the olfactory bulb which are similar in the polarity and shape to the potentials elicited by AC and DPC stimulation, it may be suggested that they also elicit synaptic depolarization of the dendrites and somata of the granule cells in the GCL. An anatomical investigation (Price & Powell, 1970) reported that some fibers from the pyriform cortex, amygdala and olfactory tubercle pass forward in the medial forebrain bundle and the association system to the anterior olfactory nucleus (AON), where they end in the deeper half of the external plexiform layer. Thus, one can assume one of the possibible passways which elicit depolarization of the granule cells following stimulation of the deep lying structures of the LOT projection areas; i.e. stimulation of these areas may activate the neurons of the AON synaptically and the activated

AON neurons then cause synaptic depolarization of the granule cells. On the other hand, it has been reported that some neurons in the anterior prepyriform cortex and the olfactory tubercle directly send their axons to the olfactory bulb (Broadwell & Jacobowitz, 1976; Dennis & Kerr, 1976). It is not possible to determine in the present experiment whether the cepolarization of the granule cells was elicited monosynaptically or di- or poly-synaptically via interneurons (e.g. AON neurons) following stimulation of the deep lying structures of the LOT projection areas.

As stated above, neurons in the nucleus of the horizontal limb of the diagonal band (NDB) send their axons to the ipsilateral olfactory bulb through the LOT and these axons terminate on the peripheral processes of the granule cells (Price, 1968; Price & Powell, 1970c, e). If the peripheral processes of the granule cells receive excitatory inputs from NDB neurons as Price and Powell suggeested, one can expect that stimulation of NDB would elicit a negative field potential in the EPL and a positive one in the GCL. However, in the present investigation, stimuli delivered to the region in or near the NDB generated a small negative field potential in the GCL which is similar in shape to the one elicited by DPC stimulation. Since, as was pointed out by Price and Powell (1970e, f), there are medial forebrain bundle fibers running in or near the NDB and these fibers terminate in the AON, it would be difficult to apply electric shocks to the NDB selectively. Thus, it is very probable that the field potential in the olfactory bulb elicited by NDB stimulation would be masked by the potentials due to the activation of the medial forebrain bundle fibers. It is, therefore, necessary to search for a method to activate the NDB selectively in order to investigate the centrifugal input from the NDB to the olfactory bulb. It is interesting to note that stimulation of the lateral hypothalamic area also elicited a negative field potential in the GCL (Fig. 32). Recent histological observations of Broadwell and Jacobowitz (1976) have pointed out that the lateral hypothalamic area represents one of the sources of direct centrifugal fibers to the main olfactory bulb, and they have also suggested that neurons of lateral hypothalamic area send their axons to the AON.

It has been shown that stimulation of the mitral cell axons or of the AC fibers elicits depolarization of the presumed granule cells (Mori & Takagi, 1977, 1978b). The present experiment showed that depolarization of the granule cells could be elicited by stimulation of DPC (and possibly by stimulation of the deep lying structures of all the LOT projection areas).

These results are in agreement with the histological evidence (Price & Powell, 1970c) that all of the extrinsic fibers from the telencephalon appear to terminate upon the granule cells and form asymmetrical synapses with the round synaptic vesicles. It has been discussed (Shepherd, 1970) that the granule cells in the olfactory bulb and the amacrine cells in the retina are very similar with respect to the following morphological and physiological characteristics. Firstly, both cells lack an axon. Secondly, both of the cells have reciprocal synapses. Thirdly, both of them are supposed to be inhibitory interneurons (Dowling & Boycott, 1966; Marchiafava, 1976; Murakami & Shimoda, 1977; Werblin & Dowling, 1969). The present experiment added another common feature between the granule cells and the amacrine cells; i.e. both cells receive a strong depolarizing action from the centrifugal fibers. It is well known that stimulation of LOT or AC usually produces IPSPs in the mitral cells. In this study, it was shown that stimulation of the deep lying structures of the LOT projection areas (e.g. the prepyform cortex and the olfactory tubercle) also invariably produced IPSPs in the mitral cells. It is noteworthy that the onset and peak-time of AC- or DPC-evoked IPSPs in the mitral cell were delayed for several milliseconds from those of EPSPs in presumed granule cells (cf. Fig. 34 and Fig. 35). According to the histological investigations (Price & Powell, 1970d; Reese & Shepherd, 1972), almost all the synapses found on the mitral cell dendrites and somata (excepting those in or around the glomerular region) are the reciprocal synapses with the peripheral processes of the granule cells. Thus, it may be reasonable to assume that the IPSPs in the mitral cells elicited by stimulation of the DPC are produced through the activation of the granule cells just as in the case of the LOT-evoked or AC-evoked IPSPs in the mitral cells. According to the present and previous investigations, the pathways for eliciting the mitral cell IPSPs following LOT, AC or DPC stimulation may be summarized as follows; LOT stimulation produces EPSPs in the peripheral processes of the granule cells mainly through the mitral-to-granule dendrodendritic excitatory synapses, while AC or DPC stimulation may elicit EPSPs in the somata or dendrites of the granule cells in the GCL. The activated granule cells in turn causes synaptic inhibition of the mitral cells through the granule-to-mitral dendrodendritic inhibitory synapses. As stated above, the anatomical investigations indicated that the granule cells receive various kinds of extrinsic inputs from the telencephalon directly or via AON neurons, but the outputs from the granule cells are only the granule-

to-mitral dendrodendritic synapses. The present experiment suggested that the granule cells do receive excitatory centrifugal influences from various areas in the basal forebrain (the anterior commissure, the deep lying structures of the LOT projection areas and possibly the lateral hypothalamic area) and that the mitral cells receive predominantly inhibitory influences via the granule cells from these basal forebrain. The functional significance of these centrifugal influences upon the mitral cells via the granule cells waits for further research.

# 4. SUMMARY

In the rabbit olfactory bulb, an analysis has been carried out on intracellular potentials recorded from mitral cells and neurons in the granule cell layer (GCL cells) in addition to the extracellular field potentials elicited by the stimulation of olfactory nerve, lateral olfactory tract, anterior commissure or various regions in the basal forebrain.

* * *

Olfactory nerve stimulation elicited fast prepotentials (FPPs) in addition to small EPSPs in mitral cells. Analysis of the natures of FPPs suggests that the primaly dendrite of the mitral cell has an ability of spike generation .....(Section A)

* * *

Most recordings from mitral cells showed large and prolonged IPSPs subsequent to the antidromic spikes following LOT stimulation. These IPSPs decreased in amplitude and then reversed in polarity by progressive increase in hyperpolarizing current applied intracellularly. They were accompanied by a prominent and long lasting conductance increase of the mitral cell membrane.

Reversed IPSPs of mitral cells having quite different time courses from the original hyperpolarizing IPSPs suggest that the inhibitory synapses are widely distributed on the soma and dendrites.

Following LOT stimulation, EPSPs could be recorded from GCL cells whose onset latency was approximately 0.6 msec shorter than that of mitral cell IPSPs. Comparison of the behavior of EPSPs in GCL cells and that of mitral cell IPSPs under various conditions of LOT stimulation suggests that these GCL cells are the inhibitory interneurons mediating mitral cell inhibition.

The results support the hypothesis of dendrodendritic pathways for activation of granule cells and subsequent inhibition of mitral cells. ..... (Section B)

* * *

Repetitive LOT stimulation caused alternation in the amplitude of successive IPSPs in mitral cells and EPSPs in presumed granule cells. The rhythmic oscillations of the membrane potential were also observed in mitral cells and presumed granule cells during odor stimulation. Analysis of their behavior and simultaneously recorded induced waves in

the GCL suggests that dendrodendritic synaptic interactions between mitral and granule cells may provide the mechanism for the generation of the rhythmic activity.....(Section C)

* * *

Most mitral cell recordings showed IPSPs with latency of 7-11 msec following AC stimulation. These IPSPs had similar sensitivity as the IPSPs evoked by lateral olfactory tract (LOT) stimulation to internally applied current and showed asymmetrical reversal during application of the hyperpolarizing current.

Volleys in the AC elicited EPSPs in type 1 GCL cells whose characteristics were in agreement with those of inhibitory interneurons inferred from the analyses of mitral cell IPSPs. It has been suggested that these type 1 GCL cells may be the common inhibitory interneurons (presumably granule cells) mediating both AC-evoked and LOT-evoked IPSPs in mitral cells.

Conditioning AC stimulation depressed the test LOT-evoked IPSPs in mitral cells and test LOT-evoked EPSPs in type 1 GCL cells. These observations are in good agreement with the hypothesis that LOT-evoked IPSPs are mainly mediated by the dendrodendritic reciprocal synapses between mitral cell dendrites and peripheral processes of granule cells. .....(Section D)

* * *

Regions which exert centrifugal influences on the olfactory bulb activity were studied applying systematic stimulation to various areas of the ipsilateral telencephalon in the rabbit. By delivering electric stimuli to the anterior commissure (AC), the deep lying structures in the projection areas of the lateral olfactory tract (LOT) and the medial forebrain bundle situated between the lateral hypothalamic area and the lateral preoptic area, negative field potentials were evoked in the granule cell layer (GCL) of the bulb.

Intracellular recordings from the mitral cells and the GCL neurons in the olfactory bulb were performed in order to clarify the modes of the centrifugal influences on the olfactory bulb neurons.

EPSPs were recorded in the GCL neurons by stimulation of the deep lying structure of the prepyriform cortex. The onset time and duration of the EPSPs corresponded well to those of the negative field potentials in the GCL. Thus, it was suggested that these negative potentials were caused by the EPSPs of the number of granule cells.

In almost all of the mitral cells, IPSPs were recorded by stimulation of the AC and the deep lying structures of the LOT projection areas. The onsets of the IPSPs were found with delays of several milliseconds from those of the negative field potentials in the GCL.

It was postulated that the excitation of the centrifugal system mainly exerts a depressive influence on the activity of the mitral cell, and that the GCL neuron (presumably the granule cell) seems to be an inhibitory interneuron interpolated between the extrinsic fibers from the telencephalon and the mitral cell.....(Section E)

## 5. ACKNOWLEDGEMENTS

I wish to thank Professor S. F. Takagi for his encouragement and support throughout this work and Professor N. Tsukahara for his helpful discussions. I also wish to thank staves of the department of physiology, and M. Nakashima, S. Kogure and M. Satou for good collaboration.
Thanks are also due to M. Iino and K. Yokozawa for excellent technical assistances, to T. Yajima for beautiful photographings and T. Wada for very good typings.
This investigation was supported by grants from the Education Ministry of Japan.

## REFERENCES


Adrian, E. D. (1950). The electrical activity of the mammalian olfactory bulb. Electroen. Neurophysiol. 2, 377-388.

Allison, A. C. (1953). The morphology of the olfactory system in the vertebrates. Biol. Rev. 28, 195-244.

Andres, K. H. (1965). Der Feinbau des Bulbus Olfactorius der Ratte unter besonderer Berücksichtigung der synaptishen Verbindungen. Z. Zellforsh. mikrosk. Anat. 65, 530-561.

Andres, K. H. (1970). Anatomy and ultrastructure of the olfactory bulb in fish, amphibia, reptiles, birds and mammals. In G. E. W. Wolstenholme and J. Knight (Eds.), Taste and Smell in Vertebrates, In: Ciba Found. Symp., Churchill, London, pp. 177-194.

Baumgarten, R. von., Green,J.D. and Mancia, M. (1962a). Recurrent inhibition in the olfactory bulb. II. Effects of antidromic stimulation of commissural fibers. J. Neurophysiol. 25, 489-500.

Baumgarten, R. von., Green, J. D., and Mangia, M. (1962b). Slow waves in the olfactory bulb and their relation to unitary discharge. Electroencephalogr. Clin. Neurophysiol., 14, 621-634.

Broadwell, R. D. (1975). Olfactory relationships of the telencephalon and diencephalon in the rabbit. I. An autoradiographic study of the efferent connections of the main and accessory olfactory bulbs. J. comp. Neurol., 163, 329-346.

Broadwell, R. D. and Jacobowitz, D. M. (1976). Olfactory relationships of the telencephalon and diencephalon in the rabbit. III. The ipsilateral centrifugal fibers to the olfactory bulbar and retrobulbar formations. J. comp. Neurol., 170, 321-346.

Cajal, S. R. (1955). Studies on the Cerebral Cortex. (Translated by Kraft, L. M.) London: Lloyd-Luke.

Callens, M. (1965). Peripheral and Central Regulatory Mechanisms of the Excitability in the Olfactory System. Brussels: Arscia Uitgaven.

Coombs, J. S., Eccles, J. C. and Fatt, P. (1955). The specific ionic conductance and the ionic movements across the motoneuronal membrane that produce the inhibitory post-synaptic potential. J. Physiol. 130, 326-373.

Dennis, B. J. and Kerr, D. I. B. (1968). An evoked potential study of centripetal and centrifugal connections of the olfactory bulb in the cat. Brain Res., 11, 373-396.

Dennis, B. J., and Kerr, D. I. B. (1975). Olfactory bulb connections with basal rhinencephalon in the ferret: an evoked potential and neuroanatomical study. J. comp. Neurol., 159, 129-148.

Dennis, B. J., and Kerr, D. I. B. (1976). Origins of olfactory bulb centrifugal fibers in the cat. Brain Res. 110, 593-600.

Dowling, J. E., and Boycott, B. B. (1966). Organization of the primate retina: electron microscopy, Proc. roy. Soc., B, 166, 80-111.

Eccles, J. C. (1964). The Physiology of Synapses. Berlin: Springer.

Eccles, J. C., Libet, B., and Young, R. R. (1958). The behaviour of chromatolysed motoneurones studied by intracellular recording. J. Physiol. (Lond.), 143, 11-40.

Eccles, J. C., Llinás, R. and Sasaki, K. (1966). Intracellularly recorded responses of the cerebellar purkinje cells. Expl. Brain Res. 1, 161-183.

Fifková, E., and Maršala, J. (1967). Stereotaxic atlases for the cat, rabbit and rat. In J. Bures, M. Petran and J. Zachar (Eds.), Electrophysiological Methods in Biological Research, Academic press, New York and London.

Cetchell, T. V. and Shepherd, G. M. (1975). Synaptic actions on mitral and tufted cells elicited by olfactory nerve volleys in the rabbit. J. Physiol., 251, 497-522.

Green, J. D., Mancia, M. and Baumgarten, R. von. (1962). Recurrent inhibition in the olfactory bulb. I. Effects of antidromic stimulation of the lateral olfactory tract. J. Neurophysiol. 25, 467-488.

Haberly, L. B., and Price, J. L. (1977). The axonal projection patterns of the mitral and tufted cells of the olfactory bulb in the rat. Brain Res., 129, 152-157.

Heimer, L. (1968). Synaptic distribution of centripetal and centrifugal nerve fibres in the olfactory system of the rat, J. Anat. (Lond.), 103, 413-432.

Hirata, Y. (1964). Some observations on the fine structure of the synapses in the olfactory bulb of the mouse, with particular reference to the atypical synaptic configuration. Archs Histol. Japan. 24, 293-302.

Kandel, E. R., Spencer, W. A. and Brinley, F. J. (1961). Electrophysiology of hippocampal neurons. I. Sequential invasion and synaptic organization. J. Neurophysiol. 24, 225-242.

Kerr, D. I. B. (1960). Properties of the olfactory efferent system. Aust. J. exp. Biol. med. Sci. 38, 29-36.

Kerr, D. I. B. and Hagbarth, K. E. (1955). An investigation of olfactory centrifugal system. J. Neurophysiol. 18, 362-374.

Komisaruk, B. R. and Beyer, C. (1972). Responses of diencephalic neurons to olfactory bulb stimulation, odor, and arousal. Brain Res., 36, 153-170.

Kuno, M. and Llinás, R. (1970). Enhancement of synaptic transmission by dendritic potentials in chromatolysed motoneurons of the cat. J. Physiol. (Lond.), 210, 807-821.

Maekawa, K. and Purpura, D. P. (1967). Properties of spontaneous and evoked synaptic activities of thalamic ventrobasal neurons. J. Neurophysiol., 30, 360-381.

Marchiafava, P. L. (1976). Centrifugal actions on amacrine and ganglion cells in the retina of the turtle. J. Physiol. (Lond.), 255, 137-155.

Miller, R. F. and Dacheux, R. (1976). Dendritic and somatic spikes in mudpuppy amacrine cells: identification and TTX sensitivity. Brain Res., 104, 157-162.

Mori, K., Kogure, S. and Takagi, S. F. (1977). Alternating responses of olfactory bulb neurons to repetitive lateral olfactory tract stimulation. Brain Res., 133, 150-155.

Mori, K. and Takagi, S. F. (1975). Spike generation in the mitral cell dendrite of the rabbit olfactory bulb. Brain Res. 100, 685-689.

Mori, K. and Takagi, S. F. (1977a). Inhibition in the olfactory bulb; dendrodendritic interactions and their relation to the induced waves. Food Intake and Chemical Senses Tokyo: Tokyo Univ. Press (in the Press).

Mori, K. and Takagi, S. F. (1977b). Inhibitory potentials in mitral cells of the rabbit olfactory bulb. Proc. Internatn. Union of Physiol. Sci. 13, 527.

Mori, K. and Takagi, S. F. (1978a). An intracellular study of dendrodendritic inhibitory synapses on mitral cells in the rabbit olfactory bulb. ~~(Submitted to~~ (J. Physiol.) In press

Mori, K. and Takagi, S. F. (1978b). Activation and inhibition of olfactory bulb neurons by anterior commissure volleys in the rabbit. ~~(Submitted to~~ (J. Physiol.) In press

Murakami, M. and Shimoda, Y. (1977). Identification of amacrine and ganglion cells in the carp retina. J. Physiol. (Lond.), 264, 801-818.

Nicoll, R. A. (1969). Inhibitory mechanisms in the rabbit olfactory bulb: dendrodendritic mechanisms. Brain Res., 14, 157-172.

Nicoll, R. A. (1970). Recurrent excitatory pathways of anterior commissure and mitral cell axons in the olfactory bulb. Brain Res., 19, 491-493.

Ochi, J. (1963). Olfactory bulb responses to antidromic olfactory tract stimulation in the rabbit. Jap. J. Physiol., 13, 113-128.

Phillips, C. G. (1959). Actions of antidromic pyramidal volleys on single Betz cells in the cat. Q.Jl exp. Physiol., 44, 1-25.

Phillips, C. G., Powell, T. P. S. and Shepherd, G. M. (1963). Responses of mitral cells to stimulation of the lateral olfactory tract in the rabbit. J. Physiol., 168, 65-88.

Pinching, A. J. (1971). Myelinated dendritic segments in the monkey olfactory bulb. Brain Res., 29, 133-138.

Pollwn, D. A. and Lux, H. D. (1966). Conductance changes during inhibitory postsynaptic potential in normal and strychninized cortical neurons. J. Neurophysiol., 29, 369-381.

Price, J. L. (1968). The termination of centrifugal fibres in the olfactory bulb. Brain Res., 7, 483-486.

Price, J. L. (1973). An autoradiographic study of complementary laminar patterns of termination of afferent fibers to the olfactory cortex. J. comp. Neurol., 150, 87-108.

Price J. L. and Powell, T. P. S. (1970a). The morphology of the granule cells of the olfactory bulb. J. Cell Sci., 7, 91-123.

Price, J. L. and Powell, T. P. S. (1970b). The synaptology of the granule cells of the olfactory bulb. J. Cell Sci., 7, 125-155.

Price, J. L. and Powell, T. P. S. (1970c). An electronmicroscopical study of the termination of the afferent fibres to the olfactory bulb from the cerebral hemisphere. J. Cell Sci. 7, 157-187.

Price, J. L. and Powell, T. P. S. (1970d). The mitral and short axon cells of the olfactory bulb. J. Cell Sci., 7, 631-651.

Price, J. L. and Powell, T. P. S. (1970e). An experimental study of the origin and the course of the centrifugal fibres to the olfactory bulb in the rat. J. Anat. (Lond.), 107, 215-237.

Price, J. L. and Powell, T. P. S. (1970f). The afferent connexions of

the nucleus of the horizontal limb of the diagonal band. J. Anat. (Lond.), 107, 239-256.

Purpura, D. P. (1966). Comparative physiology of dendrites. In G. C. Quarton, T. Melnechuck and F. O. Schmitt (Eds.), The neurosciences; A Study Program, Rockefeller Univ. Press, New York, pp. 372-393.

Purpura, D. P. and Cohen, B. (1962). Intracellular recording from thalamic neurons during recruiting responses. J. Neurophysiol., 25, 621-635.

Purpura, D, P., Desiraju, T., Prelevic, S. and Santini, M. (1968). Excitability changes in the dendrites of thalamic neurons during prolonged synaptic activation. Brain Res., 10, 457-459.

Purpura, D. P. and McMurtry, J. G. (1965). Intracellular activities and evoked potential changes during polarization of motor cortex. J. Neurophysiol., 28, 166-185.

Purpura, D. P. and Shofer, R. J. (1964). Cortical intracellular potentials during augmenting and recruiting responses. 1. Effects of injected hyperpolarizing currents on evoked membrane potential changes. J. Neurophysiol., 27, 117-132.

Purpura, D. P., Shofer, R. J. and Scarff, T. (1965). Properties of synaptic activities and spike potentials of neurons in immature neocortex. J. Neurophysiol., 28, 925-942.

Rall, W. and Shepherd, G. M. (1968). Theoretical reconstruction of field potentials and dendrodendritic synaptic interactions in olfactory bulb. J. Neurophysiol., 31, 884-915.

Rall, W., Shepherd, G. M., Reese, T. S. and Brightman, M. W. (1966). Dendrodendritic synaptic pathway for inhibition in the olfactory bulb. Exptl. Neurol., 14, 44-56.

Reese, T. S. and Shepherd, G. M. (1972). Dendrodendritic synapses in the central nervous system. Structure and function of synapses, ed. Pappas, G. D. and Purpura, D. P. pp 121-136, New York: Raven.

Ribak, C. E., Vaughn, J. E., Saito, K., Barber, R. and Roberts, E. (1977). Glutamate Decarboxylase localization in neurons of the olfactory bulb. Brain Res., 126, 1-18.

Scalia, F. (1966). Some olfactory pathways in the rabbit brain. J. comp. Neurol., 126, 285-310.

Scalia, F. and Winans, S. S. (1975). The differential projections of the olfactory bulb and accessory olfactory bulb in mammals. J. comp. Neurol.,

161, 31-56.

Scheibed, M. E. and Scheibel, A. B. (1975). Dendrite bundles, central programs and the olfactory bulb. Brain Res., 95, 407-421.

Scott, J. W. and Leonard, C. M. (1971). The olfactory connections of the lateral hypothalamus in the rat, mouse and hamster. J. comp. Neurol., 141, 331-314.

Scott, J. W. and Pfaffmann, C. (1967). Olfactory input to the hypothalamus: electrophysiological evidence. Science, 158, 1592-1594.

Shepherd, G. M. (1963). Responses of mitral cells to olfactory nerve volleys in the rabbit. J. Physiol., 168, 89-100.

Shepherd, G. M. (1963). Neuronal systems controlling mitral cell excitability. J. Physiol., 168, 101-117.

Shepherd, G. M. (1969). Dendrodendritic synaptic interactions in olfactory bulb. J. Physiol. (Lond.), 204, 132-133.

Shepherd, G. M. (1970). The olfactory bulb as a simple cortical system: experimental analysis and functional implications. In F. O. Schmitt (Ed.), The Neurosciences, Second Study Program, Rockefeller Univ. Press, New York, pp. 539-552.

Shepherd, G. M. (1972). Synaptic organization of the mammalian olfactory bulb. Physiol. Rev., 52, 864-917.

Spencer, W. A. and Kandel, E. R. (1961). Electrophysiology of hippocampal neurones. IV. Fast prepotentials. J. Neurophysiol., 24, 272-285.

Tsukahara, N. and Fuller, D. R. G. (1969). Conductance changes during pyramidally induced postsynaptic potentials in the red nucleus neurons. J. Neurophysiol., 32, 35-42.

Walsh, R. R. (1959). Olfactory bulb potentials evoked by electrical stimulation of the contralateral bulb. Amer. J. Physiol., 196, 327-329.

Werblin, F. S. and Dowling, J. E. (1969). Organization of the retina of the mudpuppy, Necturus muculosus. II. Intracellular recording. J. Neurophysiol., 32, 339-355.

Westecker, M. E. (1970). Altenating characteristics of the evoked potential in the olfactory bulb in response to repetitive stimulation of the lateral olfactory tract. Brain Res., 17, 142-144.

Westecker, M. E. (1970). Excitatory and inhibitory interactions in the olfactory bulb involving dendrodendritic synapses between mitral cells and granular cells. Pflügers Arch. ges. Physiol., 317, 173-186.

Willey, T. J. (1973). The ultrastructure of the cat olfactory bulb. J. Comp. Neurol., 152, 211-232.

Yamamoto, C., Yamamoto, T. and Iwama, K. (1963). The inhibitory system in the olfactory bulb studied by intracellular recording. J. Neurophysiol. 26, 403-415.